Pliocene Sea Ice Evolution in the Iceland and Labrador Sea – A Biomarker Approach

Caroline Clotten

Thesis for the degree of philosophiae doctor (PhD)
at the University of Bergen

2017

Date of defence: 07.12.2017

Scientific environment

This thesis was submitted for the degree doctor philosophiae (PhD) at the Department of Earth Sciences (University of Bergen, Norway). The research was performed at *Uni Research Climate AS* and *Bjerknes Centre for Climate Research* (Bergen, Norway). The lab work was carried out in collaboration with our partners at the *Alfred Wegener Institute Helmholtz Centre for Polar and Marine Research* (Bremerhaven, Germany).

This PhD was part of the *Pliocene East Greenland Current and Sea Ice Evolution (PEGSIE)* project. The main supervisor of the thesis was Dr. Stijn De Schepper (Uni Research Climate). Co-supervisors were Prof. Dr. Ruediger Stein (Alfred Wegener Institute, Germany) and Prof. Dr. Eystein Jansen (University of Bergen). This research was funded by the Norges Forskningsrådet (NFR; grant no: 229819).

Uni Research Climate, Bergen, Norway

Bjerknes Centre for Climate Research, Bergen, Norway

Alfred Wegener Institute Helmholtz Centre for Polar and Marine Research, Bremerhaven, Germany

Department of Earth Science
Faculty of Mathematics and Natural Science
University of Bergen, Bergen, Norway

Acknowledgements

After more than three amazing years that have influenced me quite a lot, I will leave Bergen with mixed feelings, but not without saying thank you to those people, who accompanied me during this part of my life.

First of all, I would like to thank my supervisor Stijn De Schepper. I am grateful that you gave me the opportunity to work in this project with you. I admit it was not always easy, but your motivating words helped me to continue. I thank you for freedom, endless patience, reading countless times through manuscripts, abstracts, posters, correcting them, and discussing data with me. You did a good job by dragging me through the last tough part of the PhD.

Ruediger Stein, I thank you for being my co-supervisor. I really enjoyed data, poster and manuscript discussions with you, which always brought me a lot further and helped to focus my mind.

I thank Eystein Jansen for co-supervising my thesis and Tim Herbert and Sofia Ribeiro for being my opponents.

I thank the admin staff and my colleagues at Uni Research Climate for a great time, but especially Tamara Trofimova and Fabian Bonitz for having amusing non-scientific conversations during breaks. Special thanks to Kerstin Perner for comfort and support, when I needed it.

Walter Luttmer for teaching me the lab techniques and for funny (and sometimes also serious) conversations during my lab work.

Kirsten Fahl. Thank you so much for “adopting” and caring for me during my stays in Bremerhaven. Your ability to bring a smile onto my face even 1000 km away was a big help. Thank you for everything you have done for me during the past three years.

Tanja Hörner, Henriette Kolling and Anne Kremer, thanks so much for your friendship and support during my stays in Bremerhaven, which wouldn’t have been half the fun without you!

I thank my friends, especially Rike Völpel, Kati Hirschmann, Nadine Broda, and Inka Schade. You are amazing friends. I learnt a lot about the meaning of friendship during the past years I couldn't always be with you.

Katharina Lefringhausen, thanks for being an awesome friend my entire life. Although physically apart, you stayed mentally by my side and advising me on how to handle a PhD. I am lucky you made these experiences before me ;)

I thank Yvonne Clotten for being the best sister I could wish for. You reminded me that there are other things in life than work. I missed you a lot during my time in Bergen.

I owe great thanks to my parents, Ilona and Hans-Josef Clotten, and my grandma Christiana Danch. You taught me to always believe in myself and never to give up. No matter how hard it seems there is always a way. What I achieved so far was only possibly because of your love and faith.

Last, but definitely not least, Steffen Paprott – I have no idea how I can thank you for all your love and support you gave me during the last years and actually almost half of my life. Thank you for letting me do my PhD abroad, although it meant additional years apart. It was not easy, but you trusted in me – and in us. You helped me handling the tension I was feeling especially towards the end and gave me confidence in myself. And for that I am endlessly thankful.

Finally, I am also grateful for Rike Völpel, Thorsten vor der Landwehr, Steffen Paprott, Katrin Hirschmann, Anne Kremer, Tanja Hörner, Henriette Kolling and Birte Westrop for reading the final thesis and spotting mistakes I wasn't able to see anymore.

Caroline Clotten

Bergen, September 2017

Abstract

Sea ice plays a crucial role in the climate system. Although this is broadly acknowledged, the role of sea ice is not fully understood, especially during warmer periods such as the Pliocene (5.88–2.58 Million years (Ma) ago). Fragmentary evidence suggests that the Arctic sea ice was reduced in the Pliocene, but that it could have been transported into the Nordic Seas, when the East Greenland Current (EGC) developed, which established the modern Nordic Seas circulation. Today the EGC is the main exporter of cooler and fresher Arctic water masses into the Nordic Seas and carries 90% of the total sea ice exported from the Arctic Ocean with it. The main objectives of this thesis are to determine the presence of (seasonal) sea ice in the Pliocene Iceland and Labrador Seas and to identify the role of the EGC and sea ice on the Pliocene (sub-)Arctic climate.

The Iceland Sea and the Labrador Sea are important and sensitive regions for determining the occurrence of sea ice and changes in the EGC and Greenland Ice Sheet (GIS). Therefore, Early Pliocene to Early Quaternary sediments were investigated from the Iceland Sea (ODP Site 907) and the Labrador Sea (IODP Site U1307) using biomarkers (IP_{25}, sterols, alkenones) to reconstruct the Pliocene paleoceanography and especially the sea ice cover in both areas. Additional information was obtained from palynological analysis of the same sites.

My analyses revealed, that sea ice occurred for the first time in the Pliocene Iceland Sea around 4.5 Ma, together with a cooling of the entire Nordic Seas. The development of a proto EGC replaced warmer Atlantic water masses in the Iceland Sea and either favored the local formation of sea ice or directly exported sea ice from the Arctic Ocean. At ~4.0 Ma, an extended interval of seasonal sea ice in the Iceland Sea occurred contemporaneously with the establishment of a large sea surface temperature (SST) gradient in the Nordic Seas: the Iceland Sea cooled further, whereas the Norwegian Sea warmed. Increased warming in the North Atlantic and Norwegian Sea at this time may have lead to increased moisture transport towards Siberia, which can ultimately led to a freshening of the Arctic Ocean, favoring sea ice production and export (**Paper I**).

Frequently occurring seasonal sea ice was reconstructed between 3.5–3.0 Ma in the Iceland Sea (**Paper II**), while the biomarker analysis indicate dominantly ice-free conditions in the Labrador Sea for approximately the same time interval (**Paper III**). This may have been the result of a weak EGC influence in the Labrador Sea, whereas the EGC influence was stronger in the Iceland Sea at times when the GIS was significantly reduced. The weaker EGC

influence in the Labrador Sea might be coinciding with a strong subpolar gyre (SPG) circulation in the Labrador Sea allowing for more advection of Atlantic water masses into the Labrador Sea (**Paper III**). Higher-than-modern alkenone-based SSTs suggest that summers in both areas were sea ice-free. After 3.0 Ma, sea ice occurred less frequently in the Iceland Sea, whereas from 2.75 Ma fluctuations in the sterol record might suggest a nearby sea ice edge (**Paper II**). The Labrador Sea received more polar water and a sea ice edge developed after ~3.1 Ma implying an enhanced southward flow of the EGC (**Paper III**). The enhanced southward penetration of polar waters might agree with a weaker SPG circulation. As such, a sea ice edge and an intensified EGC might have acted as a positive feedback for the expansion of the GIS during the Northern Hemisphere glaciation by stronger sea ice albedo feedbacks and isolation of Greenland from warm Atlantic water masses, respectively.

List of publications

I. Clotten, C., Stein, R., Fahl, K., Schreck, M., De Schepper, S. On the Causes of Sea Ice in the Early Pliocene Iceland Sea. *Manuscript in preparation for Geology*.

II. Clotten, C., Stein, R., Fahl, K., De Schepper, S. (accepted). Seasonal sea ice cover during the warm Pliocene: evidence from the Iceland Sea (ODP Site 907). *Earth and Planetary Science Letters, accepted pending minor revisions [status 19/09/2017]*.

III. Clotten, C., Stein, R., Fahl, K., De Schepper, S. Sea ice presence in the Labrador Sea prior to the Northern Hemisphere Glaciation. *Manuscript in preparation for Quaternary Science Reviews*.

IV. Schreck, M., Nam, S.-I., Clotten, C., Fahl, K., De Schepper, S., Forwick, M., Matthiessen, J. (2017). Neogene dinoflagellate cysts and acritarchs from the high northern latitudes and their relation to sea surface temperature. *Marine Micropaleontology*, doi.org/10.1016/j.marmicro.2017.09.003

Contents

1 Introduction

1.1 Sea ice

Sea ice is frozen ocean water that forms and melts exclusively in the ocean, and as such is independent from ice on land (e.g. ice sheets on Greenland). Sea ice grows and melts seasonally (first-year ice), but especially in the central Arctic Ocean and close to Antarctica, perennial sea ice remains over several years (multi-year ice). Sea ice that drifts on the open ocean and is propelled by wind and currents is termed pack ice, whereas stationary sea ice attached to the coast is called land fast ice.

Although sea ice occurs mainly in the polar regions of both hemispheres, it is a critical component in the polar and global climate system. Sea ice acts as an isolator between the ocean and atmosphere, limiting heat, moisture and gas exchange when it is present (Dieckmann and Hellmer, 2010). Sea ice also has a high albedo, meaning that most (~90 %) of the incoming solar radiation is reflected back into space, whereas energy is absorbed by the dark surrounding, lower albedo water (*Figure 1.1*). Decreasing sea ice leads to a reduction in Earth's albedo and thus increases the temperature in both atmosphere and ocean, which in turn adds further to thinning and melting of sea ice (Serreze and Barry, 2011). Sea ice is also important for deep-water formation. Cooling and freezing of surface waters results in salt release (brine formation) to the surface ocean. These denser and cooler surface waters sink towards the bottom of the ocean and form deep-water masses (Rudels and Quadfasel, 1991),

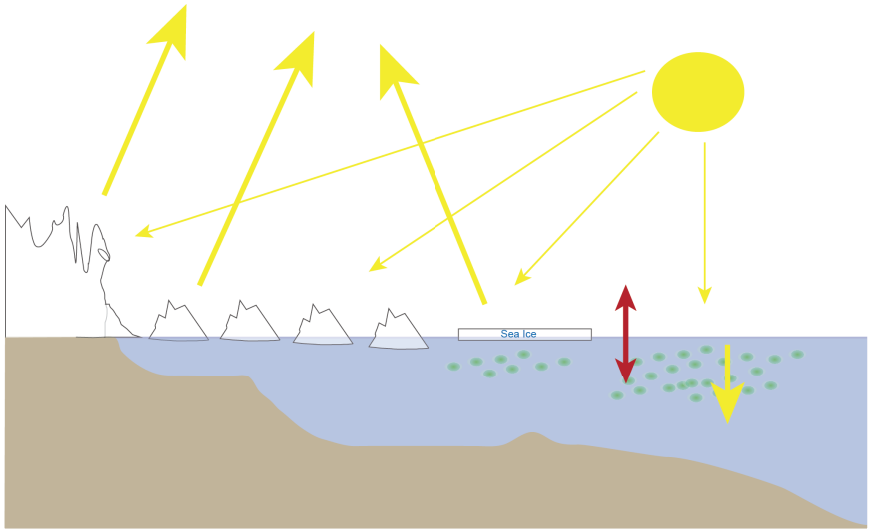

Figure 1.1: *Schematic illustration of role of sea ice in the climate system. Yellow arrows indicate the incoming and reflected solar radiation, red arrow indicates the heat exchange between ocean and atmosphere. Green dots represent marine phytoplankton, which is higher in open ocean environments than below sea ice.*

which enhances the deep-ocean circulation and ventilation (Killworth, 1983). The export of Arctic sea ice towards the North Atlantic affects the ocean circulation by decreasing the sea surface salinity and increasing the surface stratification, which can potentially disturb the thermohaline circulation (THC; e.g. Dickson et al., 2007).

Sea ice is not only important for physical aspects of the environment, but also for the biosphere. It provides an unique life habitat for mammals like seals and the iconic polar bear, but also for phytoplankton (Gosselin et al., 1997). Starting in late autumn, sea ice algae (mainly diatoms) are incorporated into sea ice, where they hibernate in small channels formed during sea ice formation (Gradinger and Ikävalko, 1998). In spring, when sufficient light and nutrients become available the algae start to grow (Horner, 1985). Thus, sea ice algae, adapted and bound to this specific environment, contribute to organic carbon and biomass release (Gosselin et al., 1997; Gradinger, 2009) and form the basic level of the Arctic food chain by photosynthesis (Arrigo et al., 2010). Interestingly, some of those algae synthesize specific biomarkers, which can be found in geological records and are used to reconstruct past sea ice cover (e.g. Belt et al., 2007; Brown et al., 2014; see also chapter 2.1). The consequences and implications of the ongoing sea ice decrease for the (macro-)faunal communities and the climate are not yet fully understood because sea ice as a climate component only gained attention as an important climate feature in the past decades (Dieckmann and Hellmer, 2010).

Today the central Arctic Ocean is perennially covered with sea ice, while the marginal seas including the Iceland and Labrador seas experience high seasonality of sea ice extent (*Figure 1.2)*. During winter (February/March), sea ice cover is largest (*Figure 1.2A*), while it decreases during summer (*Figure 1.2B*). Since the beginning of the satellite data records in 1978, Arctic sea ice extent declined (~3.8% per decade) with larger losses in summer and autumn (Stroeve et al., 2007; Vaughan et al., 2013). Not only the sea ice extent is decreasing, but also older, thicker sea ice is declining at a high rate (13.5 % per decade; Vaughan et al., 2013). In summer 2012, the lowest extent of sea ice was recorded within the satellite era (*Figure 1.3*). In fact, summers of 2007, 2011, 2012, 2016 and 2017 have all shown very low sea ice extents (*Figure 1.3*). Based on the rapidly diminishing sea ice extent, the Arctic Ocean may be seasonally sea ice-free in summer by the middle of the century (Wang and Overland, 2012). Stroeve et al. (2007; *Figure 1.4*) showed that the recent sea ice loss is faster than model simulations predicted, therefore an ice free Arctic Ocean might occur sooner and probably more abrupt than slowly due to amplifying feedback mechanisms within the Arctic climate system (polar amplification; Allison et al., 2009; Serreze and Barry, 2011).

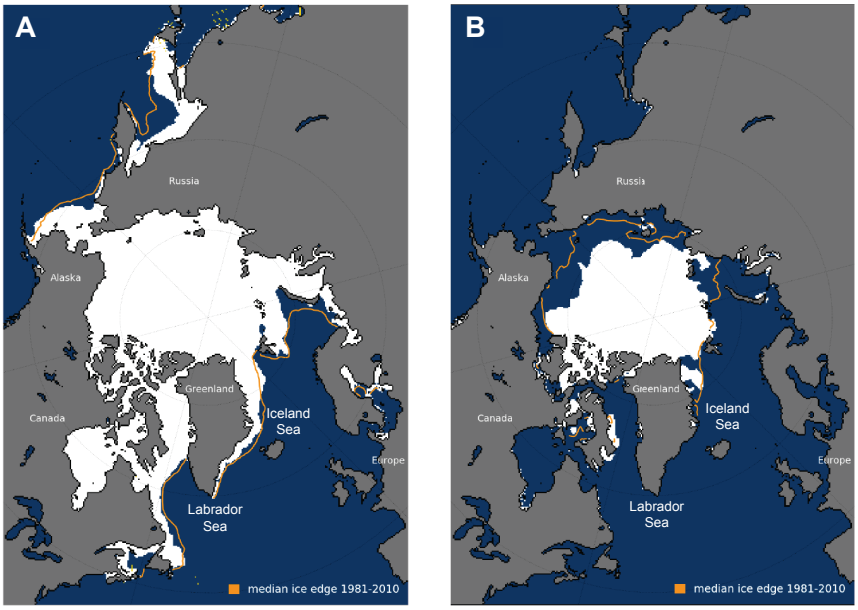

Figure 1.2: *Modern Arctic Ocean sea ice extent for A) March 2017 and B) August 2017. Orange lines indicate the median sea ice extent from 1981–2010. Reconstructions based on data from* http://nsidc.org/arcticseaicenews/

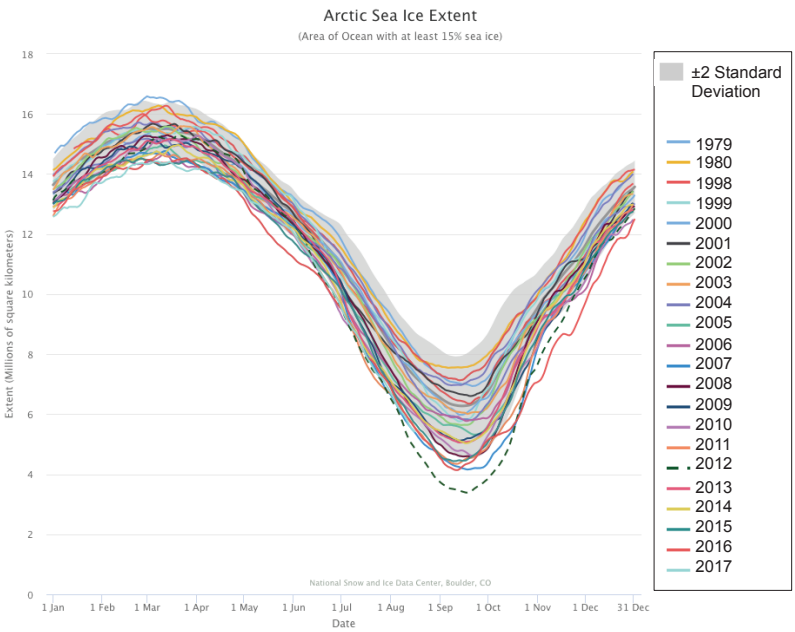

Figure 1.3: *Annual Arctic sea ice extent for different years. Gray shaded area shows the 2sd of the mean between 1981-2010 (black line). Reconstructions based on data from* http://nsidc.org/arcticseaicenews/

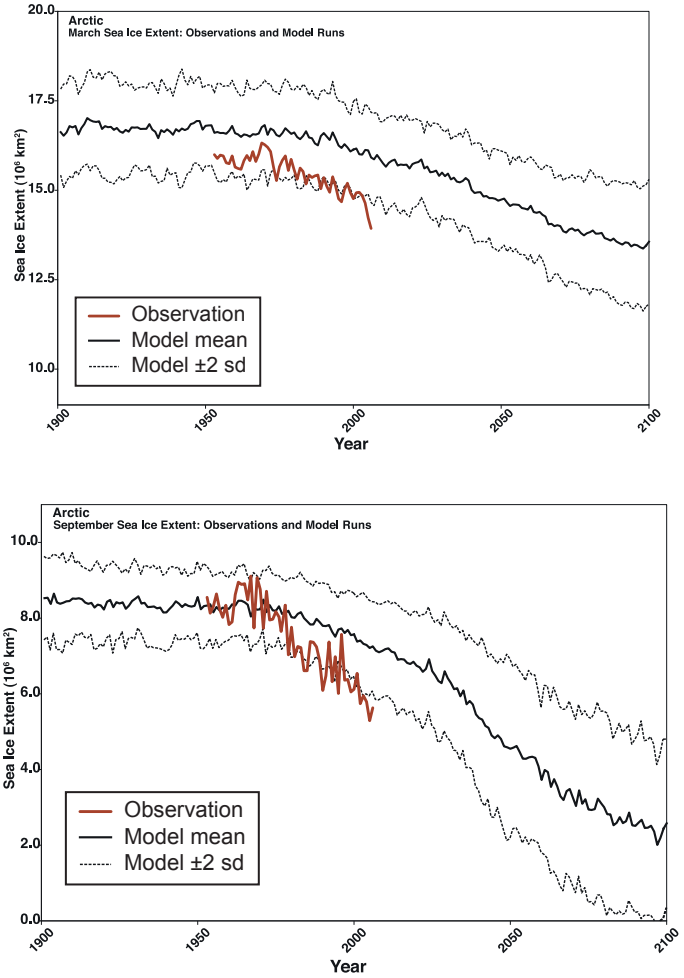

Figure 1.4: *Upper panel shows Arctic March, lower panel Arctic September sea ice extent (x10^6 km^2) from observations (thick red line) and the multi-model ensemble mean (solid black line) and standard deviation (dotted black line) from different 18 IPCC AR4 climate models (individual models not shown here). Figure of Stroeve et al. (2007).*

Evidence for the very first sea ice occurrence in the Arctic Ocean comes from iron (Fe) grains in marine deposits with an Eocene age (~44 Ma) recovered from the ACEX (Arctic Coring Expedition) drill site (Darby, 2014). Sea ice is the most likely delivery agent for these grains, which initially occur in short intervals, indicating that perennial sea ice occurred ephemerally until ~37 Ma. Based on Strontium, Lead, and Neodymium isotope records from the same core, a continuous Arctic sea ice cover for the past 15 Ma is proposed (Haley et al., 2008a; 2008b). These findings are in agreement with provenance studies of Fe-oxide grains suggesting a perennial sea ice cover in the central Arctic Ocean from the middle Miocene (~14 Ma)

onwards (Darby, 2008). This fits into the context of a transition to globally cooler conditions during the Neogene (e.g. Zachos et al., 2001) and in the Arctic as indicated by substantial glaciations in the northern Barents Sea area (Knies and Gaina, 2008). Recently, seasonal sea ice conditions with ice free summers were demonstrated to occur in the central Arctic Ocean during the Late Miocene (Stein et al., 2016). The first sea ice in the marginal Arctic Ocean (Yermak Plateau) emerged around 4.0 Ma in the Early Pliocene possibly due to the opening of the Bering Strait and uplift of the circum-Arctic topography (Knies et al., 2014a). After 4.0 Ma, sea ice expanded and a modern winter maximum was established around 2.5 Ma on the Yermak Plateau (Knies et al., 2014a).

While sea ice is documented outside the Arctic Ocean, i.e. in the Nordic Seas (Hoff et al., 2016; Kolling et al., 2017) and Labrador Sea (Weckström et al., 2013) during the Late Quaternary, there is currently no evidence for sea ice in those regions in older times. The significance of sea ice on local and global scale is widely accepted, but the causes and consequences of a reduced sea ice cover in a globally warm world are not fully understood. A recent study has shown that the loss of sea ice enhances surface melting of the modern Greenland Ice Sheet (GIS; Liu et al., 2016). Without sea ice, heat exchange from the ocean into the atmosphere increases, resulting in advection of warm air masses and thus warming over Greenland (Ballantyne et al., 2013), which potentially hampers sustaining a GIS and may ultimately lead to melting of the GIS. In the light of the ongoing climate change, it is crucial to know how sea ice waning in the Northern Hemisphere will affect the GIS as well as the THC, which distributes heat over the globe. Therefore, collecting data about the sea ice extent in the geological past, and especially in times with a globally warm climate such as the Pliocene is essential to better understand the future climate in the Arctic.

1.2 Nordic Seas and Labrador Sea oceanography

The Nordic Seas (Greenland, Norwegian, and Iceland Sea) connect the Arctic Ocean and the North Atlantic (*Figure 1.5A*; Blindheim and Østerhus, 2005). The Nordic Seas surface circulation is dominated by the inflow of relatively warm (~10 ºC) and saline (~35 psu) waters of the North Atlantic Current (NAC) in the east over the Greenland-Scotland Ridge (GSR; Blindheim and Østerhus, 2005), and the outflow in the west of the East Greenland Current (EGC), which exports cold (<0 ºC), fresher (30 psu) and nutrient depleted water masses over the Denmark Strait into the Labrador Sea (Aagaard and Coachman, 1968a, b; Hopkins, 1991). This results in a strong temperature and salinity gradient between the east and the west Nordic Seas surface waters (*Figure 1.5A*). Due to the warm Atlantic water inflow, the eastern margin of the Nordic Seas is sea ice-free. North of Scandinavia the NAC divides into two branches: about one-third flows eastward into Barents Sea, and two-third form the West Spitsbergen

Current (WSC), which flows northward into the eastern Fram Strait. There, water masses cool due to heat release into the atmosphere, get denser and sink to the seafloor (Blindheim and Østerhus, 2005). Only a small part of the WSC reaches the Arctic Ocean, where it submerges under a layer of cold and fresh Arctic water exiting the Arctic Ocean (Johannessen, 1986). The main part of the WSC is deflected southwestward as the Return Atlantic Current (RAC), where it dips in the western Fram Strait under the cold waters exiting the Arctic Ocean as the EGC. This mixture of polar surface and Atlantic subsurface waters flows southward along the eastern margin of Greenland (Blindheim and Østerhus, 2005; Rudels et al., 2002). At approximately 68 ºN, a small part of the EGC bifurcates north of Iceland to form the East Icelandic Current (EIC). Its water masses can be found in a depth of 0–50 m (Rudels et al., 2002). West of Iceland, warm Atlantic water enters the Nordic Seas as the Irminger Current (IC) to flow northward towards Iceland. North of Iceland, the EIC and IC mix and flow eastwards. Thereby they form the southern boundary of a gyre in the Iceland Sea where polar and Atlantic waters mix (*Figure 1.5A*; Baumann et al., 1996; Rudels et al., 2002).

The other branch of the IC flows into the Labrador Sea, where it meets the polar, cool and fresher surface waters of the EGC. Both water masses mix as they round the southern tip of Greenland and form the West Greenland Current (WGC; Fratantoni and Pickart, 2007), which flows northwestward along the west coast of Greenland (Clarke and Gascard, 1983; Schmidt and Send, 2007). A branch of the WGC feeds the Labrador Current (LC), which brings cool and fresh Arctic waters southward along the Canadian Coast towards the North Atlantic (Schmidt and Send, 2007; and refs therein). Together with the NAC, the EGC, IC and LC form the subpolar gyre (SPG; *Figure 1.5A*), which is driven by the regional wind system and buoyancy differences of the different water masses in the Labrador Sea (Hátún et al., 2005). In a depth of 700–2500 m, cooler (3.5 ºC) and fresher (34.9 psu) Labrador Sea Water (LSW) is formed by convective overturning in the Labrador Sea off the east coast of Greenland (Dickson and Brown, 1994; Schmitz, 1996). Deep-water masses originating from the Greenland and Iceland seas as well as from the Norwegian Sea enter the Labrador Sea over the Denmark Strait as Denmark Scotland Overflow Water (DSOW; <3500 m) and Iceland-Scotland Ridge as Iceland Scotland Overflow Water (ISOW; 2500–3500 m), respectively (Evans et al., 2007; Pickart, 1992).

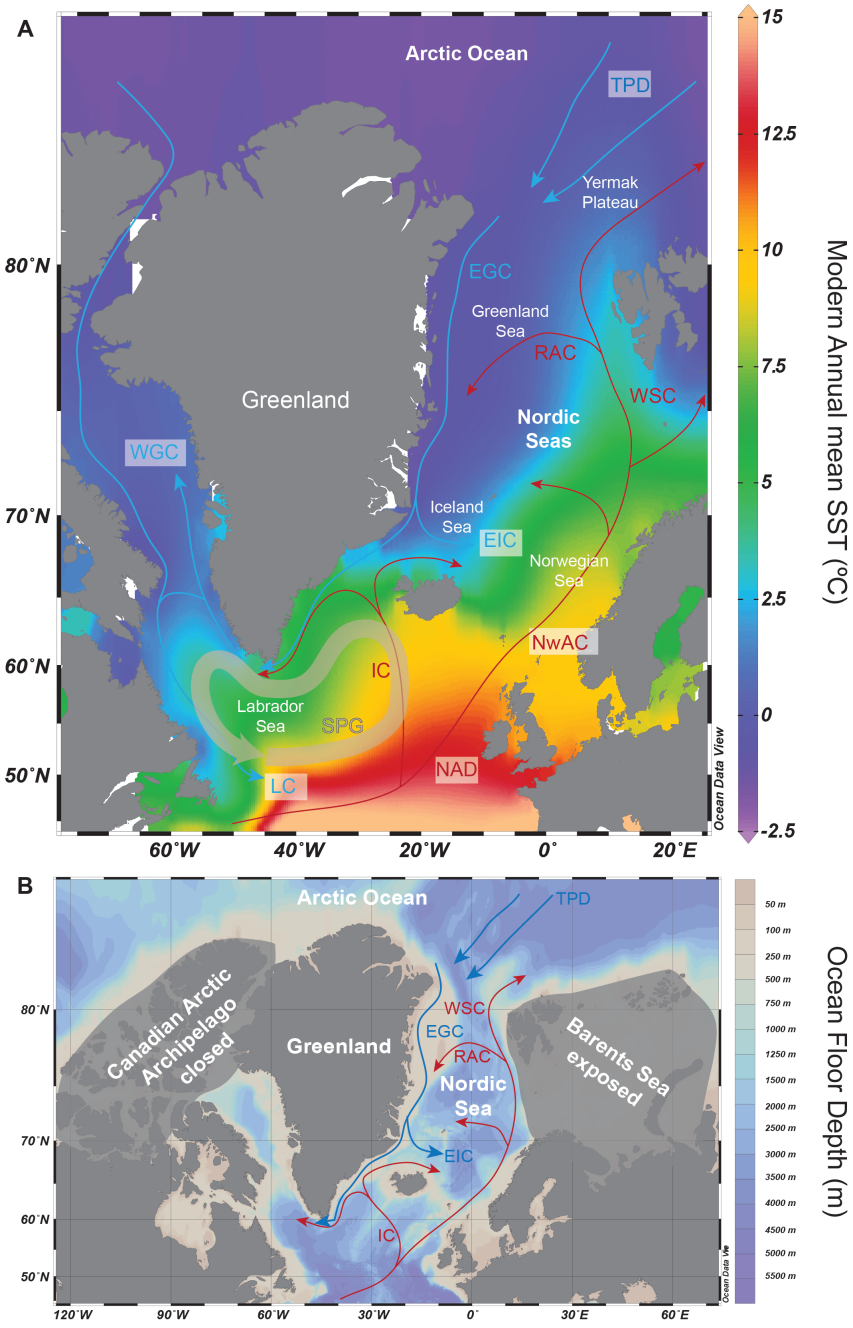

Figure 1.5: *A) Modern oceanography of the Nordic Seas after Blindheim and Østerhus (2005) and modern annual SSTs (Locarnini et al., 2013). B) Pliocene paleoceanography and paleogeography. Exposed Barents Sea is based on Zieba et al. (2017) and closed Canadian Arctic Archipelago based on Matthiessen et al. (2009). Red arrows indicate important warm surface currents: NAD = North Atlantic Drift, NWAC = Norwegian Atlantic Current, WSC = West Spitsbergen Current, RAC = Return Atlantic Current, IC = Irminger Current. Blue arrows show important cool water surface currents: TPD = Transpolar Drift, EGC = East Greenland Current, EIC = East Icelandic Current, WGC = West Greenland Current, LC = Labrador Current. Subpolar gyre (SPG) is shown in light brown.*

Together with the LSW, these water masses form the North Atlantic Western Boundary Undercurrent (WBUC; Dickson and Brown, 1994; Schmitz, 1996). The Nordic Seas and the Labrador Sea are an important source for the North Atlantic Deep Water (NADW). NADW is produced by sufficient atmospheric cooling and the cyclonic SPG circulation allows surface water to be mixed into greater depth (Dickson and Brown, 1994; Schmitz, 1996). Additional overflow of the dense DSOW and ISOW into the Labrador Sea drive the global thermohaline circulation.

1.3 Pliocene climate and paleoceanography in the Arctic and Nordic Seas

The Pliocene is an epoch that extends from 5.33 to 2.58 Ma and is embraced by the older Miocene Epoch and the younger Pleistocene Epoch (Hilgen et al., 2012). Stratigraphically, the Pliocene is subdivided into two stages: the Early Pliocene or Zanclean (5.33–3.60 Ma) and the Late Pliocene or Piacenzian (3.60–2.58 Ma; *Figure 1.6*). The base of the Zanclean lies within the Gilbert Chron (Van Couvering et al., 2000). The Zanclean top also corresponds to the base of the younger Piacenzian at 3.60 Ma, marked by the Gilbert-Gauss magnetic reversal (Castradori et al., 1998) and marine isotope stage (MIS) MG8 (Shackleton et al., 1995). The Piacenzian top is magnetostratigraphically defined by the Gauss/Matuyama reversal and corresponds to MIS 103 (Gibbard et al., 2010).

The Pliocene has long been considered to be a warm and climatological stable time period (Dowsett et al., 2005; Draut et al., 2003; Haywood et al., 2013) with high CO_2 concentrations (e.g. Kürschner et al., 1996). Evidence for rather warm, stable conditions and reduced continental ice sheets comes from the global $\delta^{18}O$ stack of benthic foraminifera (Lisiecki and Raymo, 2005), which shows low variability in the Early Pliocene, although larger Quaternary-like variability appears in the latest Pliocene (< 3.0 Ma; *Figure 1.6)*. The interpreted Pliocene stability adds to a number of other reasons such as globally high temperatures, high CO_2 levels and reduced ice sheets (Dolan et al., 2011; Haywood et al., 2016a; Martínez-Botí et al., 2015) for why the Pliocene and specifically the mid Piacenzian Warm Period (mPWP) have been studied as a potential analogue for our planets' climate by the end of this century. However, like other past warm events, the mPWP is not a perfect analogue for the future climate due to paleogeographic and topographic differences (i.e. ocean gateways, mountain range elevation) and a climate in equilibrium to a long-term CO_2 forcing – in contrast to the ongoing, transient forcing (Haywood et al., 2011). Therefore, a time slice around the interglacial peak of MIS KM5c (~3.205 Ma; *Figure 1.6*) is currently in the focus of the Pliocene scientific community, both from a modeling (e.g. PlioMIP2; Haywood et al., 2016b) and data perspective (e.g. Dowsett et al., 2016). A time slice, rather than the time slab approach used in the mPWP reconstructions (PRISM; e.g. Dowsett, 2007; 2010), avoids averaging several, different warm

intervals within the mPWP (Haywood et al., 2013). Averaging these warm intervals may give the impression of a warm and stable climate, but a few recent Pliocene studies demonstrated that mPWP and also Pliocene climate, especially in the Nordic Seas and the Arctic, was more variable and possibly not as warm as previously thought (Bachem et al., 2017; Knies et al., 2014a; Risebrobakken et al., 2016).

Early Pliocene

The period between 4.4 and 4.0 Ma was probably the warmest period within the Pliocene with a global temperature higher by about ~4 ºC compared to modern values (Brierley and Fedorov, 2010). This period was characterized by both weak meridional and zonal SST gradients resulting from stable high tropic warm pool SSTs and warm high latitude oceans (Fedorov et al., 2013). This resulted in a weaker atmospheric circulation (e.g. Brierley and Fedorov, 2010; Brierley et al., 2009) and a deeper thermocline in the tropics (Fedorov et al., 2013). Reconstructed atmospheric CO_2 concentrations range between 380 and 400 ppm (*Figure 1.6;* e.g. Pagani et al., 2010; Seki et al., 2010) comparable to modern values of 405.07 ppm in August 2017 (www.esrl.noaa.gov/gmd/ccgg/trends/). Only small fluctuations of global ice volume occurred in the Early Pliocene (*Figure 1.6*; Lisiecki and Raymo, 2005), but it is evident that occasional expansion of local ice sheets in the Arctic region produced icebergs and ice-rafted debris (IRD) (Knies and Gaina, 2008; Knies et al., 2014b). IRD was recorded in the Irminger Basin (St. John and Krissek, 2002) and Iceland Sea between 4.9 and 4.8 Ma, and again around 4.0 Ma in the Iceland Sea (Fronval and Jansen, 1996). Together with the occurrence of IRD in the Labrador Sea at 4.0 Ma (Wolf and Thiede, 1991), this suggests that also an ice sheet occasionally occurred on Greenland at this time.

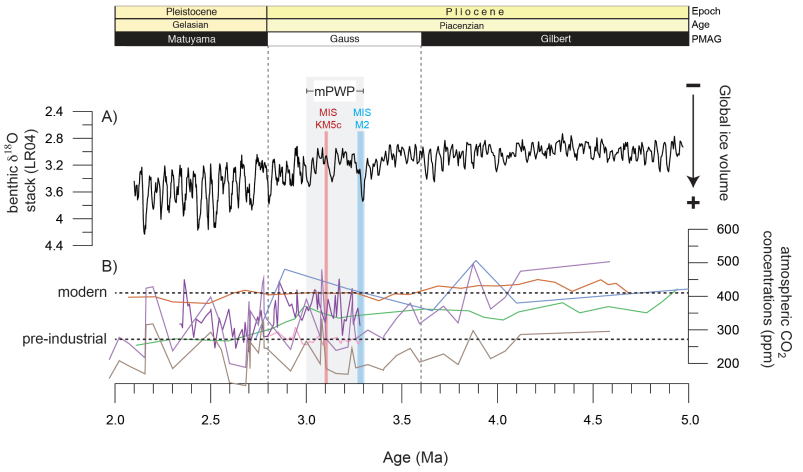

Figure 1.6: *Pliocene/Early Pleistocene changes in A) $\delta^{18}O$ of benthic foraminifera (Lisiecki and Raymo, 2005) and B) atmospheric CO_2 concentrations (Badger et al., 2013 pink line; Bartoli et al., 2011 brown line; Martínez-Botí et al., 2015 purple line ; Seki et al., 2010 orange and green line; Stap et al., 2016 blue line).*

By the Early Pliocene, the Atlantic–Pacific Ocean gateways had not reached their modern setting and were undergoing important changes. Between 4.7 and 4.2 Ma, the Central American Seaway (CAS; *Figure 1.7*) shoaled (e.g. Haug et al., 2001; Steph et al., 2006; 2010), which was suggested to result in an increased Atlantic Meridional Overturning Circulation (AMOC) and northward heat transport (Haug and Tiedemann, 1998; Steph et al., 2010). However, Bell et al. (2015) have recently questioned the role of the Early Pliocene CAS shoaling on deep-water formation and the Pliocene climate evolution. Nevertheless, CAS shoaling between 4.7–4.2 Ma might have affected flow direction through the Bering Strait. The

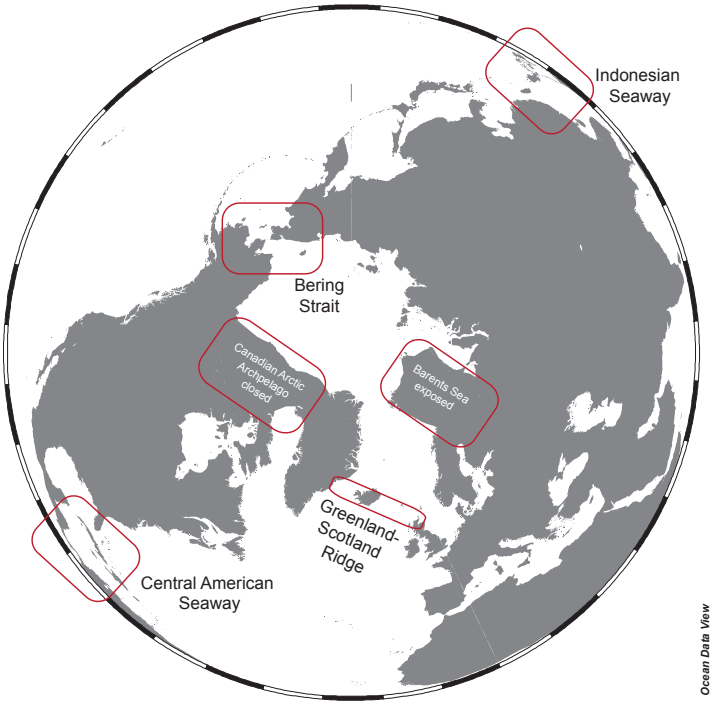

Figure 1.7: *Important gateways that underwent changes in the Miocene and Pliocene.*

Bering Strait (*Figure 1.7*), already open since the Late Miocene (7.4–7.3 Ma), was, together with the Fram Strait, the only high-latitude connection for water exchange between the Arctic Ocean and the Atlantic (Knies et al., 2014b; Matthiessen et al., 2009). At this time, the Canadian Arctic Archipelago (CAA) was closed and the Barents Sea sub-aerially exposed (*Figure 1.7*; Matthiessen et al., 2009; Torsvik et al., 2002; Zieba et al., 2017).

The water flow through the Bering Strait was at first mainly in southward direction, i.e. from the Arctic Ocean into the Pacific (Marincovich and Gladenkov, 1999, 2001). Modeling studies indicate that CAS shoaling leads to reversal of the flow through the Bering Strait, i.e. flow from the Pacific into the Arctic (Maier-Reimer et al., 1990; Sarnthein et al., 2009). CAS

closure leads to the build-up of a Pacific-Atlantic salinity contrast and increases the steric sea level height of the Pacific relative to the Atlantic (Schneider and Schmittner, 2006), which favors changing the flow direction through the Bering Strait. This flow reversal around 4.5 Ma likely increased the inflow of Pacific waters via the Arctic Ocean into the Nordic Seas and thereby exporting polar water masses southwards. This is indicated by the arrival of boreal Pacific molluscs in the Iceland Sea (Durham and MacNeil, 1967; Marincovich and Gladenkov, 2001; Verhoeven et al., 2011), and the accumulation of sea ice related diatoms in the Labrador Sea indicating surface cooling (Bohrmann et al., 1990). Further, changes in sedimentology in the Fram Strait region around this time have been related to increased sea ice export from the Arctic (Knies et al., 2014b). This evidence together with dinoflagellate cyst assemblage turnovers in the Nordic Seas led De Schepper et al. (2015) to propose the onset of a proto-EGC in the Early Pliocene related to ocean gateway changes, i.e. opening of the Bering Strait and closing of the CAS. The onset of the EGC initiated a major change in the Nordic Seas surface circulation. The zonal SST gradient, which is characteristic for the modern Nordic Seas due to cool low salinity water outflow in the western Nordic Seas and warm saline water inflow in the eastern Nordic Seas (*Figure 1.5A*), only developed around 4.0 Ma (Bachem et al., 2017).

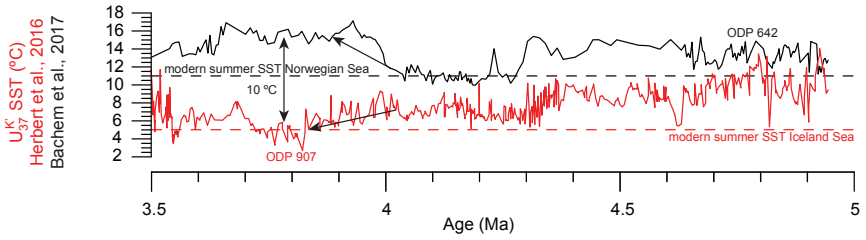

Figure 1.8: *SST comparison between the Norwegian Sea (Bachem et al., 2017; black line) and the Iceland Sea (Herbert et al., 2016; red line). Dashed lines indicate modern summer SSTs after Locarnini et al. (2013).*

From around 4.0 Ma, the Iceland Sea gradually cooled while the Norwegian Sea rapidly warmed, resulting in a SST gradient of ~10 °C. This is 4 °C higher than the modern value (*Figure 1.8*; Bachem et al., 2017; Herbert et al., 2016) and point to major oceanographic changes around that time. The onset of an early EGC likely cooled the Iceland Sea and an observed sea surface productivity decrease was proposed to be related to the occurrence of sea ice (De Schepper et al., 2015; Schreck et al., 2013; Shipboard Scientific Party, 1996; Stabell and Koç, 1996). However, no direct evidence of sea ice has been reported. The export of sea ice might be possible because it was suggested that perennial sea ice may have occurred in the central Arctic Ocean as early as 15 Ma (Haley et al., 2008b). Late Miocene reconstructions indicate a seasonal sea ice cover in the Arctic (Stein et al., 2016) and Early Pliocene sea ice reconstructions in the marginal Arctic Ocean indicate the first seasonal sea ice around 4.0 Ma

(Knies et al., 2014a). *Thus, whether sea ice occurred in the Early Pliocene Iceland Sea when an early EGC was established has so far not been assessed using direct sea ice proxies.*

Mid Pliocene

Probably the best investigated time interval in the Pliocene is the mid Piacenzian Warm Period (mPWP, 3.264–3.025 Ma). This interval has been the focus of both the Pliocene Research, Interpretation and Synoptic Mapping project (PRISM; Dowsett et al., 2010) and the Pliocene Model Intercomparison Project (PlioMIP; Haywood et al., 2013). Generally, the mPWP is characterized by higher CO_2 levels, reduced continental ice sheets, and higher sea levels (refs in Haywood et al., 2016a). The global atmospheric CO_2 concentrations were lower than in the Early Pliocene, but still higher or possibly in the same range as the pre-industrial values of 280 ppm (*Figure 1.6*). Estimates range between 365–415 ppm (Pagani et al., 2010; Seki et al., 2010) or as low as 270–300 ppm (Badger et al., 2013). The global $\delta^{18}O$ stack indicates a slight trend towards increasing ice volume with increasing variability within the mPWP compared to the Early Pliocene (*Figure 1.6A*). IRD input (as evidence for a larger GIS) is increasing in the western Nordic Seas (Fronval and Jansen, 1996; Jansen et al., 2000) and Labrador Sea (Sarnthein et al., 2009; Wolf and Thiede, 1991). Model studies suggest that glaciations on Greenland were restricted to southeast Greenland (Dolan et al., 2011; Koenig et al., 2015), but indications for small ice sheets were also found on Iceland (Eiríksson and Geirsdóttir, 1991). The rather small continental ice sheets on Greenland and possibly Iceland are in agreement with a higher-than-modern sea level of ~22 ± 10 m (Miller et al., 2012).

The mPWP follows a major glacial event during MIS M2 (~3.3 Ma; Lisiecki and Raymo, 2005). This large MIS M2 glaciation was rather short and is often seen as a failed attempt to start an large Northern Hemisphere glaciation (Haug and Tiedemann, 1998). While the mechanism behind MIS M2 remains enigmatic (Tan et al., 2017), it is clear that a considerable cooling occurred in the North Atlantic (De Schepper et al., 2013; 2009; Lawrence et al., 2009; Naafs et al., 2010). The cooling was indicated by a shift from warm water to cold-water dinoflagellate species and a decrease of SSTs of 3–4 ºC. After this brief glacial, SSTs and warm dinoflagellate species returned to the pre-M2 state (De Schepper et al., 2013; 2009; Lawrence et al., 2009; Naafs et al., 2010). It was shown in a model experiment that potentially larger-than-modern ice sheets during MIS M2 do not contradict the North Atlantic paleoenvironmental proxy data (Dolan et al., 2015). It was proposed that the cooling resulted from a reduced northward heat transport due to a re-opening of the CAS (De Schepper et al., 2013; 2009). However, a recent modeling experiment indicated that the CAS opening only resulted in a small expansion of the Northern Hemisphere ice sheets and could not trigger the MIS M2 glaciation alone (Tan et al., 2017). These authors proposed that besides an open CAS,

low CO_2 levels (220 ppm), and suitable orbital parameters were necessary for the MIS M2 glaciation.

During the mPWP reconstructed global atmospheric temperatures were higher than today (2–3ºC; Dowsett et al., 2010; Salzmann et al., 2011), with the Arctic region reaching temperatures of up to ~8–11 ºC warmer than modern (Brigham-Grette, 2013; Csank et al., 2013). This is in agreement with significantly warmer Nordic Seas and Arctic Ocean SSTs during the mPWP that were up to 5 and 16 ºC higher than today, respectively (Robinson, 2009). Based on these high temperature values, Arctic Pliocene sea ice extent during winter was interpreted to correspond to modern summer minimum conditions (Dowsett et al., 2010), whereas summers were sea ice free. This implies that the marginal Arctic Ocean was seasonally sea ice-free, and consequently, that both the Iceland and Labrador seas were year-round ice-free. Recent studies now indicate that the SSTs in the Nordic Seas were likely only 2–3 ºC higher compared to today (e.g. Bachem et al., 2017; 2016). At the same time, the EGC was already established in the Early Pliocene (De Schepper et al., 2015) and could potentially have exported sea ice from the Arctic. With seasonal sea ice, comparable to modern summer conditions, occurring on the Yermak Plateau around this time (Knies et al., 2014a), an active EGC could have transported or favored sea ice formation in the Iceland and Labrador seas. *Yet, direct evidence for sea ice in the Iceland and Labrador seas during the globally warm climate of the mid Piacenzian is currently lacking*.

Late Pliocene

Following the mPWP, global ice volume gradually increased towards the intensification of the Northern Hemisphere glaciation (iNHG), when the amplitude of the glacial/interglacial cycles increased strongly (*Figure 1.6*; Lisiecki and Raymo, 2005). Continental ice sheets especially expanded in the Northern Hemisphere, where increasing amounts of IRD are detected in marine sediments in the Barents Sea area (Knies et al., 2009; 2014b), the Iceland Sea (Jansen et al., 2000), the Labrador Sea (Sarnthein et al., 2009), the Norwegian Sea (Henrich et al., 1989) and the North Atlantic (Kleiven et al., 2002). Later (~2.64 Ma) also North American ice sheets extended onto the continental shelf consistent with a gradually southward extension of the ice sheets in the Northern Hemisphere during the iNHG (Bailey et al., 2013).

The mechanisms and causes of the iNHG remain an intriguing scientific topic. Several hypotheses were proposed including changes of orbital parameters, ocean gateways, and atmospheric CO_2. Generally, the build-up of ice sheets in the Northern Hemisphere requires sufficient moisture supply and cool enough temperatures so that the accumulated snow does not melt during summer. Around 3.0 Ma, the obliquity cycle (41,000 years) – influencing the distribution of solar insolation – was proposed to have changed from low-amplitude before

3.0 Ma to high-amplitude obliquity. This led to cooler summers, favorable for ice sheet growth (Haug and Tiedemann, 1998). The moisture supply towards the high latitudes was proposed to result from the closure/shoaling of the CAS (Haug and Tiedemann, 1998), which was the most favored theory for the iNHG for a long time. Due to the CAS closure the deep-water formation increased, which enhanced the evaporative cooling and thus directly provided moisture for the ice sheet growth (Haug and Tiedemann, 1998). It was further hypothesized by Driscoll and Haug (1998) that the CAS closure increased the moisture supply towards Eurasia, which in turn increased the freshwater input by Siberian rivers into the Arctic Ocean. The consequently reduced salinity allowed enhanced sea ice formation, increasing the albedo feedback and thereby contributing to cooling and ice growth in the Northern Hemisphere. This theory was questioned by Klocker et al. (2005), who showed in a model study that the CAS closure did not promote ice accumulation. Additionally, Lunt et al. (2008) showed that the increased moisture transport was most likely not enough to trigger the expansion of Northern Hemisphere ice sheets.

Alternatively, the closure of the Indonesian Seaway (*Figure 1.7*) was suggested to cause cooler conditions in North America via teleconnections and thus favoring the growth of large ice sheets (Cane and Molnar, 2001). This hypothesis could not be confirmed in model studies (Brierley and Fedorov, 2016; Jochum, 2009; Krebs et al., 2011). Another explanation is the termination of the 'permanent El Niño' state around 3.0 Ma that ended the heat transport to the north (Brierley and Fedorov, 2010; Wara et al., 2005). While record of proxy data in the equatorial Pacific region suggest El Niño patterns comparable to modern one (Molnar and Cane, 2002), a model study showed that warm conditions in North America (i.e. no ice sheets) also occurred during warm Pliocene conditions without a 'permanent' El Niño state (Haywood and Valdes, 2004).

Finally, the decrease of atmospheric CO_2 (Badger et al., 2013; Bartoli et al., 2011; Martínez-Botí et al., 2015; Pagani et al., 2010; Seki et al., 2010; *Figure 1.6*) was argued to be the most likely candidate for the growth of the Northern Hemisphere ice sheets (e.g. Lunt et al., 2008). The CO_2 decrease could be related to (1) increased stratification in the North Pacific, which increased the biological pump and thus removed CO_2 from the atmosphere (Haug et al., 1999), (2) the uplift of the Rocky Mountains and Himalayan, which removed CO_2 out of the atmosphere due to increased chemical weathering (Raymo et al., 1988; Ruddiman and Kutzbach, 1989), and/or (3) promoted sea ice formation in the Southern Ocean and thus a stronger stratification of the water column (Woodard et al., 2014), which contributed to CO_2 storage in the deep ocean (Lang et al., 2016).

Sarnthein et al. (2009) demonstrated a freshening and cooling of the EGC around 3.0 Ma. They proposed that a cooler and fresher EGC would isolate Greenland from warm Atlantic waters

and poleward heat transport, thereby promoting a persistent glaciation of Greenland. An enhanced EGC could have brought sea ice along with it, but there is no direct evidence for sea ice along the East Greenland Coast. The only sea ice record for the Pliocene comes from the marginal Arctic Ocean indicating that sea ice started to expand to modern winter maximum around 2.75 Ma (Knies et al., 2014a). *The hypothesis that a cool, fresh EGC exporting sea ice and isolating Greenland from warm Atlantic waters (Sarnthein et al., 2009), has not been confirmed by direct evidence for sea ice presence along eastern Greenland during the intensification of the Northern Hemisphere glaciation.*

1.4 Research questions and objectives

There is no doubt about the importance of sea ice for the Arctic and global climate system. Thus, procuring knowledge of its evolution during past warmer time intervals (e.g. Pliocene) is of great significance. The role of sea ice during past warmer than modern time intervals such as the Pliocene is, however, neither well documented nor understood. Both study areas (Iceland and Labrador Sea) provide an ideal location to test the sea ice biomarker IP_{25} (see Chapter 2.1) during warmer climate conditions and in areas outside the marginal Arctic Ocean environment, for which the sea ice proxy was developed. Highly variable (spatial and temporal) modern sea ice coverage characterizes both study areas due to the dynamics between cool and warm water masses. Previous research demonstrated that the Nordic Seas underwent significant changes during the Pliocene and that conditions were far from stable (Bachem et al., 2017; De Schepper et al., 2015; Risebrobakken et al., 2016). The state of the Arctic gateways might have also played a more significant role than previously thought (Otto-Bliesner et al., 2017). Based on the unresolved role of sea ice during the Pliocene, there are three research questions that are addressed:

- *Did sea ice occur in the Early Pliocene Iceland Sea when an early EGC was established?*
- *Could sea ice occur in the Iceland and Labrador seas during the globally warm climate of the warm mid Piacenzian?*
- *Was sea ice present in the Iceland and Labrador seas and what was its role during the intensification of the Northern Hemisphere?*

Therefore, to address the research questions, the specific objectives of this thesis were:

- To determine the presence of (seasonal) sea ice in the Pliocene Iceland and Labrador Seas.
- To identify potential mechanisms controlling the Pliocene sea ice occurrence and the consequences for the Greenland Ice Sheet.

2 Methods

The recent evolution of the Arctic sea ice cover is well recorded by instrumental records (e.g. satellite data), but its development through Earth's history is poorly documented. To obtain information about sea ice evolution further back in time, marine sediment cores as well as ice cores can be investigated. Different proxy approaches can be used to reconstruct paleo sea ice (review in e.g. de Vernal et al., 2013):

- Sedimentary analyses
- Micropaleontological analyses such as assemblages of fossil diatoms, dinoflagellate cysts (dinocysts), foraminifera and/or ostracodes
- Geochemical analyses such as $\delta^{18}O$ in foraminiferal tests, highly branched isoprenoids (HBIs) and/or sea salt in ice cores.

Sedimentary records can provide information on sea ice: lithogenic particles (e.g. iron grains) picked up during sea ice formation have been associated with sea ice transport and were used to reconstruct Arctic sea ice in the Miocene (e.g. Darby, 2014).

The analyses of microfossils (e.g. dinocysts, diatoms, foraminifera) in marine sediment are common techniques in paleoceanography. These fossil groups are a good tool to reconstruct sea ice because some species are directly dependent on sea ice or are feeding on sea ice related prey and can thus be very abundant in sea ice influenced areas. For example, the dinoflagellate species *Polarella glacialis* is known to live in sea ice (e.g. Montresor et al., 1999) and their cysts have recently been reported in the sediment from the seasonally sea ice covered Hudson Bay (Heikkilä et al., 2016). Several species (e.g. *Brigantedinium*) commonly occur in seasonal sea ice environments, but dinocysts are usually not recorded in sediments underneath permanent sea ice. In general, dinocysts have a better preservation in the northern high latitude oceans, where preservation of calcareous organisms and opal-building organisms (diatoms) is problematic (e.g. Armand and Leventer, 2010; Henrich et al., 2002; Stabell and Koç, 1996; Weckström et al., 2013). The calcareous and siliceous fossil record might therefore be biased due to dissolution, leading to inaccuracies in the interpretation using these proxies. When diatoms are well preserved, they are very abundant and can be used for quantitative reconstructions (Weckström et al., 2013) and some species are directly related to sea ice occurrence (Gersonde and Zielinski, 2000). When foraminifera are preserved, they are carriers of geochemical information, e.g. $\delta^{18}O$. Foraminiferal $\delta^{18}O$ can provide information about brine and sea ice formation rates. This method is also not flawless because $\delta^{18}O$ is depending on ocean temperature and salinity as well as metabolic effects of

the foraminifera themselves. Therefore, additional information on the ocean conditions, when the foraminifera calcified, is needed to receive reliable information on paleo sea ice cover (Hillaire-Marcel and de Vernal, 2008). In the Pliocene Iceland and Labrador seas, carbonate dissolution of planktonic foraminifera, low-diversity planktonic foraminifera assemblages (Baumann et al., 1996; Henrich et al., 2002; Jansen et al., 2000), and scarce diatom assemblages (Stabell and Koç, 1996) are known problems that limit sea ice reconstructions.

Over the last decade, the study of organic biomarkers has gained importance in sea ice cover reconstructions (e.g. Belt et al., 2007; Knies et al., 2014a; Kolling et al., 2017; Müller et al., 2011; Stein et al., 2016). Small amounts of organic molecules produced by organisms living in the upper ocean and buried in the sediment, can provide useful information about abiotic conditions at the time of their growth (Thomas et al., 2010). Highly branched isoprenoids (HBI) can give direct information on spring sea ice cover in the Northern Hemisphere (IP_{25} (see below); e.g. Belt et al., 2007; Müller et al., 2009) and potentially in the Southern Hemisphere ($IPSO_{25}$; Belt et al., 2016). In contrast to the HBI-monoene (IP_{25}), the HBI-diene ($IPSO_{25}$) was found in sediments from both, the Arctic and Antarctic Ocean (Belt et al., 2007; Massé et al., 2011). The similar variability and co-occurrence of both IP_{25} and the HBI-diene in Antarctic sediments are thus thought to be produced by sea ice diatoms (Massé et al., 2011). However, the HBI-diene was also found in the Peru upwelling region (Volkman et al., 1983), indicating that this compound might not strictly be depending on sea ice to be synthesized. Although it has been shown that this method is currently probably the most accurate way to reconstruct past sea ice cover, further improvement of this method is needed (see below).

The discovery and development of the biogeochemical sea ice proxy IP_{25} (ice proxy with 25 carbon atoms) a decade ago (Belt et al., 2007), has thus been a big step forward for sea ice reconstructions. Especially by incorporating dinoflagellate cysts, indicating (shifts in) productivity and therefore changing oceanographic conditions, biomarkers (IP_{25} and sterols) are currently the best tools for reconstructing sea ice conditions in the Northern Hemisphere.

2.1 Indicator for sea ice

Past sea ice cover in the Arctic and subarctic Ocean can be reconstructed using the biomarker IP_{25} (Belt et al., 2007). IP_{25} is a highly branched isoprenoid (HBI) monoene (*Figure 2.1*) that is synthesized by specific Arctic sea ice diatoms *(Pleurosigma stuxbergii var. rhomboides, Haslea crucigeroides, H. kjellmanii*, and/or *H. spicula*; Brown et al., 2014). These microalgae occupy the underside of sea ice, where they receive enough nutrient-rich water and light, penetrating through the ice, which favors their growth (Thomas and Dieckmann, 2008). When the ice melts or the diatoms die, their frustules may not be preserved in the sediment, but their

chemical biomarkers are documented in marine sediments. The highest accumulation (90%) of IP_{25} concentrations occurs from mid-March to May in first year sea ice (Brown et al., 2011), indicating a seasonal signal of IP_{25}. Müller et al. (2011) studied sediment surface samples in the western and eastern Nordic Seas and demonstrated that the biomarker reconstructions mirror the modern satellite-derived spring sea ice distribution. Thus, the specific, sensitive and stable biomarker IP_{25} can be used to reconstruct the presence/absence of Arctic spring sea ice.

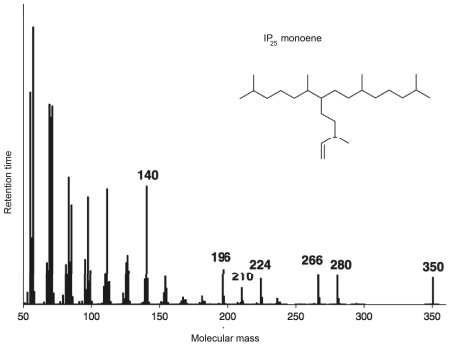

Figure 2.1: *Mass spectrum and chemical structure of the IP_{25} HBI monoene. Modified after Belt et al. (2007).*

A weakness of applying IP_{25} is that it is not possible to distinguish between a permanent sea ice cover and ice-free conditions since IP_{25} is absent in both scenarios (Belt et al., 2007; Müller et al., 2009). Under ice-free conditions, no life habitat is provided for the sea ice diatoms. On the other hand, if the sea ice cover is too thick or snow accumulates on top, light penetration is hampered, preventing sea ice algae growth (*Figure 2.2*). In order to overcome this problem, Müller et al. (2011) combined IP_{25} with marine phytoplankton biomarkers (e.g. brassicasterol and dinosterol, see *Chapter 2.2*), which are absent under severe sea ice conditions. By determining the phytoplankton maker IP_{25} index (PIP_{25} index; Eq. 1, *Figure 2.2.*), the distinction between these two scenarios became possible.

$$PIP_{25} = \frac{IP_{25}}{(IP_{25} + Phytoplankton\ biomarker \cdot c)} \quad (1)$$

$$c = \frac{mean\ IP_{25}\ concentrations}{mean\ phytoplankton\ biomarker\ concentrations} \quad (2).$$

The resulting PIP_{25} index, developed for sea ice margin scenarios, allows semi-quantitative estimation of the sea ice cover (Müller et al., 2011; *Figure 2.2*). In general, this approach works well in areas, which are influenced by multi-year sea ice such as continental margins of East Greenland and West Spitsbergen, where the PIP_{25} index showed a good correlation with satellite-derived spring sea ice data (Müller et al., 2011). The application of this proxy is, however, limited when IP_{25} and the phytoplankton biomarker are in-phase (e.g. coevally low or high; Müller et al., 2011; 2012). Similar observations were made by Weckström et al. (2013), who stress to act with caution, when applying PIP_{25} index under different environmental settings as prevailing in the Arctic Ocean. Especially, because there could be

other factors than sea ice (e.g. nutrients, light availability) that control the phytoplankton productivity. Thus, it was recommended by Müller et al. (2012) to interpret the IP_{25} and phytoplankton record also individually.

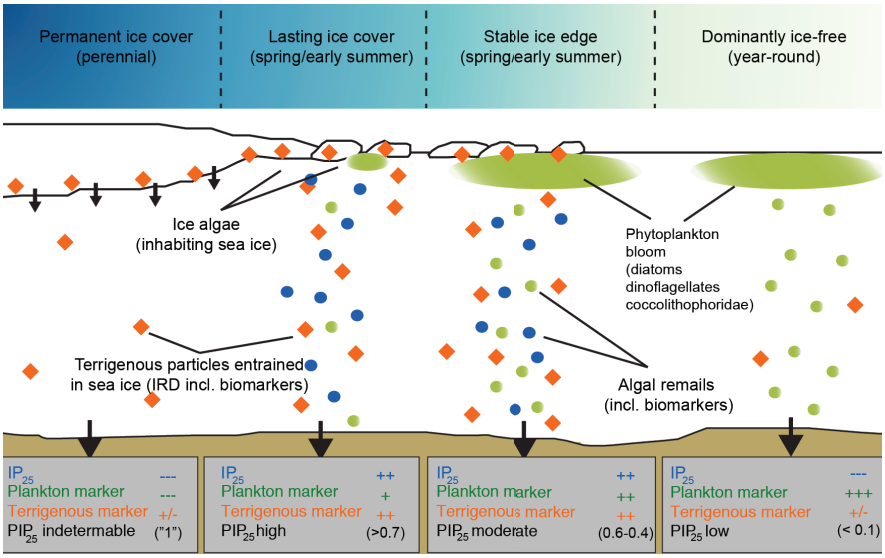

Figure 2.2: *Generalized scheme illustrating spring sea ice and phytoplankton conditions and the respective sedimentary contents of IP_{25}, marine and terrigenous biomarkers (including IRD) as well as the calculated PIP_{25} index. Modified after Stein et al. (2016).*

An additional important, yet problematic factor in Eq. 1 is the balance factor c (Eq. 2). The factor c was introduced to compensate for the higher phytoplankton concentrations compared to IP_{25} concentrations (Müller et al., 2011). The PIP_{25} index is strongly dependent on the balance factor c, which is calculated for each data set specifically. This could result in shifts in the PIP_{25} record, which in turn influences the interpretation of the sea ice conditions (Belt and Müller, 2013). Recently, Smik et al. (2016) presented HBI-triene (a variation of the HBI-monoene IP_{25}) as a potential substitute for brassicasterol when calculating the P_BIP_{25} index (PIP_{25} index with brassicasterol). The authors claim that this approach is less dependent on the balance factor c and may have significant positive outcomes for down-core semi-quantitative sea ice reconstructions.

Even though IP_{25} and PIP_{25} have their limitations, it is currently a solid, reliable and accurate approach to reconstruct the past sea ice cover in the Northern Hemisphere. This was successfully demonstrated in Quaternary sea ice reconstructions in different parts of the Arctic and sub-Arctic Oceans (e.g. Cabedo-Sanz et al., 2013; Hoff et al., 2016; Hörner et al., 2017; Müller et al., 2009) and in the Labrador Sea (Weckström et al., 2013). The proxy was also used to reconstruct the Pliocene sea ice in the Arctic Ocean (Knies et al., 2014a) and recently even for reconstructions of the Miocene sea ice extent in the central Arctic Ocean

(Stein et al., 2016), demonstrating the good stability of the biomarker over long geological times.

2.2 Indicator for organic carbon source

Sterols are valuable biomarkers for assigning the source of organic matter in water and sediments (Rontani et al., 2014) and can be used to identify (paleo-)environmental changes. Sterols are relatively stable over long geological timescales and have structural features (e.g. positions of double bounds), which are restricted to a few groups of organisms (Volkman, 1986). Specific sterols (e.g. brassicasterol and dinosterol; *Figure 2.3*) can often be used as an indicator for marine phytoplankton production (Volkman, 1986; Volkman et al., 1993) and can thus serve as a proxy for open ocean conditions (for a critical review see Belt et al., 2013; Fahl and Stein, 1999; Xiao et al., 2013). These sterols can only be produced by phytoplankton living under ice-free conditions. Their abundance increases close to a sea ice edge (Stein and Stax, 1991) or oceanic fronts (Hirche et al., 1991) due to higher abundance of nutrients favoring phytoplankton growth.

Dinosterol is almost exclusively produced by (marine) dinoflagellates, although it is not found in all dinoflagellate species (Volkman et al., 1993 and refs therein). When comparing dinosterol with dinocyst concentrations, they often do not correlate (Boere et al., 2009; Mouradian et al., 2007; paper II). Why dinosterol and dinoflagellate cysts are not produced or preserved in the same sediment samples remains enigmatic. Several reasons might be considered to explain the findings. It is assumed that dinoflagellates synthesize/contain dinosterol at any stage of their living cycle, whereas dinocysts, which are later found in the sediment, reflect their dormancy phase (Head, 1996; Mouradian et al., 2007). Heterotrophic dinoflagellates have 4–12 times higher dinosterol concentrations compared to autotrophic species, making heterotrophic dinoflagellates a major source of dinosterol in sediments (Amo et al., 2010). Heterotrophic dinoflagellate cysts (e.g. round brown cysts, *Islandinium*) are typically associated with sea ice environments (de Vernal and Rochon, 2011; Marret and Zonneveld, 2003), but are also most prone to degradation (Zonneveld et al., 2001). In contrast, dinosterol is more resistant against degradation and shows a good stability toward diagenetic reworking in sediments. Further, dinosterol is not produced by all species (e.g. *Polarella glacialis*; Boere et al., 2009), the quantities of dinosterol vary among different dinoflagellate species (Volkman, 2003) and not all dinoflagellates produce cysts (Head, 1996).

In contrast to dinosterol, brassicasterol can be synthesized by coccolithophores and diatoms (living in the marine realm), but also by freshwater diatoms and eventually sea ice diatoms (Belt et al., 2013; Fahl and Stein, 2012; Huang and Meinschein, 1976; Volkman, 1986). Thus, its origin is often unclear as it can also reflect fluvial input from land (especially in shelf

areas; Fahl and Stein, 1999). Weckström et al. (2013) also noted that drift ice can positively influence the growth of brassicasterol-synthesizing phytoplankton by surface stratification due to sea ice melt and associated release of nutrients (Dieckmann and Thomas, 2003). This can potentially increase brassicasterol concentrations suggesting reduced sea ice conditions, which might subsequently lead to a misinterpretation of the data (Belt et al., 2013). This stresses that in areas other than the (marginal) Arctic Ocean, other factors (e.g. nutrient) may have a stronger control over productivity than sea ice.

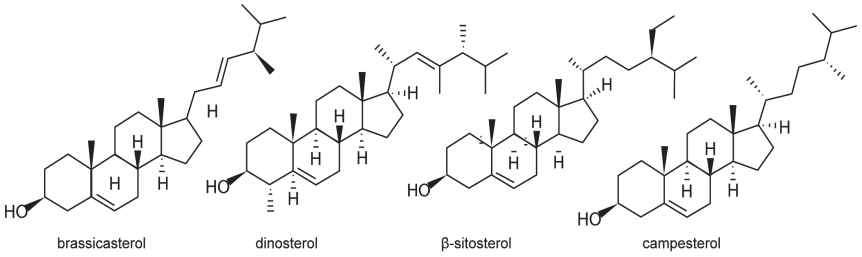

Figure 2.3: *Chemical structures of applied sterols. Source: http://www.chemfaces.com/series/S0204-1.html*

Campesterol and β-sitosterol (*Figure 2.3*) are primarily produced by terrigenous vascular plants (Huang and Meinschein, 1976, 1979; Volkman, 1986; Yunker et al., 1995). Thus, their occurrence in the sediment reflects terrestrial input, although it was shown that marine sea grass might produce these sterols as well (Rontani et al., 2014; Volkman et al., 2008). Nonetheless, β-sitosterol and campesterol have been successfully applied for terrigenous input in the Arctic Ocean (e.g. Fahl and Stein, 1999; Xiao et al., 2013).

2.3 Indicator for sea surface temperature

A widely used approach for reconstructing paleo sea surface temperatures is the U^K_{37} index (e.g. Brassell et al., 1986; Prahl and Wakeham, 1987; Rosell-Melé et al., 2001). The U^K_{37} index is based on long-chain C_{37} alkenones (ketone with 37 carbon atoms) synthesized by haptophyte algae (coccolithophores) living in 0–10 m water depths (mixed layer; e.g. Brassell et al., 1986; Prahl and Wakeham, 1987). The U^K_{37} index reflects the ratio of these C_{37} alkenones, characterized by different numbers of double bonds, i.e. di-($C_{37:2}$), tri-($C_{37:3}$), and tetra-($C_{37:4}$) methyl unsaturated ketones (*Figure 2.4*) that correlates with SST (Brassell et al., 1986):

$$U^K_{37} = \frac{C_{37:2} - C_{37:4}}{C_{37:2} + C_{37:3} + C_{37:4}} \quad (3).$$

The original index was modified to $U_{37}^{K\prime}$ (Prahl and Wakeham, 1987), which only considers the di- and tri-unsaturated ketones. I used this calibration for my studies, since no $C_{37:4}$ alkenones were detected in the sediments of the Iceland and Labrador seas:

$$U_{37}^{K\prime} = \frac{C_{37:2}}{C_{37:2}+C_{37:3}} \quad (4).$$

Different calibrations, derived from experiments and field studies, translate the $U_{37}^{K\prime}$ index into SSTs (e.g. Conte et al., 2006; Müller et al., 1998; Prahl and Wakeham, 1987; Sicre et al., 2002). The $U_{37}^{K\prime}$ index was converted to SST according to the World Ocean surface sediment vs. measured mean annual temperature calibration of Müller et al. (1998):

$$U_{37}^{K\prime} = 0.033\mathrm{T} + 0.044 \quad (5).$$

The error for the calculated SST values is ± 1.0 ºC for the entire temperature range (0–27 ºC; Müller et al., 1998). This calibration was developed from sediment surface samples between 60 ºN and 60 ºS, because $U_{37}^{K\prime}$ core-top measurements seemed to be biased by ice rafting in the Greenland and Norwegian Sea (Müller et al., 1998) implying that the $U_{37}^{K\prime}$ is more scattered in the lower temperature range (<10 ºC) than for the mean, i.e. the error might be higher. Müller et al. (1998) consider their calibration as an annual mean SST, although the correlation to summer SSTs is equally significant (r^2 = 0.981 and r^2 = 0.980, respectively). For polar and sub-polar regions, interpreting the results as summer SSTs is more accurate since alkenone production there is limited to the summer months due to low solar insolation in winter (e.g. Andruleit, 1997). Hence, our SST reconstructions for the Iceland and Labrador seas rather suggest summer SSTs, which has also been shown in previous studies in the Norwegian Sea and North Atlantic (Bachem et al., 2016; Filippova et al., 2016; Lawrence et al., 2009). When reconstructing paleo SSTs based on alkenones, lateral advection and resuspension of this molecular components has to be considered (Conte et al., 2006; Ohkouchi et al., 2002). Further, the Greenland Ice Sheet may erode older (e.g. Cretaceous, Paleogene) sediments, including its fossil content and biomarkers, which can be transported by icebergs into the Nordic Seas and North Atlantic. Inclusion of such reworked alkenones in Pliocene samples thus has the potential to shift the signal towards higher temperatures (Filippova et al., 2016).

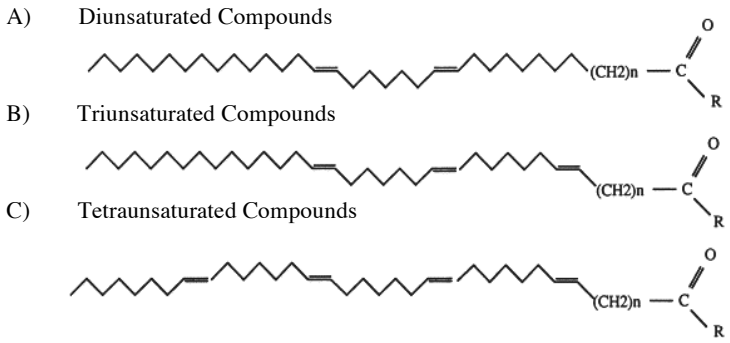

Figure 2.4: *Chemical structures of di-, tri-, and tetra-unsaturated C_{37} alkenones. Taken from Conte et al. (1998).*

The cosmopolitan species *Emiliani huxleyi* is thought to be the main producer of alkenones in Quaternary sediments. In pre-Quaternary sediments, alkenones are endorsed to coccolithophores of the family *Gephyrocapsaceae*. Pliocene SST records (e.g. Lawrence et al., 2009; Naafs et al., 2010) have shown that these species can also be used for $U_{37}^{K\prime}$ without showing substantial differences to *E. huxleyi* (Schreck et al., 2013 and refs therein). The application of $U_{37}^{K\prime}$ SST proxy necessitates that the relative abundance of the $C_{37:2}$ and $C_{37:3}$ alkenones are unchanged during deposition and diagenesis (Lawrence et al., 2007). Despite the fact that several studies have shown a high degradation of C_{37} alkenones, the $U_{37}^{K\prime}$ index remains constant during diagenesis (Lawrence et al., 2007 and refs therein).

All lab work was performed at the Alfred Wegener Institute, Bremerhaven (Germany). Details of the sample preparation and analysis are described in Fahl and Stein (2012) and paper II.

3 Summary of papers

Paper I: *On the Causes of Sea Ice in the Early Pliocene Iceland Sea*

In paper I, we investigate the earliest occurrence of sea ice in the Early Pliocene Iceland Sea (ODP Site 907) based on biomarker (IP_{25}, sterols, alkenones) and palynological data for the time interval between 5.0 to 3.0 Ma. Firstly, our results show that sea ice appeared first in the Iceland Sea around 4.5 Ma together with a decrease in dinoflagellate concentration and a major change in the Nordic Seas surface ocean conditions (De Schepper et al., 2015). Cooling of the summer SSTs only occurred 200 ka after the first evidence for sea ice appeared. The sea surface changes were most likely linked to cooler water masses exiting the Arctic Ocean and replacing the warm Atlantic water masses on the western side of the Nordic Seas. The development of a proto EGC (De Schepper et al., 2015) may have favored the formation of sea ice in the Iceland Sea or exported sea ice directly from the Arctic Ocean.
Secondly, at ~4.0 Ma an extended interval of seasonal sea ice occurred in the Iceland Sea and in the Fram Strait. This widespread development of sea ice may have occurred as a consequence of cooling in the Iceland Sea (Herbert et al., 2016) and contemporaneous warming the North Atlantic (Lawrence et al., 2009) and the Norwegian Sea (Bachem et al., 2017), which essentially developed a strong zonal temperature gradient in the Nordic Seas around 4.0 Ma (Bachem et al., 2017). Increased northward heat transport into the eastern Nordic Seas may have increased the moisture transport towards Siberia. Ultimately, this led to a freshening of the Arctic Ocean, which favored sea ice formation. The resulting outflow of fresher water and possibly sea ice from the Arctic likely contributed to an increased sea ice formation/occurrence in the Iceland Sea.

Paper II: *Seasonal sea ice cover during the warm Pliocene: evidence from the Iceland Sea (ODP Site 907)*

In paper II, sea ice and summer SSTs in the Iceland Sea (ODP Site 907) for the time interval between 3.50 and 2.40 Ma were reconstructed using organic biomarkers (IP_{25}, sterols, alkenones), with additional palynological data. We show that between 3.50–3.00 Ma, including the mid Piacenzian Warm Period (3.26–3.03 Ma; Dowsett et al., 2010), seasonal sea ice with occasionally ice-free intervals existed in the Iceland Sea. Summers were ice free as

indicated by our alkenone-based summer SSTs, which are similar to modern values. The EGC may have transported sea ice into the Iceland Sea and/or brought cooler and fresher waters favoring local sea ice formation. After 3.00 Ma, sea ice occurred less frequently in the Iceland Sea. Nevertheless, a longer period with seasonal sea ice extending to the study site between 2.81 and 2.74 Ma may have acted as a positive feedback for the build-up of the Greenland Ice Sheet (GIS) around 2.75 Ma. Primary productivity increased slightly as evidenced by our biomarkers, and appears to reveal glacial/interglacial variability from 2.75 Ma onwards. We interpreted those productivity variations in the Iceland Sea to reflect shifts of a sea ice edge along the East Greenland margin.

Paper III: *Sea Ice Expansion in the Labrador Sea prior to the Intensification of the Northern Hemisphere Glaciation*

Paper III focuses on the EGC and its links to the GIS and the subpolar gyre (SPG) prior to and during the intensification of the Northern Hemisphere Glaciation (iNHG). We analyzed biomarkers (IP_{25}, sterols, alkenones) from the Labrador Sea (IODP Site U1307) between 3.56 and 2.28 Ma. Our sea ice and SST reconstructions indicate dominantly ice-free conditions between 3.56 and 3.10 Ma, resulting from a weak EGC and thus enhanced advection of Atlantic waters into the Labrador Sea. This might have been related to a generally strong/expanded SPG transporting warm Atlantic water via the Irminger Current into the Labrador Sea, blocking the southward flow of the EGC. The GIS was generally reduced during this period, but expanded during marine isotope stage M2 (~3.3 Ma; Dolan et al., 2015; Koenig et al., 2015). Interestingly, between 3.32 and 3.18 Ma, a stable ice edge occurred in the Labrador Sea possibly due to stronger EGC influence and a reduction of Atlantic water influence.

After ~3.10 Ma, polar water influence increased as indicated by a freshening and the development of a stable sea ice edge in the Labrador Sea, suggesting an enhanced southward flow of the EGC. Enhanced EGC influence together with less Atlantic water influence suggests a weakened SPG circulation. Sea ice in the Labrador Sea, a weak SPG and a stronger EGC likely increased the isolation of Greenland from warm Atlantic water masses as well as sea ice albedo feedbacks, which both favored the expansion of the GIS and thus ultimately may have played a role in the iNHG around 2.7 Ma.

4 Synthesis and outlook

My research on the evolution of the sea ice extent and the East Greenland Current in the Iceland and Labrador seas contributes significantly to the knowledge of the Pliocene (sub-) Arctic climate and paleoceanography. Using the sea ice proxy IP_{25}, I demonstrated for the first time that sea ice occurred in the Iceland and Labrador seas during the globally warm Pliocene. The multi-proxy approach of biomarkers (IP_{25}, sterols, alkenones) and palynology allowed addressing the research questions.

Did sea ice occur in the Early Pliocene Iceland Sea when an early EGC was established?

Following a previous cooling trend from 11 to 8 ºC between 4.9 and 4.5 Ma in the Iceland Sea (Herbert et al., 2016), I showed that sea ice first occurred in the Iceland Sea during the Early Pliocene (~4.5 Ma, paper I). This was most likely related to significant circulation changes in the Nordic Seas, related to the onset of an early EGC (De Schepper et al., 2015). Sea ice occurrence itself was not accompanied by direct cooling. The trend towards permanently cooler and fresher conditions took place approximately 100 ka later, when the sea surface conditions in the Norwegian Sea cooled as well. This indicates enhanced EGC influence in the entire Nordic Seas, which could have favored also sea ice presence in the Iceland Sea. Summer sea surface temperatures (SSTs) between 4.9 and 4.0 Ma were 2–5 ºC higher than modern values of 5 ºC (Locarnini et al., 2013), suggesting either a seasonal sea ice cover or drift sea ice transported over a short distance from the North into the Iceland Sea. At 4.0 Ma, seasonal sea ice developed in the Iceland Sea (paper I) and was accompanied by the absence of dinocysts (De Schepper et al., 2015; Schreck et al., 2013) and a decrease in the SSTs from ~8 to 2 ºC (Herbert et al., 2016), which is well below the modern summer SSTs. Contemporaneously, SSTs in both the North Atlantic (Lawrence et al., 2009) and the Norwegian Sea (Bachem et al., 2017) increased strongly, which likely increased moisture transport to the North (Bachem et al., 2017; Driscoll and Haug, 1998). This may have also increased the moisture supply to Siberia, followed by increased river runoff towards the north to ultimately freshen the Arctic Ocean and facilitate sea ice formation. This is in agreement with a sea ice record from the marginally Arctic Ocean Yermak Plateau, which indicates the first sea ice occurrence at ~3.9 Ma (Knies et al., 2014a). The resulting outflow from the Arctic might then have contributed to increased sea ice formation/occurrence in the Iceland Sea.

Can sea ice occur in the Iceland and Labrador Seas during the globally warm climate of the warm mid Pliocene?

Sea ice continued to occur in the Iceland Sea between 3.5 and 3.0 Ma including the warm mid Pliocene (paper II), but was mainly absent in the Labrador Sea (paper III). This might have been related to warm water advection from the North Atlantic into the Labrador Sea via the Irminger Current, which blocked the southward flow of the EGC. As a result, cooler, fresher polar waters including sea ice could not be transported beyond the Iceland Sea. Summer SSTs in both the Iceland and Labrador Sea were respectively 2–3 ºC and 3–4 ºC on average higher during the Pliocene than compared to modern. This suggests that increased warm Atlantic water influence might have been related to a stronger subpolar gyre (SPG) transporting more warm Atlantic water via the Irminger Current into the Labrador Sea.
This state was interrupted by a major glacial event during MIS M2, when sea ice evidence was recorded in the Labrador Sea. We interpret this as increased transport of cool polar water via the EGC, which directly transported sea ice southward or created favorable conditions for the development of a stable sea ice edge. This coincides with a SST cooling of up to 3–4 ºC in the eastern North Atlantic (De Schepper et al., 2013; 2009; Lawrence et al., 2009). The reduced northward heat flow via the NAD system likely influenced the Labrador Sea and might have co-occurred with a weakened/contracted SPG. As such, the cool water EGC likely effectively isolated Greenland from the relatively warmer Atlantic water masses, which is favorable for ice sheet expansion on Greenland (Sarnthein et al., 2009).

Was sea ice present in the Iceland and Labrador seas and what was its role during the intensification of the Northern Hemisphere?

Between ~3.0 and ~2.4 Ma, sea ice only existed occasionally in the Iceland Sea while a sea ice edge developed along eastern Greenland (paper II), and occurred frequently in the Labrador Sea (paper III). This could be related to an increased southward flow of the EGC favoring sea ice occurrence in the Labrador Sea, while the reduced EGC influence allowed only for occasional sea ice occurrence in the Iceland Sea. A stronger EGC reaching the Labrador Sea, would have isolated Greenland from warmer Atlantic water masses (see also Sarnthein et al., 2009). In addition, the development of a stable sea ice edge along the coast of eastern Greenland could have increased sea ice albedo feedbacks. Both would have likely favored the ice sheet growth as evidenced by the increased ice-rafted debris deposition in the Iceland and Labrador seas (Jansen et al., 2000; St. John and Krissek, 2002; Wolf and Thiede, 1991). Sea ice increased especially between 3.10 and 2.75 Ma in the Labrador Sea, well

before the intensification of the Northern Hemisphere glaciation (~2.75 Ma; Mudelsee and Raymo, 2005) and might thus have significantly contributed to the Greenland Ice Sheet (GIS) expansion.

After the GIS expansion around 2.75 Ma, a strong variability on possibly glacial/interglacial timescales was observed in the SST and sterols in the Iceland Sea (paper II) that may be related to the development of a nearby sea ice edge along the East Greenland coast. Occasionally, a sea ice edge also developed in the Labrador Sea after 2.70 Ma. The development of a sea ice edge could be related to a pronounced cooling in the North Atlantic (Lawrence et al., 2009) and a southward shift of the Arctic Front (Naafs et al., 2010) that would have hampered Atlantic water from entering the Iceland Sea.

Outlook

It was shown previously that IP_{25} and sterols could be used to reconstruct Pliocene sea ice (Knies et al., 2014a). By applying the same biomarker approach and combining the record with alkenone and palynology data on Pliocene sediments from the Iceland and Labrador seas, I could demonstrate that these proxies are vital and useful tools to assess the paleo sea ice cover, where other proxies (e.g. foraminifera) cannot be used. This knowledge promotes further paleo sea ice studies in other Arctic areas, where Pliocene sediments can be found (e.g. Baffin Bay, Kara Sea, and Bering Strait). The recently discovered HBI-diene ($IPSO_{25}$; Belt et al., 2016) for sea ice and HBI-triene (Smik et al., 2016) as a substitute for brassicasterol might be tested here as well or even in the Pliocene Southern Ocean. Using these proxies in older sediments, their stability and applicability on older geological records can be tested.

As briefly discussed in Chapter 2.1, the PIP_{25} index allows semi-quantitative estimation of the sea ice cover. When applying the PIP_{25} approach to our data from the Iceland Sea (*Figure 4.1A; paper II*) and the Labrador Sea (*Figure 4.1B; paper III*), often a permanent sea ice cover is reconstructed. However, a permanent sea ice cover is unlikely since in both regions alkenone SSTs could (almost) always be measured throughout the entire studied interval. Reconstructed SSTs are often above, but also drop below the modern values. Nevertheless, even the cooler than modern SSTs imply that the alkenone producing organisms, i.e. calcareous nannofossils, were present during at least part of the year (most likely summer). As a consequence, the frequent occurrence of permanent sea ice cover as reconstructed by the PIP_{25} index is thus very unrealistic. In a few samples of the Iceland Sea ODP Site 907, alkenone SSTs could not be determined (*Figure 4.1A* opened and filled circles; see also paper II), suggesting that at those occasions, a permanent sea ice cannot be excluded. However, during these times, the PIP_{25} index suggests ice-free conditions. The PIP_{25} index

was developed for the Arctic region, where a permanent sea ice cover occurs today. It has been shown in a study from the southwest Labrador Sea that the PIP_{25} results differed from observed (historic/satellite) sea ice data (Weckström et al., 2013). Therefore, the index may not work in the Iceland and Labrador seas, where other factors (e.g. nutrients) may have more influence the occurrence of brassicasterol and dinosterol synthesizing organisms than sea ice. Additionally, the temporal resolution in our samples may be also problematic because (1) one sample already integrates 1,000 years, in which sea ice cover is variable and (2) the resolution for the studies between samples is ~7,000 years. Thus, further detailed, high-resolution investigations are needed to confirm the possibility of short-lived year-round sea ice cover.

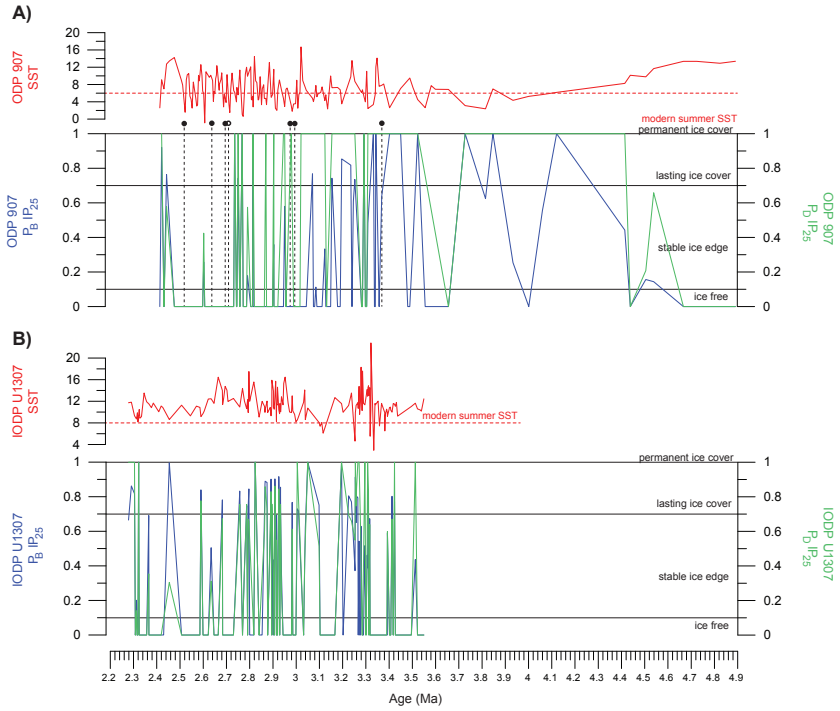

Fig. 4.1: *Calculated PIP_{25} index with brassicasterol (blue line) and dinosterol (green line) and reconstructed SST in °C of A) ODP Site 907 and B) IODP Site U1307. The results often indicate "permanent" sea ice conditions, which seems unrealistic considering warmer as today SSTs and the modern oceanographic situation.*

Although I demonstrated the presence of sea ice in both study areas, it remains unclear if the sea ice was formed locally or if it was transported. This knowledge may help to better understand the role of the EGC and whether sea ice could be formed locally in the Iceland Sea, which was the case for instance in the 1970s during the Great Salinity Anomaly (GSA; Bersch et al., 2007). During this event high amounts of freshwater were derived into the Labrador Sea, reducing the winter convection and thus the production of deep-water masses

(e.g. Belkin, 2004). The resulting change in the atmospheric pressure system caused an advance of the polar front into the Iceland Sea and led to local sea ice formation (Ólafsson, 1999). To identify whether sea ice was locally formed or transported, sedimentological data (e.g. Andrews et al., 2016; Cabedo-Sanz et al., 2016) is needed preferably on the same samples as the biomarker reconstruction to shed light on the local/regional development of the sea ice.

Understanding the history of key elements in the climate system (e.g. EGC, SPG circulation, and sea ice development close to the east Greenland coast), helps to gain a more detailed picture of the regional Pliocene paleoceanography and paleoclimatology. The development of the EGC has been investigated between 5.0 and 2.4 Ma in the Iceland Sea (paper I and II) and between 3.6 and 2.3 Ma (paper III). While it was shown in paper I that the first sea ice in the Pliocene Iceland Sea occurred most likely with the onset of the EGC ~4.5 Ma, it remains unclear if the EGC penetrated into the Labrador Sea. The accumulation of sea ice related diatoms in the Labrador Sea indicates surface cooling (Bohrmann et al., 1990), but direct evidence for sea ice is missing. Unfortunately, the record of IODP Site U1307 does not contain sediments older than ~3.6 Ma, whereas the sedimentological record of the neighboring ODP Site 646 dates back until the Late Miocene (Shipboard Scientific Party, 1986). Sedimentological and palynological data (de Vernal and Mudie, 1989; Korstgard and Nielsen, 1989; Wolf and Thiede, 1991) indicate the potential of this site to elucidate the Labrador Sea's paleoceanography. Extending IP_{25} studies into the Early Pliocene will therefore provide additional information on the evolution of sea ice in the Labrador Sea and the role of the EGC.

As proposed in paper III, the subpolar gyre (SPG) might have played a role in the Pliocene climate transition. Investigating the SPG during changing climates might help to understand how important and sensitive the SPG was/is to Arctic fresher water and sea ice input via the EGC. Therefore, areas influenced by all surface currents (EGC, WGC, LC, NAD) that form the SPG should be studied to see, which triggers have the potential to influence the gyre circulation. Surface water conditions can be reconstructed using temperature/salinity proxies (e.g. foraminifera and/or coccolithophores) or fossil assemblages (e.g. dinoflagellates). Especially the focus on the position and shifts of the frontal zones (i.e. Arctic Front) would be very relevant to understand the SPG evolution. For understanding future climate changes, studies on decadal/centennial timescales are crucial. On the other hand, long-term, high-resolution studies in warm time intervals (e.g. Pliocene) can give insights in the underlying links between the SPG circulation and GIS evolution.

After 2.75 Ma, sterols and SSTs in the Iceland Sea were probably changing on glacial/interglacial timescales related to a sea ice edge close to Greenland (paper II). A sea ice

edge likely also influenced the sterols in the Labrador Sea (paper III) as they were fluctuating in agreement with IP_{25}. To get better insights into potential glacial/interglacial variability in the marine productivity, an associated sea ice margin and SSTs, high-resolution records should be procured. The detection of glacial/interglacial variability in records that are not a direct proxy for continental ice might help to provide new insights into ice sheet expansion, maybe also in combination with benthic $\delta^{18}O$ records. This could be tested in the late Pliocene/early Pleistocene transitions, when glacials became more pronounced. A supposedly promising site may be ODP Site 987 close to the eastern Greenland coast and directly underlying the EGC. I started to analyze samples of the Pliocene section (5.00–2.54 Ma) in low resolution. My preliminary biomarker analysis (not included in this thesis) indicates year-round ice-free conditions as suggested by the absence of IP_{25} and high concentrations of brassicasterol and dinosterol as well as average summer SSTs of 12.5 ºC. Preliminary analysis of the dinocyst assemblage shows high amounts of reworked material that is most likely derived from pre-Neogene sediment on Greenland. This might indicate dilution by allochthonous material brought to the study site by the EGC or more likely from Greenland. ODP Site 987 is located off the Scoresby Sund, which was suggested to be the major drainage pathway of the eastern GIS (Solgaard et al., 2011). However, the site is also known to be affected by slide deposits during the Pleistocene related to the waning and waxing of the GIS (Laberg et al., 2013) and might therefore not be an ideal site to Pliocene study sea ice evolution.

Finally, the results of my studies provide an improvement to define the boundary conditions for model experiments. Using this new sea ice reconstructions, it can now be more accurately tested in model experiments how the Greenland Ice Sheet behaves, when sea ice is present in the Iceland and Labrador seas under relatively high CO_2 conditions (Early to mid Pliocene). Furthermore, the effect of closing and opening gateways in the Early Pliocene (CAS and Bering Strait, respectively) on the EGC, Arctic sea ice cover, and Greenland temperature and mass balance can be better simulated.

The new results of the studies presented here shed light on the state of the Pliocene sea ice cover in the subarctic seas and demonstrated that seas ice was present during this warm climate period. The encouraging findings illustrate that further studies are needed to better understand changes in key climate components and regions.

5 References

Aagaard, K., and Coachman, L. K., 1968a, The East Greenland Current North of Denmark Strait: Part I Arctic, v. 21, no. 3, p. 181-200. doi. jstor.org/stable/40507537

-, 1968b, The East Greenland Current North of Denmark Strait: Part II: Arctic, v. 21, no. 4, p. 267-290. doi. jstor.org/stable/40507576

Allison, I., Bindoff, N. L., Bindschadler, R. A., Cox, P. M., de Noblet, N., England, M. H., Francis, J. E., Gruber, N., Haywood, A. M., Karoly, D. J., Kaser, G., Le Quéré, C., Lenton, T. M., Mann, M. E., McNeil, B. I., Pitman, A. J., Rahmstorf, S., Rignot, E., Schellnhuber, H. J., Schneider, S. H., Sherwood, S. C., Somerville, R. C. J., Steffen, K., Steig, E. J., Visbeck, M., and Weaver, A. J., 2009, The Copenhagen Diagnosis, 2009: Updating the World on the Latest Climate Science., Sydney, Australia, The University of New South Wales Climate Change Research Centre (CCRC), 1-62 p.:

Amo, M., Suzuki, N., Kawamura, H., Yamaguchi, A., Takano, Y., and Horiguchi, T., 2010, Sterol composition of dinoflagellates: Different abundance and composition in heterotrophic species and resting cysts: Geochemical Journal, v. 44, p. 225-231. doi. 10.2343/geochemj.1.0063

Andrews, J. T., Stein, R., Moros, M., and Perner, K., 2016, Late Quaternary changes in sediment composition on the NE Greenland margin (~73° N) with a focus on the fjords and shelf: Boreas, v. 45, no. 3, p. 381-397. doi. 10.1111/bor.12169

Andruleit, H., 1997, Coccolithophore fluxes in the Norwegian-Greenland Sea: seasonality and assemblage alterations: Marine Micropaleontology, v. 31, p. 45-64. doi. 10.1016/S0377-8398(96)00055-2

Armand, L. K., and Leventer, A., 2010, Palaeo Sea ice Distribution and Reconstruction Derived from the Geological Record, *in* Thomas, D. N., and Dieckmann, G. S., eds., Sea Ice, Blackwell Publishing Ltd, p. 469-530.

Arrigo, K. R., Mock, T., and Lizotte, M. P., 2010, Primary Producers and Sea Ice *in* Dieckmann, G., and Thomas, D. N., eds., Sea Ice, Blackwell Publishing Ltd, p. 283-325.

Bachem, P. E., Risebrobakken, B., De Schepper, S., and McClymont, E. L., 2017, Highly variable Pliocene sea surface conditions in the Norwegian Sea: Climate of the Past, p. 1-25. doi. 10.5194/cp-2016-131

Bachem, P. E., Risebrobakken, B., and McClymont, E. L., 2016, Sea surface temperature variability in the Norwegian Sea during the late Pliocene linked to subpolar gyre strength and radiative forcing: Earth and Planetary Science Letters, v. 446, p. 113-122. doi. 10.1016/j.epsl.2016.04.024

Badger, M. P., Schmidt, D. N., Mackensen, A., and Pancost, R. D., 2013, High-resolution alkenone palaeobarometry indicates relatively stable pCO(2) during the Pliocene (3.3-2.8 Ma): Philos Trans A Math Phys Eng Sci, v. 371, no. 2001, p. 2-16. doi. 10.1098/rsta.2013.0094

Bailey, I., Hole, G. M., Foster, G. L., Wilson, P. A., Storey, C. D., Trueman, C. N., and Raymo, M. E., 2013, An alternative suggestion for the Pliocene onset of major northern hemisphere glaciation based on the geochemical provenance of North Atlantic Ocean ice-rafted debris: Quaternary Science Reviews, v. 75, p. 181-194. doi. 10.1016/j.quascirev.2013.06.004

Ballantyne, A. P., Axford, Y., Miller, G. H., Otto-Bliesner, B. L., Rosenbloom, N., and White, J. W. C., 2013, The amplification of Arctic terrestrial surface temperatures by reduced sea-ice extent during the Pliocene: Palaeogeography, Palaeoclimatology, Palaeoecology, v. 386, p. 59-67. doi. 10.1016/j.palaeo.2013.05.002

Bartoli, G., Hönisch, B., and Zeebe, R. E., 2011, Atmospheric CO2decline during the Pliocene intensification of Northern Hemisphere glaciations: Paleoceanography, v. 26, no. 4, p. PA4213. doi. 10.1029/2010pa002055

Baumann, K.-H., Meggers, H., and Henrich, R., 1996, Variations in Surface Water Mass Conditions in the Norwegian-Greenland Sea: Evidence from Pliocene/Pleistocene Calcareous Plankton Records (Sites 644,907, 909): Proceedings of the Ocean Drilling Program, Scientific Results, v. 151, p. 493-514. doi. 10.2973/odp.proc.sr.151.138.1996

Belkin, I. M., 2004, Propagation of the "Great Salinity Anomaly" of the 1990s around the northern North Atlantic.: Geophysical Research Letters, v. 31, no. 8, p. L08306. doi. 10.1029/2003GL019334

Bell, D. B., Jung, S. J., Kroon, D., Hodell, D. A., Lourens, L. J., and Raymo, M. E., 2015, Atlantic deep-water response to the Early Pliocene shoaling of the Central American seaway.: Scientific reports, v. 5, p. 5:12252, 12251-12212. doi. 10.1038/srep12252

Belt, S. T., Brown, T. A., Ringrose, A. E., Cabedo-Sanz, P., Mundy, C. J., Gosselin, M., and Poulin, M., 2013, Quantitative measurement of the sea ice diatom biomarker IP25 and sterols in Arctic sea ice and underlying sediments: Further considerations for palaeo sea ice reconstruction: Organic Geochemistry, v. 62, p. 33-45. doi. 10.1016/j.orggeochem.2013.07.002

Belt, S. T., Massé, G., Rowland, S. J., Poulin, M., Michel, C., and LeBlanc, B., 2007, A novel chemical fossil of palaeo sea ice: IP25: Organic Geochemistry, v. 38, no. 1, p. 16-27. doi. 10.1016/j.orggeochem.2006.09.013

Belt, S. T., and Müller, J., 2013, The Arctic sea ice biomarker IP25: a review of current understanding, recommendations for future research and applications in palaeo sea ice reconstructions: Quaternary Science Reviews, v. 79, p. 9-25. doi. 10.1016/j.quascirev.2012.12.001

Belt, S. T., Smik, L., Brown, T. A., Kim, J. H., Rowland, S. J., Allen, C. S., Gal, J.-K., Shin, K.-H., Lee, J. I., and Taylor, K. W. R., 2016, Source identification and distribution reveals the potential of the geochemical Antarctic sea ice proxy IPSO25. : Nature Communications, v. 7, p. 7:12655, 12651-12610. doi. 10.1038/ncomms12655

Bersch, M., Yashayaev, I., and Koltermann, K. P., 2007, Recent changes of the thermohaline circulation in the subpolar North Atlantic.: Ocean Dynamics, v. 57, p. 223-235. doi. 10.1007/s10236-007-0104-7

Blindheim, J., and Østerhus, S., 2005, The Nordic Seas: Main Oceanographic Features, *in* Drange, H., Dokken, T., Furevik, T., Gerdes, R., and Berger, W., eds., The Nordic Seas: An Integrated Perspective, p. 11-37.

Boere, A. C., Abbas, B., Rijpstra, W. I., Versteegh, G. J., Volkman, J. K., Sinninghe Damste, J. S., and Coolen, M. J., 2009, Late-Holocene succession of dinoflagellates in an Antarctic fjord using a multi-proxy approach: paleoenvironmental genomics, lipid biomarkers and palynomorphs: Geobiology, v. 7, no. 3, p. 265-281. doi. 10.1111/j.1472-4669.2009.00202.x

Bohrmann, G., Henrich, R., and Thiede, J., 1990, Miocene to Quaternary Palaeoceanography in the Northern North Atlantic: Variability of Carbonate and Biogenic Opal Accumulation, *in* Thiede, U. B. a. J., ed., Geological History of the Polar Oceans: Arctic Versus Antarctic, Kluwer Academic Publishers, p. 647-675.

Brassell, S. C., Eglinton, G., Marlowe, I. T., Pflaumann, U., and Sarnthein, M., 1986, Molecular stratigraphy: a new tool for climatic assessment: Nature, v. 320, p. 129-133. doi. 10.1038/320129a0

Brierley, C. M., and Fedorov, A. V., 2010, Relative importance of meridional and zonal sea surface temperature gradients for the onset of the ice ages and Pliocene-Pleistocene climate evolution: Paleoceanography, v. 25, no. 2, p. PA2214. doi. 10.1029/2009pa001809

Brierley, C. M., and Fedorov, A. V., 2016, Comparing the impacts of Miocene–Pliocene changes in inter-ocean gateways on climate: Central American Seaway, Bering Strait, and Indonesia: Earth and Planetary Science Letters, v. 444, p. 116-130. doi. 10.1016/j.epsl.2016.03.010

Brierley, C. M., Fedorov, A. V., Liu, Z., Herbert, T. D., Lawrence, K. T., and LaRiviere, J. P., 2009, Greatly expanded tropical warm pool and weakened Hadley circulation in the early Pliocene: Science, v. 323, no. 5922, p. 1714-1718. doi. 10.1126/science.1167625

Brigham-Grette, J. M., Martin; Minyuk, Pavel; Andrei Andreev, Pavel Tarasov, DeConto, Roberto; Koenig, Sebastian; Nowaczyk, Norbert; Wennrich, Volker; Rosén, Peter; Haltia, Eeva; Cook, Tim; Gebhardt, Catalina; Meyer-Jacob, Carsten; Snyder, Jeff; Herzschuh, Ulrike, 2013, Pliocene Warmth, Polar Amplification, and Stepped Pleistocene Cooling recorded in NE Arctic Russia: Science, v. 340, p. 1421-1427. doi. 10.1126/science.1233137

Brown, T. A., Belt, S. T., Philippe, B., Mundy, C. J., Massé, G., Poulin, M., and Gosselin, M., 2011, Temporal and vertical variations of lipid biomarkers during a bottom ice diatom bloom in the Canadian Beaufort Sea: further evidence for the use of the IP25 biomarker as a proxy for spring Arctic sea ice: Polar Biology, v. 34, no. 12, p. 1857-1868. doi. 10.1007/s00300-010-0942-5

Brown, T. A., Belt, S. T., Tatarek, A., and Mundy, C. J., 2014, Source identification of the Arctic sea ice proxy IP25: Nat Commun, v. 5, p. 4197. doi. 10.1038/ncomms5197

Cabedo-Sanz, P., Belt, S. T., Jennings, A. E., Andrews, J. T., and Geirsdóttir, Á., 2016, Variability in drift ice export from the Arctic Ocean to the North Icelandic Shelf over the last 8000 years: A multi-proxy evaluation: Quaternary Science Reviews, v. 146, p. 99-115. doi. 10.1016/j.quascirev.2016.06.012

Cabedo-Sanz, P., Belt, S. T., Knies, J., and Husum, K., 2013, Identification of contrasting seasonal sea ice conditions during the Younger Dryas: Quaternary Science Reviews, v. 79, p. 74-86. doi. 10.1016/j.quascirev.2012.10.028

Cane, M. A., and Molnar, P., 2001, Closing of the Indonesian seaway as a precursor to east African aridification around 3–4 million years ago: Nature, v. 411, p. 157-162. doi. 10.1038/35075500

Castradori, D., Rio, D., Hilgen, F. J., and Lourens, L. J., 1998, The global standard stratotype-section and point (GSSP) of the Piacenzian Stage (Middle Pliocene). Episodes, v. 21, p. 88-93. doi. n/a

Clarke, R. A., and Gascard, J. C., 1983, The formation of Labrador Sea water. Part I: Large-scale processes: Journal of Physical Oceanography, v. 13, no. 10, p. 1764-1778. doi. 10.1175/1520-0485(1983)013<1764:TFOLSW>2.0.CO;2

Conte, M. H., Sicre, M.-A., Rühlemann, C., Weber, J. C., Schulte, S., Schulz-Bull, D., and Blanz, T., 2006, Global temperature calibration of the alkenone unsaturation index (UK'_{37}) in surface waters and comparison with surface sediments: Geochemistry, Geophysics, Geosystems, v. 7, no. 2, p. Q02005, 02001-02022. doi. 10.1029/2005gc001054

Conte, M. H., Thompson, A., Lesley, D., and Harris, R. P., 1998, Genetic and Physiological Influences on the Alkenone/Alkenoate Versus Growth Temperature Relationship in Emiliania huxleyi and Gephyrocapsa Oceanica: Geochimica et Cosmochimica Acta, v. 62, no. 1, p. 51-68. doi. 10.1016/S0016-7037(97)00327-X

Csank, A. Z., Fortier, D., and Leavitt, S. W., 2013, Annually resolved temperature reconstructions from a late Pliocene–early Pleistocene polar forest on Bylot Island, Canada.: Palaeogeography, Palaeoclimatology, Palaeoecology, v. 369, p. 313-322. doi. 10.1016/j.palaeo.2012.10.040

Darby, D. A., 2008, Arctic perennial ice cover over the last 14 million years: Paleoceanography, v. 23, no. 1, p. PA1S07. doi. 10.1029/2007pa001479

Darby, D. A., 2014, Ephemeral formation of perennial sea ice in the Arctic Ocean during the middle Eocene: Nature Geoscience, v. 7, no. 3, p. 210-213. doi. DOI: 10.1038/NGEO2068

De Schepper, S., Groeneveld, J., Naafs, B. D., Van Renterghem, C., Hennissen, J., Head, M. J., Louwye, S., and Fabian, K., 2013, Northern hemisphere glaciation during the globally warm early Late Pliocene: PLoS One, v. 8, no. 12, p. e81508. doi. 10.1371/journal.pone.0081508

De Schepper, S., Head, M. J., and Groeneveld, J., 2009, North Atlantic Current variability through marine isotope stage M2 (circa 3.3 Ma) during the mid-Pliocene: Paleoceanography, v. 24, no. 4, p. PA4206. doi. 10.1029/2008pa001725

De Schepper, S., Schreck, M., Beck, K. M., Matthiessen, J., Fahl, K., and Mangerud, G., 2015, Early Pliocene onset of modern Nordic Seas circulation related to ocean gateway changes: Nat Commun, v. 6, p. 8659. doi. 10.1038/ncomms9659

de Vernal, A., Gersonde, R., Goosse, H., Seidenkrantz, M.-S., and Wolff, E. W., 2013, Sea ice in the paleoclimate system: the challenge of reconstructing sea ice from proxies – an introduction: Quaternary Science Reviews, v. 79, p. 1-8. doi. 10.1016/j.quascirev.2013.08.009

de Vernal, A., and Mudie, P. J., 1989, Pliocene and Pleistocene palynostratigraphy at ODP Sites 646 and 647, eastern and southern Labrador Sea: Proceedings of the Ocean Drilling Program, Scientific Results, v. 105, p. 401–422. doi. doi:10.2973/odp.proc.sr.105.134.1989

de Vernal, A., and Rochon, A., 2011, Dinocysts as tracers of sea-surface conditions and sea-ice cover in polar and subpolar environments: IOP Conference Series: Earth and Environmental Science, v. 14, p. 012007; 012001-012022. doi. 10.1088/1755-1315/14/1/012007

Dickson, R., Rudels, B., Dye, S., Karcher, M., Meincke, J., and Yashayaev, I., 2007, Current estimates of freshwater flux through Arctic and subarctic seas: Progress in Oceanography, v. 73, no. 3, p. 210-230. doi. 10.1016/j.pocean.2006.12.003

Dickson, R. R., and Brown, J., 1994, The production of North Atlantic Deep Water: Sources, rates, and pathways: Journal of Geophysical Research, v. 99, no. C6, p. 12,319-341. doi. 10.1029/94jc00530

Dieckmann, G. S., and Hellmer, H. H., 2010, The Importance of Sea Ice: An Overview, *in* Thomas, D. N., and Dieckmann, G. S., eds., Sea ice, Blackwell Publishing Ltd, p. 1-22.

Dieckmann, G. S., and Thomas, D. N., 2003, Sea ice : an introduction to its physics, chemistry, biology and geology, *in* Thomas, D. N., and Dieckmann, G. S., eds., Sea ice, Blackwell Sciences, p. 1-400.

Dolan, A. M., Haywood, A. M., Hill, D. J., Dowsett, H. J., Hunter, S. J., Lunt, D. J., and Pickering, S. J., 2011, Sensitivity of Pliocene ice sheets to orbital forcing: Palaeogeography, Palaeoclimatology, Palaeoecology, v. 309, no. 1-2, p. 98-110. doi. 10.1016/j.palaeo.2011.03.030

Dolan, A. M., Haywood, A. M., Hunter, S. J., Tindall, J. C., Dowsett, H. J., Hill, D. J., and Pickering, S. J., 2015, Modelling the enigmatic Late Pliocene Glacial Event — Marine Isotope Stage M2: Global and Planetary Change, v. 128, p. 47-60. doi. 10.1016/j.gloplacha.2015.02.001

Dowsett, H. J., 2007, The PRISM palaeoclimate reconstruction and Pliocene sea-surface temperature, *in* Williams, M., Haywood, A. M., Gregory, F. J., and Schmidt, D. N., eds., Deep-Time Perspectives on Climate Change, The Micropalaeontological Society Special Publications, p. 459-480.

Dowsett, H. J., Chandler, M. A., Cronin, T. M., and Dwyer, G. S., 2005, Middle Pliocene sea surface temperature variability.: Palaeogeography, v. 20, no. 2, p. PA2014. doi. 10.1029/2005PA001133

Dowsett, H. J., Dolan, A. M., Rowley, D., Moucha, R., Forte, A. M., Mitrovica, J. X., Pound, M. J., Salzmann, U., Robinson, M. M., Chandler, M. A., Foley, K., and Haywood, A. M., 2016, The PRISM4 (mid-Piacenzian) paleoenvironmental reconstruction: Climate of the Past, v. 12, p. 1519-1538. doi. 10.5194/cp-12-1519-2016

Dowsett, H. J., Robinson, M. M., Haywood, A. M., Salzmann, U., Hill, D. J., Sohl, L., Chandler, M. A., Williams, M., Foley, K., and Stoll, D., 2010, The PRISM3D paleoenvironmental reconstruction: Stratigraphy, v. 7, p. 123–139. doi. pubs.er.usgs.gov/publication/70044350

Draut, A. E., Raymo, M. E., McManus, J. F., and Oppo, D. W., 2003, Climate stability during the Pliocene warm period.: Palaeogeography, v. 18, no. 4, p. 1078. doi. 10.1029/2003PA000889

Driscoll, N. W., and Haug, G. H., 1998, A Short Circuit in Thermohaline Circulation: A Cause for Northern Hemisphere Glaciation?: Science, v. 282, p. 436-438. doi. 10.1126/science.282.5388.436

Durham, J. W., and MacNeil, F. S., 1967, Cenozoic migrations of marine invertebrates through the Bering Strait region, *in* Hopkins, D. M., ed., The Bering Land Bridge: Stanford, CA, Stanford University Press, p. 326-349.

Eiríksson, J., and Geirsdóttir, Á., 1991, A record of Pliocene and Pleistocene glaciations and climatic changes in the North Atlantic based on variations in volcanic and sedimentary facies in Iceland: Marine Geology, v. 101, p. 147-159. doi. 10.1016/0025-3227(91)90068-F

Evans, H. F., Channell, J. E. T., Stoner, J. S., Hillaire-Marcel, C., Wright, J. D., Neitzke, L. C., and Mountain, G. S., 2007, Paleointensity-assisted chronostratigraphy of detrital layers on the Eirik Drift (North Atlantic) since marine isotope stage 11: Geochemistry, Geophysics, Geosystems, v. 8, no. 11, p. GC001720. doi. 10.1029/2007gc001720

Fahl, K., and Stein, R., 1999, Biomarkers as organic-carbon-source and environmental indicators in the Late Quaternary Arctic Ocean-problems and perspectives: Marine Chemistry, v. 63, p. 293–309. doi. 10.1016/S0304-4203(98)00068-1

Fahl, K., and Stein, R., 2012, Modern seasonal variability and deglacial/Holocene change of central Arctic Ocean sea-ice cover: New insights from biomarker proxy records: Earth and Planetary Science Letters, v. 351-352, p. 123-133. doi. 10.1016/j.epsl.2012.07.009

Fedorov, A. V., Brierley, C. M., Lawrence, K. T., Liu, Z., Dekens, P. S., and Ravelo, A. C., 2013, Patterns and mechanisms of early Pliocene warmth: Nature, v. 496, no. 7443, p. 43-49. doi. 10.1038/nature12003

Filippova, A., Kienast, M., Frank, M., and Schneider, R. R., 2016, Alkenone paleothermometry in the North Atlantic: A review and synthesis of surface sediment data and calibrations: Geochemistry, Geophysics, Geosystems, v. 17, no. 4, p. 1370-1382. doi. 10.1002/2015gc006106

Fratantoni, P. S., and Pickart, R. S., 2007, The Western North Atlantic Shelfbreak Current System in Summer: Journal of Physical Oceanography, v. 37, no. 10, p. 2509-2533. doi. 10.1175/jpo3123.1

Fronval, T., and Jansen, E., 1996, Late Neogene Paleoclimates and Paleoceanography in the Iceland-Norwegian Sea: Evidence from the Iceland and Vøring Plateaus: Proceedings of the Ocean Drilling Program, Scientific Results, v. 151, p. 455-468. doi. 10.2973/odp.proc.sr.151.134.1996

Gersonde, R., and Zielinski, U., 2000, The reconstruction of the late Quaternary sea-ice distribution e the use of diatoms as a proxy for sea-ice.: Palaeogeography, Palaeoclimatology, Palaeoecology, v. 162, p. 263-286. doi. 10.1016/S0031-0182(00)00131-0

Gibbard, P. L., Head, M. J., and Walker, M. J., 2010, Formal ratification of the Quaternary System/Period and the Pleistocene Series/Epoch with a base at 2.58 Ma.: Journal of Quaternary Science, v. 25, no. 2, p. 96-102. doi. 10.1002/jqs.1338

Gosselin, M., Levasseur, M., Wheeler, P. A., Horner, R. A., and Booth, B. C., 1997, New measurements of phytoplankton and ice algal production in the Arctic Ocean: Deep Sea Research Part II: Topical Studies in Oceanography, v. 44, no. 8, p. 1623-1644. doi. 10.1016/S0967-0645(97)00054-4

Gradinger, R., 2009, Sea-ice algae: Major contributors to primary production and algal biomass in the Chukchi and Beaufort Seas during May/June 2002: Deep Sea Research Part II: Topical Studies in Oceanography, v. 56, no. 17, p. 1201-1212. doi. 10.1016/j.dsr2.2008.10.016

Gradinger, R., and Ikävalko, J., 1998, Organism incorporation into newly forming Arctic sea ice in the Greenland Sea: Journal of Plankton Research, v. 20, no. 5, p. 871-886. doi. 10.1093/plankt/20.5.871

Haley, B. A., Frank, M., Spielhagen, R. F., and Eisenhauer, A., 2008a, Influence of brine formation on Arctic Ocean circulation over the past 15 million years: Nature Geoscience, v. 1, no. 1, p. 68-72. doi. 10.1038/ngeo.2007.5

Haley, B. A., Frank, M., Spielhagen, R. F., and Fietzke, J., 2008b, Radiogenic isotope record of Arctic Ocean circulation and weathering inputs of the past 15 million years: Paleoceanography, v. 23, no. 1, p. PA1S13. doi. 10.1029/2007pa001486

Hátún, H., Sando, A. B., Drange, H., Hansen, B., and Valdimarsson, H., 2005, Influence of the Atlantic subpolar gyre on the thermohaline circulation: Science, v. 309, no. 5742, p. 1841-1844. doi. 10.1126/science.1114777

Haug, G. H., Sigman, D. M., Tiedemann, R., Pedersen, T. F., and Sarnthein, M., 1999, Onset of permanent stratification in the subarctic Pacific Ocean: Nature, v. 401, no. 6755, p. 779-782. doi. 10.1038/44550

Haug, G. H., and Tiedemann, R., 1998, Effect of the formation of the Isthmus of Panama on Atlantic Ocean thermohaline circulation: Nature, v. 393, p. 673-676. doi. 10.1038/31447

Haug, G. H., Tiedemann, R., Zahn, R., and Ravelo, A. C., 2001, Role of Panama uplift on oceanic freshwater balance.: Geology, v. 29, no. 3, p. 207-210. doi. 10.1130/0091-7613(2001)029<0207:ROPUOO>2.0.CO;2

Haywood, A. M., Dowsett, H. J., and Dolan, A. M., 2016a, Integrating geological archives and climate models for the mid-Pliocene warm period: Nat Commun, v. 7, p. 10646. doi. 10.1038/ncomms10646

Haywood, A. M., Dowsett, H. J., Dolan, A. M., Rowley, D., Abe-Ouchi, A., Otto-Bliesner, B., Chandler, M. A., Hunter, S. J., Lunt, D. J., Pound, M., and Salzmann, U., 2016b, The Pliocene Model Intercomparison Project (PlioMIP) Phase 2: scientific objectives and experimental design: Climate of the Past, v. 12, no. 3, p. 663-675. doi. 10.5194/cp-12-663-2016

Haywood, A. M., Hill, D. J., Dolan, A. M., Otto-Bliesner, B. L., Bragg, F., Chan, W. L., Chandler, M. A., Contoux, C., Dowsett, H. J., Jost, A., Kamae, Y., Lohmann, G., Lunt, D. J., Abe-Ouchi, A., Pickering, S. J., Ramstein, G., Rosenbloom, N. A., Salzmann, U., Sohl, L., Stepanek, C., Ueda, H., Yan, Q., and Zhang, Z., 2013, Large-scale features of Pliocene climate: results from the Pliocene Model Intercomparison Project: Climate of the Past, v. 9, no. 1, p. 191-209. doi. 10.5194/cp-9-191-2013

Haywood, A. M., Ridgwell, A., Lunt, D. J., Hill, D. J., Pound, M. J., Dowsett, H. J., Dolan, A. M., Francis, J. E., and Williams, M., 2011, Are there pre-Quaternary geological analogues for a future greenhouse warming?: Philos Trans A Math Phys Eng Sci, v. 369, no. 1938, p. 933-956. doi. 10.1098/rsta.2010.0317

Haywood, A. M., and Valdes, P. J., 2004, Modelling Pliocene warmth: contribution of atmosphere, oceans and cryosphere: Earth and Planetary Science Letters, v. 218, no. 3-4, p. 363-377. doi. 10.1016/s0012-821x(03)00685-x

Head, M. J., 1996, Modern dinoflagellate cysts and their biological affinities, *in* J., J., and C., M. D., eds., Palynology: Principles and Applications Salt Lake City, UT, American Association of Stratigraphic Palynologists Foundation,, p. 1197–1248.

Heikkilä, M., Pospelova, V., Forest, A., Stern, G. A., Fortier, L., and Macdonald, R. W., 2016, Dinoflagellate cyst production over an annual cycle in seasonally ice-covered Hudson Bay.: Marine Micropaleontology,, v. 125, p. 1-24. doi. 10.1016/j.marmicro.2016.02.005

Henrich, R., Baumann, K.-H., Huber, R., and Meggers, H., 2002, Carbonate preservation records of the past 3 Myr in the Norwegian-Greenland Sea and the northern North Atlantic: implications for the history of NADW production: Marine Geology, v. 184, p. 17-39. doi. 10.1016/S0025-3227(01)00279-1

Henrich, R., Wolf, T., Bohrmann, G., and Thiede, J., 1989, Cenozoic Paleoclimatic and Paleoceanographic Changes in the Northern Hemisphere revealed by Variability of coarse-fraction Composition in Sediments from the Vøring Plateau - ODP Leg 104 Drill Sites: Proceedings of the Ocean Drilling Program, Scientific Results, v. 104, p. 75-188. doi. 10.2973/odp.proc.sr.104.196.1989

Herbert, T. D., Lawrence, K. T., Tzanova, A., Peterson, L. C., Caballero-Gill, R., and Kelly, C. S., 2016, Late Miocene global cooling and the rise of modern ecosystems: Nature Geoscience, p. 1-5. doi. 10.1038/ngeo2813

Hilgen, F. J., Lourens, L. J., Van Dam, J. A., Beu, A. G., Boyes, A. F., Cooper, R. A., Krijgsman, W., Ogg, J. G., Piller, W. E., and Wilson, D. S., 2012, The Neogene Period, p. 923-978. doi. 10.1016/b978-0-444-59425-9.00029-9

Hillaire-Marcel, C., and de Vernal, A., 2008, Stable isotope clue to episodic sea ice formation in the glacial North Atlantic: Earth and Planetary Science Letters, v. 268, no. 1, p. 143-150. doi. 10.1016/j.epsl.2008.01.012

Hirche, H. J., Baumann, M. E. M., Kattner, G., and Gradinger, R., 1991, Plankton distribution and the impact of copepod grazing on primary production in Fram Strait, Greenland Sea: Journal of Marine Systems, v. 2, no. 3-4, p. 477-494. doi. 10.1016/0924-7963(91)90048-Y

Hoff, U., Rasmussen, T. L., Stein, R., Ezat, M. M., and Fahl, K., 2016, Sea ice and millennial-scale climate variability in the Nordic seas 90 kyr ago to present: Nat Commun, p. 7:12247. doi. 10.1038/nprot.2016.089

Hopkins, T. S., 1991, The GIN Sea - A synthesis of its physical oceanography and literature review: Earth-Science Reviews, v. 30, p. 175-318 doi. 10.1016/0012-8252(91)90001-V

Horner, R. A., 1985, Ecology of sea ice microalgae, *in* Horner, R. A., ed., Sea ice biota: CRC Press, Boca Raton, p. 83-103.

Hörner, T., Stein, R., and Fahl, K., 2017, Evidence for Holocene centennial variability in sea ice cover based on IP25 biomarker reconstruction in the southern Kara Sea (Arctic Ocean): Geo-Marine Letters, p. 1-12. doi. 10.1007/s00367-017-0501-y

Huang, W.-Y., and Meinschein, W. G., 1976, Sterols as source indicators of organic materials in sediments: Geochimica and Cosmochimica Acta, v. 40, p. 323-330. doi. 10.1016/0016-7037(76)90210-6

-, 1979, Sterols as ecological indicators: Geochimica and Cosmochimica Acta, v. 43, p. 739-745. doi. 10.1016/0016-7037(79)90257-6

Jansen, E., Fronval, T., Rack, F., and Channell, J. E. T., 2000, Pliocene-Pleistocene ice rafting history and cyclicity in the Nordic Seas during the last 3.5 Myr: Paleoceanography, v. 15, no. 6, p. 709-721. doi. 10.1029/1999pa000435

Jochum, M., Fox-Kemper, B., Molnar, P.H., Shields, C., , 2009, Differences in the Indonesian seaway in a coupled climate model and their relevance to Pliocene climate and El Niño.: Paleoceanography, v. 24, no. 1, p. PA1212. doi. 10.1029/2008PA001678.

Johannessen, O. M., 1986, Brief overview of the physical oceanography, *in* Hurdle, B. G., ed., The Nordic Seas New York, Springer p. 103-128.

Killworth, P. D., 1983, Deep convection in the World Ocean: Reviews of Geophysics, v. 21, no. 1, p. 1-26. doi. 10.1029/RG021i001p00001

Kleiven, H. F., Jansen, E., Fronval, T., and Smith, T. M., 2002, Intensification of Northern Hemisphere glaciations in the circum Atlantic region (3.5–2.4 Ma) - ice-rafted detritus evidence: Palaeogeography, Palaeoclimatology, Palaeoecology, v. 184, p. 213-223. doi. 10.1016/S0031-0182(01)00407-2

Klocker, A., Prange, M., and Schulz, M., 2005, Testing the influence of the Central American Seaway on orbitally forced Northern Hemisphere glaciation.: Geophysical Research Letters, v. 32, no. 3, p. L03703. doi. 10.1029/2004GL021564

Knies, J., Cabedo-Sanz, P., Belt, S. T., Baranwal, S., Fietz, S., and Rosell-Melé, A., 2014a, The emergence of modern sea ice cover in the Arctic Ocean: Nat Commun, v. 5, p. 5:5608. doi. 10.1038/ncomms6608

Knies, J., and Gaina, C., 2008, Middle Miocene ice sheet expansion in the Arctic: Views from the Barents Sea. : Geochemistry, Geophysics, Geosystems, v. 9, no. 2, p. Q02015. doi. 10.1029/2007GC001824

Knies, J., Matthiessen, J., Vogt, C., Laberg, J. S., Hjelstuene, B. O., Smelror, M., Larsen, E., Andreasen, K., Eidvin, T., and Vorren, T. O., 2009, The Plio-Pleistocene glaciation of the Barents Sea–Svalbard region: a new model based on revised chronostratigraphy: Quaternary Science Reviews v. 28, p. 812–829. doi. 10.1016/j.quascirev.20

Knies, J., Mattingsdal, R., Fabian, K., Grøsfjeld, K., Baranwal, S., Husum, K., De Schepper, S., Vogt, C., Andersen, N., Matthiessen, J., Andreassen, K., Jokat, W., Nam, S.-I., and Gaina, C., 2014b, Effect of early Pliocene uplift on late Pliocene cooling in the Arctic–Atlantic gateway: Earth and Planetary Science Letters, v. 387, p. 132-144. doi. 10.1016/j.epsl.2013.11.007

Koenig, S. J., Dolan, A. M., de Boer, B., Stone, E. J., Hill, D. J., DeConto, R. M., Abe-Ouchi, A., Lunt, D. J., Pollard, D., Quiquet, A., Saito, F., Savage, J., and van de Wal, R., 2015, Ice sheet model dependency of the simulated Greenland Ice Sheet in the mid-Pliocene: Climate of the Past, v. 11, no. 3, p. 369-381. doi. 10.5194/cp-11-369-2015

Kolling, H. M., Stein, R., Fahl, K., Perner, K., and Moros, M., 2017, Short-term variability in late Holocene sea ice cover on the East Greenland Shelf and its driving mechanisms: Palaeogeography, Palaeoclimatology, Palaeoecology, p. 1-15. doi. 10.1016/j.palaeo.2017.06.024

Korstgard, J. A., and Nielsen, O. B., 1989, Provenance of Dropstones in Baffin Bay and Labrador Sea, Leg 105: Proceedings of the Ocean Drilling Program, Scientific Results, v. 105, p. 65-69. doi. doi:10.2973/odp.proc.sr.105.200.1989

Krebs, U., Park, W., and Schneider, B., 2011, Pliocene aridification of Australia caused by tectonically induced weakening of the Indonesian throughflow.: Palaeogeography, Palaeoclimatology, Palaeoecology, v. 309, p. 111–117. doi. 10.1016/j.palaeo.2011.06.002.

Kürschner, W. M., van der Burgh, J., Visscher, H., and Dilcher, D. L., 1996, Oak leaves as biosensors of late Neogene and early Pleistocene paleoatmospheric CO2 concentrations.: Marine Micropaleontology, v. 27, no. 1-4, p. 299-312. doi. 10.1016/0377-8398(95)00067-4

Laberg, J. S., Forwick, M., Husum, K., and Nielsen, T., 2013, A re-evaluation of the Pleistocene behavior of the Scoresby Sund sector of the Greenland Ice Sheet: Geology, v. 41, no. 12, p. 1231-1234. doi. 10.1130/g34784.1

Lang, D. C., Bailey, I., Wilson, P. A., Chalk, T. B., Foster, G. L., and Gutjahr, M., 2016, Incursions of southern-sourced water into the deep North Atlantic during late Pliocene glacial intensification: Nature Geoscience, v. 9, p. 375–379. doi. 10.1038/NGEO2688.

Lawrence, K. T., Herbert, T. D., Brown, C. M., Raymo, M. E., and Haywood, A. M., 2009, High-amplitude variations in North Atlantic sea surface temperature during the early Pliocene warm period: Paleoceanography, v. 24, no. 2, p. PA2218. doi. 10.1029/2008pa001669

Lawrence, K. T., Herbert, T. D., Dekens, P. S., and Ravelo, A. C., 2007, The application of the alkenone organic proxy to the study of Plio-Pleistocene climate, *in* Williams, M., Haywood, A. M., Gregory, F. J., and Schmidt, D. N., eds., Deep-Time Perspectives on Climate Change: Marrying the Signal from Computer Models and Biological Proxies: London, The Micropalaeontological Society, Special Publication, p. 539-562.

Lisiecki, L. E., and Raymo, M. E., 2005, A Pliocene-Pleistocene stack of 57 globally distributed benthic δ18O records: Paleoceanography, v. 20, no. 1, p. PA1003. doi. 10.1029/2004pa001071

Liu, J., Chen, Z., Francis, J. E., Song, M., Mote, T., and Hu, Y., 2016, Has Arctic Sea Ice Loss Contributed to Increased Surface Melting of the Greenland Ice Sheet?: Journal of Climate, v. 29, p. 3373-3386. doi. 10.1175/JCLI-D-15-0391.1

Locarnini, R. A., Mishonov, A. V., Antonov, J. I., Boyer, T. P., Garcia, H. E., Baranova, O. K., Zweng, M. M., Paver, C. R., Reagan, J. R., Johnson, D. R., Hamilton, M., and Seidov, D., 2013, World Ocean Atlas 2013, Volume 1: Temperature, *in* Levitus, S., and Mishonov, A. V., eds., NOAA Atlas NESDIS 73, p. 40 pp.

Lunt, D. J., Foster, G. L., Haywood, A. M., and Stone, E. J., 2008, Late Pliocene Greenland glaciation controlled by a decline in atmospheric CO2 levels: Nature, v. 454, no. 7208, p. 1102-1105. doi. 10.1038/nature07223

Maier-Reimer, E., Mikolajewicz, U., and Crowley, T., 1990, Ocean general circulation model sensitivity experiment with an open Central American Isthmus.: Palaeogeography, v. 5, no. 3, p. 349-366. doi. 10.1029/PA005i003p00349

Marincovich, L. J., and Gladenkov, A. Y., 1999, Evidence for an early opening of the Bering Strait: Nature, v. 397, p. 149-151. doi. 10.1038/16446

-, 2001, New evidence for the age of Bering Strait: Quaternary Science Reviews, v. 20, p. 329-335. doi. 10.1016/S0277-3791(00)00113-X

Marret, F., and Zonneveld, K. A. F., 2003, Atlas of modern organic-walled dinoflagellate cyst distribution: Review of Palaeobotany and Palynology, v. 125, no. 1, p. 1-200. doi. 10.1016/S0034-6667(02)00229-4

Martínez-Botí, M. A., Foster, G. L., Chalk, T. B., Rohling, E. J., Sexton, P. F., Lunt, D. J., Pancost, R. D., Badger, M. P. S., and Schmidt, D. N., 2015, Plio-Pleistocene climate sensitivity evaluated using high-resolution CO2 records: Nature, v. 518, no. 7537, p. 49-54. doi. 10.1038/nature14145

Massé, G., Belt, S. T., Crosta, X., Schmidt, S., Snape, I., Thomas, D. N., and Rowland, S. J., 2011, Highly branched isoprenoids as proxies for variable sea ice conditions in the Southern Ocean: Antarctic Science, v. 23, no. 05, p. 487-498. doi. 10.1017/s0954102011000381

Matthiessen, J., Knies, J., Vogt, C., and Stein, R., 2009, Pliocene palaeoceanography of the Arctic Ocean and subarctic seas: Philos Trans A Math Phys Eng Sci, v. 367, no. 1886, p. 21-48. doi. 10.1098/rsta.2008.0203

Miller, K. G., Wright, J. D., Browning, J. V., Kulpecz, A., Kominz, M., Naish, T. R., Cramer, B. S., Rosenthal, Y., Peltier, W. R., and Sosdian, S., 2012, High tide of the warm Pliocene: Implications of global sea level for Antarctic deglaciation: Geology, v. 40, no. 5, p. 407-410. doi. 10.1130/g32869.1

Molnar, P., and Cane, M. A., 2002, El Niño's tropical climate and teleconnections as a blueprint for pre‐Ice Age climates: Paleoceanography, v. 17, no. 2, p. 1021. doi. 10.1029/2001PA000663

Montresor, M., Procaccini, G., and Stoecker, D. K., 1999, Polarella glacialis, gen. nov., sp. nov. (Dinophyceae): Suessiaceae are still alive!. Journal of Phycology, v. 35, no. 1, p. 186-197. doi. 10.1046/j.1529-8817.1999.3510186.x

Mouradian, M., Panetta, R. J., de Vernal, A., and Gélinas, Y., 2007, Dinosterols or dinocysts to estimate dinoflagellate contributions to marine sedimentary organic matter?: Limnol. Oceanogr., v. 52, no. 6, p. 2569-2581. doi. 10.4319/lo.2007.52.6.2569

Mudelsee, M., and Raymo, M. E., 2005, Slow dynamics of the Northern Hemisphere glaciation: Paleoceanography, v. 20, no. 4, p. PA4022. doi. 10.1029/2005pa001153

Müller, J., Massé, G., Stein, R., and Belt, S. T., 2009, Variability of sea-ice conditions in the Fram Strait over the past 30,000 years: Nature Geoscience, v. 2, no. 11, p. 772-776. doi. 10.1038/ngeo665

Müller, J., Wagner, A., Fahl, K., Stein, R., Prange, M., and Lohmann, G., 2011, Towards quantitative sea ice reconstructions in the northern North Atlantic: A combined biomarker and numerical modelling approach: Earth and Planetary Science Letters, v. 306, no. 3-4, p. 137-148. doi. 10.1016/j.epsl.2011.04.011

Müller, J., Werner, K., Stein, R., Fahl, K., Moros, M., and Jansen, E., 2012, Holocene cooling culminates in sea ice oscillations in Fram Strait: Quaternary Science Reviews, v. 47, p. 1-14. doi. 10.1016/j.quascirev.2012.04.024

Müller, P. J., Kirst, G., Ruhland, G., von Storch, I., and Rosell-Melé, A., 1998, Calibration of the alkenone paleotemperature index UK'37 based on core-tops from the 37 eastern South Atlantic and the global ocean (60°N-60°S): Geochimica and Cosmochimica Acta, v. 62, no. 10, p. 1757-1772. doi. 10.1016/S0016-7037(98)00097-0

Naafs, B. D. A., Stein, R., Hefter, J., Khélifi, N., De Schepper, S., and Haug, G. H., 2010, Late Pliocene changes in the North Atlantic Current: Earth and Planetary Science Letters, v. 298, no. 3-4, p. 434-442. doi. 10.1016/j.epsl.2010.08.023

Ohkouchi, N., Eglinton, T. I., Keigwin, L. D., and Hayes, J. M., 2002, Spatial and Temporal Offsets Between Proxy Records in a Sediment Drift: Science, v. 298, p. 1224-1227. doi. 10.1126/science.1075287

Ólafsson, J., 1999, Connections between oceanic conditions off N-Iceland, LakeMyvatn temperature, regional wind direction variability and the North Atlantic Oscillation: Rit Fiskideild, v. 16, p. 41-58. doi. n/a

Otto-Bliesner, B. L., Jahn, A., Feng, R., Brady, E. C., Hu, A., and Löfverström, M., 2017, Amplified North Atlantic warming in the late Pliocene by changes in Arctic gateways: Geophysical Research Letters, v. 44, no. 2, p. 957-964. doi. 10.1002/2016gl071805

Pagani, M., Liu, Z., LaRiviere, J., and Ravelo, A. C., 2010, High Earth-system climate sensitivity determined from Pliocene carbon dioxide concentrations: Nature Geoscience, v. 3, no. 1, p. 27-30. doi. 10.1038/ngeo724

Pickart, R. S., 1992, Space—Time Variability of the Deep Western Boundary Current Oxygen Core: American Meteorological Society, v. 22, p. 1047-1061. doi. 10.1175/1520-0485(1992)022<1047:SVOTDW>2.0.CO;2

Prahl, F. G., and Wakeham, S. G., 1987, Calibration of unsaturationpatterns in long-chain keto compositions for palaeotemperature assesment: Nature, v. 330, p. 367-369. doi. 10.1038/330367a0

Raymo, M. E., Ruddiman, W. F., and Froelich, P. N., 1988, Influence of late Cenozoic mountain building on ocean geochemical cycles: Geology, v. 16, no. 7, p. 649-653. doi. 10.1130/0091-7613(1988)016<0649:IOLCMB>2.3.CO;2

Risebrobakken, B., Andersson, C., De Schepper, S., and McClymont, E. L., 2016, Low-frequency Pliocene climate variability in the eastern Nordic Seas: Palaeogeography, v. 31, p. PA002918. doi. 10.1002/ 2015PA002918.

Robinson, M. M., 2009, New quantitative evidence of extreme warmth in the Pliocene Arctic: Stratigraphy, v. 6, no. 4, p. 265-275. doi. 10.1130/0091-7613(1988)016<0649:IOLCMB>2.3.CO;2

Rontani, J.-F., Charrière, B., Sempéré, R., Doxaran, D., Vaultier, F., Vonk, J. E., and Volkman, J. K., 2014, Degradation of sterols and terrigenous organic matter in waters of the Mackenzie Shelf, Canadian Arctic: Organic Geochemistry, v. 75, p. 61-73. doi. 10.1016/j.orggeochem.2014.06.002

Rosell-Melé, A., Bard, E., Emeis, K.-C., Grimalt, J. O., Müller, P., Schneider, R., Bouloubassi, I., Epstein, B., Fahl, K., Fluegge, A., Freeman, K., Goñi, M., U. Güntner, U., Hartz, D., Hellebust, S., Herbert, T., Ikehara, M., Ishiwatari, R., Kawamura, K., Kenig, F., de Leeuw, J., Lehman, S., Mejanelle, L., Ohkouchi, N., Pancost, R. D., Pelejero, C., Prahl, F., Quinn, J., Rontani, J.-F., Rostek, F., Rullkötter, J., Sachs, J., Blanz, T., Sawada, K., Schulz-Bull, D., Sikes, E., Sonzogni, C., Ternois, Y., Versteegh, G. J. M., Volkman, J. K., and Wakeham, S. G., 2001, Precision of the current methods to measure the alkenone proxy UK37 alkenone abundance in sediments: Results of an interlaboratory comparison study: Geochemistry Geophysics Geosystems, v. 2, p. 2000GC000141. doi. 10.1029/2000GC000141

Ruddiman, W. F., and Kutzbach, J. E., 1989, Forcing of Late Cenozoic Northern Hemisphere climate by plateau uplift in southern Asia and the American West: Journal of Geophysical Research, v. 94, p. 18409–18427. doi. 10.1029/JD094iD15p18409

Rudels, B., Fahrbach, E., Meincke, J., Budéus, G., and Eriksson, P., 2002, The East Greenland Current and its contribution to the Denmark Strait overflow: ICES Journal of Marine Science, v. 59, no. 6, p. 1133-1154. doi. 10.1006/jmsc.2002.1284

Rudels, B., and Quadfasel, D., 1991, Convection and deep water formation in the Arctic Ocean-Greenland Sea System: Journal of Marine Systems, v. 2, p. 435-450. doi. 10.1016/0924-7963(91)90045-V

Salzmann, U., Williams, M., Haywood, A. M., Johnson, A. L. A., Kender, S., and Zalasiewicz, J., 2011, Climate and environment of a Pliocene warm world: Palaeogeography, Palaeoclimatology, Palaeoecology, v. 309, no. 1-2, p. 1-8. doi. 10.1016/j.palaeo.2011.05.044

Sarnthein, M., Bartoli, G., Prange, M., Schmittner, A., Schneider, B., Weinelt, M., Andersen, N., and Garbe-Schönberg, D., 2009, Mid-Pliocene shifts in ocean overturning circulation and the onset of Quaternary-style climates: Climate of the Past, v. 5, p. 269-283. doi. 10.5194/cp-5-269-2009

Schmidt, S., and Send, U., 2007, Origin and Composition of Seasonal Labrador Sea Freshwater: Journal of Physical Oceanography, v. 37, no. 6, p. 1445-1454. doi. 10.1175/jpo3065.1

Schmitz, W. J. J., 1996, On the World Ocean Circulation. Volume I, Some Global Feature/North Atlantic Circulation (Technical Report WHOI-96-03). Woods Hole Oceanographic Institution, Woods Hole, MA., p. 1-143. doi. hdl.handle.net/1912/355

Schneider, B., and Schmittner, A., 2006, Simulating the impact of the Panamanian seaway closure on ocean circulation, marine productivity and nutrient cycling.: Earth and Planetary Science Letters, v. 246, no. 3, p. 367-380. doi. 10.1016/j.epsl.2006.04.028

Schreck, M., Meheust, M., Stein, R., and Matthiessen, J., 2013, Response of marine palynomorphs to Neogene climate cooling in the Iceland Sea (ODP Hole 907A): Marine Micropaleontology, v. 101, p. 49-67. doi. 10.1016/j.marmicro.2013.03.003

Seki, O., Foster, G. L., Schmidt, D. N., Mackensen, A., Kawamura, K., and Pancost, R. D., 2010, Alkenone and boron-based Pliocene pCO2 records: Earth and Planetary Science Letters, v. 292, no. 1-2, p. 201-211. doi. 10.1016/j.epsl.2010.01.037

Serreze, M. C., and Barry, R. G., 2011, Processes and impacts of Arctic amplification: A research synthesis: Global and Planetary Change, v. 77, no. 1-2, p. 85-96. doi. 10.1016/j.gloplacha.2011.03.004

Shackleton, N. J., Hall, M. A., and Pate, D., 1995, Pliocene stable isotope stratigraphy of Site 864., *in* Pisias, N. G., Mayer, L. A., Janecek, T. R., Palmer-Julson, A., and van Andel, T. H., eds., Proceedings of the Ocean Drilling Program, Scientific Results Volume 138: College Station, TX Ocean Drilling Program, p. 337-355.

Shipboard Scientific Party, 1986, Site 646: Proc, Init. Repts. (Pt. A), ODP, 105., p. 419-674. doi. 10.2973/odp.proc.ir.105.105.1987

-, 1996, SITE 907 (Revisited): Proceedings of the Ocean Drilling Program, Initial Reports, v. 162, p. 223-252. doi. doi:10.2973/odp.proc.ir.162.107.1996

Sicre, M. A., Bard, E., Ezat, U., and Rostek, F., 2002, Alkenone distributions in the North Atlantic and Nordic sea surface waters: Geochemistry Geophysics Geosystems, v. 3, no. 2, p. GC000159. doi. 10.1029/2001GC000159

Smik, L., Cabedo-Sanz, P., and Belt, S. T., 2016, Semi-quantitative estimates of paleo Arctic sea ice concentration based on source-specific highly branched isoprenoid alkenes: A further development of the PIP25 index: Organic Geochemistry, v. 92, p. 63-69. doi. 10.1016/j.orggeochem.2015.12.007

Solgaard, A. M., Reeh, N., Japsen, P., and Nielsen, T., 2011, Snapshots of the Greenland Ice Sheet configuration in the Pliocene to early Pleistocene.: Journal of Glaciology, v. 57, p. 871-880. doi. 10.3189/002214311798043816.

St. John, K. E. K., and Krissek, L. A., 2002, The late Miocene to Pleistocene ice-rafting history of southeast Greenland: Boreas, v. 31, p. 28-35. doi. 10.1111/j.1502-3885.2002.tb01053.x

Stabell, B., and Koç, N., 1996, Recent to Middle Miocene Diatom Productivity at Site 907, Iceland Plateau: Proceedings of the Ocean Drilling Program, Scientific Results, p. 483-492. doi. hdl.handle.net/11250/174192

Stap, L. B., de Boer, B., Ziegler, M., Bintanja, R., Lourens, L. J., and van de Wal, R. S. W., 2016, CO2 over the past 5 million years: Continuous simulation and new δ 11B-based proxy data: Earth and Planetary Science Letters, v. 439, p. 1-10. doi. 10.1016/j.epsl.2016.01.022

Stein, R., Fahl, K., Schreck, M., Knorr, G., Niessen, F., Forwick, M., Gebhardt, C., Jensen, L., Kaminski, M., Kopf, A., Matthiessen, J., Jokat, W., and Lohmann, G., 2016, Evidence for ice-free summers in the late Miocene central Arctic Ocean: Nature Communications, v. 7, p. 11148. doi. 10.1038/ncomms11148

Stein, R., and Stax, R., 1991, Late Quaternary Organic Carbon Cycles and Paleoproductivity in the Labrador Sea: Geo-Marine Letters, v. 11, p. 90-95. doi. 10.1007/BF02431035

Steph, S., Tiedemann, R., Prange, M., Groeneveld, J., Nürnberg, D., Reuning, L., Schulz, M., and Haug, G. H., 2006, Changes in Caribbean surface hydrography during the Pliocene shoaling of the Central American Seaway: Paleoceanography, v. 21, no. 4, p. PA4221. doi. 10.1029/2004pa001092

Steph, S., Tiedemann, R., Prange, M., Groeneveld, J., Schulz, M., Timmermann, A., Nürnberg, D., Rühlemann, C., Saukel, C., and Haug, G. H., 2010, Early Pliocene increase in thermohaline overturning: A precondition for the development of the modern equatorial Pacific cold tongue: Paleoceanography, v. 25, no. 2, p. PA2202. doi. 10.1029/2008pa001645

Stroeve, J., Holland, M. M., Meier, W., Scambos, T., and Serreze, M., 2007, Arctic sea ice decline: Faster than forecast: Geophysical Research Letters, v. 34, no. 9, p. L09501. doi. 10.1029/2007gl029703

Tan, N., Ramstein, G., Dumas, C., Contoux, C., Ladant, J.-B., Sepulchre, P., Zhang, Z., and De Schepper, S., 2017, Exploring the MIS M2 glaciation occurring during a warm and high atmospheric CO 2 Pliocene background climate: Earth and Planetary Science Letters, v. 472, p. 266-276. doi. 10.1016/j.epsl.2017.04.050

Thomas, D. N., and Dieckmann, G. S., 2008, Sea ice: an introduction to its physics, chemistry, biology and geology., p. 1-250. doi.

Thomas, D. N., Papadimitriou, S., and Michel, C., 2010, Biogeochemistry of Sea Ice, *in* Dieckmann, G. S., and Thomas, D. N., eds., Sea Ice: Chichester, UK, Wiley-Blackwell, p. 325-467.

Torsvik, T. H., Carlos, D., Mosar, J., Cocks, L. R. M., and Malme, T. N., 2002, Global reconstructions and North Atlantic paleogeography 440 Ma to recent, *in* Eide, E. A., ed., BATLAS—Mid Norway plate reconstruction atlas with global and Atlantic perspectives Trondheim, Norway, Norsk Geologiske Undersøgelser, p. 18–39.

Van Couvering, J. A., Castradori, D., Cita, M. B., Hilgen, F. J., and Rio, D., 2000, The base of the Zanclean Stage and of the Pliocene Series.: Episodes, v. 23, no. 3, p. 179-187. doi. n/a

Vaughan, D. G., Cosimo, J. C., Allison, I., Carrasco, J., Kaser, G., Kwok, R., Mote, P., Murray, T., Paul, F., Ren, J., Rignot, E., Solomina, O., Steffen, K., and Zhang, T., 2013, Observations: Cryosphere., *in* Stocker, T. F., Qin, D., Plattner, G.-K., Tignor, M., Allen, S. K., Boschung, J., Nauels, A., Xia, Y., Bex, V., and Midgley, P. M., eds., Climate Change 2013: The Physical Science Basis. Contribution of Working Group I to the Fifth Assessment Report of the Intergovernmental Panel on Climate Change Cambridge, United Kingdom and New York, NY, USA., Cambridge University Press, p. 317-382.

Verhoeven, K., Louwye, S., Eiríksson, J., and De Schepper, S., 2011, A new age model for the Pliocene–Pleistocene Tjörnes section on Iceland: Its implication for the timing of North Atlantic–Pacific palaeoceanographic pathways: Palaeogeography, Palaeoclimatology, Palaeoecology v. 309, p. 33-52. doi. 10.1016/j.palaeo.2011.04.001

Volkman, J. K., 1986, A review of sterol markers for marine and terrigenous organic matter: Organic Geochemistry, v. 9, no. 2, p. 83-99. doi. 10.1016/0146-6380(86)90089-6

Volkman, J. K., 2003, Sterols in microorganisms: Applied Microbiology and Biotechnology, v. 60, p. 495–506. doi. 10.1007/s00253-002-1172-8

Volkman, J. K., Barrett, S. M., Dunstan, G. A., and Jeffrey, S. W., 1993, Geochemical significance of the occurrence of dinosterol and other 4-methyl sterols in a marine diatom: Organic Geochemistry, v. 20, no. 1, p. 7-15. doi. 10.1016/0146-6380(93)90076-N

Volkman, J. K., Farrington, J. W., Gagosian, R. B., and Wakeham, S. G., 1983, Lipid composition of coastal marine sediments from the Peru upwelling region: Advances in Organic Geochemistry, v. 1981, p. 228-240. doi. n/a

Volkman, J. K., Revill, A. T., Holdsworth, D. G., and Fredericks, D., 2008, Organic matter sources in an enclosed coastal inlet assessed using lipid biomarkers and stable isotopes: Organic Geochemistry, v. 39, no. 6, p. 689-710. doi. 10.1016/j.orggeochem.2008.02.014

Wang, M., and Overland, J. E., 2012, A sea ice free summer Arctic within 30 years: An update from CMIP5 models: Geophysical Research Letters, v. 39, no. 18, p. L18501. doi. 10.1029/2012gl052868

Wara, M. W., Ravelo, A. C., and Delaney, M. L., 2005, Permanent El Nino-like conditions during the Pliocene warm period: Science, v. 309, no. 5735, p. 758-761. doi. 10.1126/science.1112596

Weckström, K., Massé, G., Collins, L. G., Hanhijärvi, S., Bouloubassi, I., Sicre, M.-A., Seidenkrantz, M.-S., Schmidt, S., Andersen, T. J., Andersen, M. L., Hill, B., and Kuijpers, A., 2013, Evaluation of the sea ice proxy IP25 against observational and diatom proxy data in the SW Labrador Sea: Quaternary Science Reviews, v. 79, p. 53-62. doi. 10.1016/j.quascirev.2013.02.012

Wolf, T. C. W., and Thiede, J., 1991, History of terrigenous sedimentation during the past 10 m.y. in the North Atlantic (ODP Legs 104 and 105 and DSDP Leg 81): Marine Geology, v. 10, p. 83-102. doi. 10.1016/0025-3227(91)90064-B

Woodard, S. C., Rosenthal, Y., Miller, K. G., Wright, J. D., Chiu, B. K., and Lawrence, K. T., 2014, Antarctic role in Northern Hemisphere glaciation: Science, v. 346, no. 6211, p. 847-851. doi. 10.1126/science.1255586

Xiao, X., Fahl, K., and Stein, R., 2013, Biomarker distributions in surface sediments from the Kara and Laptev seas (Arctic Ocean): indicators for organic-carbon sources and sea-ice coverage: Quaternary Science Reviews, v. 79, p. 40-52. doi. 10.1016/j.quascirev.2012.11.028

Yunker, M. B., Macdonald, R. W., Veltkamp, D. J., and Cretney, W. J., 1995, Terrestrial and marine biomarkers in a seasonally ice-covered Arctic estuary - integration of multivariate and biomarker approaches: Marine Chemistry, v. 49, p. 1-50. doi. 10.1016/0304-4203(94)00057-K

Zachos, J., Pagani, M., Sloan, L., Thomas, E., and Billups, K., 2001, Trends, Rhythms, and Aberrations in Global Climate 65 Ma to Present: Science, v. 292, p. 686-693. doi. 10.1126/science.1059412, 2001.

Zieba, K. J., Omosanya, K. O., and Knies, J., 2017, A flexural isostasy model for the Pleistocene evolution of the Barents Sea bathymetry: Norwegian Journal of Geology, p. 1-19. doi. 10.17850/njg97-1-01

Zonneveld, K. A. F., Versteegh, G. J. M., and de Lange, G. J., 2001, Palaeoproductivity and post-depositional aerobic organic matter decay reflected by dinoflagellate cyst assemblages of the Eastern Mediterranean S1 sapropel: Marine Geology, v. 172, p. 181-195. doi. 10.1016/S0025-3227(00)00134-1

6.2 Paper II

Seasonal sea ice cover during the warm Pliocene: evidence from the Iceland Sea (ODP Site 907)

Clotten, C., Stein, R., Fahl, K., De Schepper, S. (accepted). Seasonal sea ice cover during the warm Pliocene: Evidence from the Iceland Sea (ODP Site 907), *Earth and Planetary Science Letters*.

Seasonal sea ice cover during the warm Pliocene: Evidence from the Iceland Sea (ODP Site 907)

Caroline Clotten[1*], Ruediger Stein[2,3], Kirsten Fahl[2], Stijn De Schepper[1]

[1] *Uni Research Climate, Bjerknes Centre for Climate Research, Jahnebakken 5, 5007 Bergen, Norway.*

[2] *Alfred Wegener Institute Helmholtz Centre for Polar and Marine Research, Am Alten Hafen 26, 27568 Bremerhaven, Germany.*

[3] *Department of Geosciences (FB5), Klagenfurter Str. 4, University of Bremen, 28359 Bremen, Germany*

[*]*corresponding author: caroline.clotten@uni.no*

Abstract

Sea ice is a critical component in the Arctic and global climate system, yet little is known about its extent and variability during past warm intervals, such as the Pliocene (5.33–2.58 Ma). Here, we present the first multi-proxy (IP_{25}, sterols, alkenones, palynology) sea ice reconstructions for the Late Pliocene Iceland Sea (ODP Site 907). Our interpretation of a seasonal sea ice cover with occasional ice-free intervals between 3.50–3.00 Ma is supported by reconstructed alkenone-based summer sea surface temperatures, which are similar to modern values. As evidenced from brassicasterol and dinosterol, primary productivity was low between 3.50 and 3.00 Ma and the site experienced generally oligotrophic conditions. The EGC (and EIC) may have transported sea ice into the Iceland Sea and/or brought cooler and fresher waters favoring local sea ice formation.

Between 3.00 and 2.40 Ma, the Iceland Sea is mainly sea ice-free, but seasonal sea ice occurred between 2.81 and 2.74 Ma. Sea ice extending into the Iceland Sea at this time may have acted as a positive feedback for the build-up of the GIS, which underwent a major expansion ~2.75 Ma. Thereafter, most likely a stable ice edge developed close to Greenland, possibly shifting with the expansion and retreat of the GIS and affecting the productivity in the Iceland Sea.

Keywords

Pliocene | Sea ice | East Greenland Current | IP_{25} | Sterols | Alkenones

1. Introduction

The modern sea ice cover is rapidly diminishing in the Arctic Ocean and seasonally ice-free conditions are projected for the middle of the 21st century (Wang and Overland, 2012). Satellite data document the Arctic sea ice evolution over the past decades, but its development throughout Earth's history is poorly known, even though sea ice is a very crucial and sensitive component in the climate system. Sea ice influences heat, moisture and gas exchange between ocean and atmosphere, Earth's albedo and primary production (e.g. de Vernal et al., 2013a). Also, brine rejection during sea ice formation affects ocean circulation and deep-ocean ventilation due to production of dense water masses (Aagaard and Carmack, 1989).

To understand sea ice variability in a globally warmer world, it is essential to document sea ice extent, and understand the underlying mechanisms that govern sea ice distribution during past warm climates. The Pliocene (5.33–2.58 Ma) is one period in Earth's history that experienced sustained intervals of global temperatures higher than preindustrial (Dowsett et al., 2013). The Pliocene is also characterized by a gradual transition from the relatively warm climates of the Early Pliocene towards cooler conditions in the Late Pliocene and early Quaternary. The Late Pliocene (3.60–2.58 Ma) had atmospheric CO_2 levels ranging between 250 and 450 ppm, global annual mean temperatures ~3 ºC higher than today, higher sea level, and reduced continental ice sheets (e.g. Dolan et al., 2015; Haywood et al., 2016; Martínez-Botí et al., 2015). Late Pliocene sea surface temperatures (SSTs) in the Norwegian Sea (Ocean Drilling Program (ODP) Site 642; Bachem et al., 2016; Fig. 1) and in the Iceland Sea (Herbert et al., 2016) were generally 2–3 ºC higher than today, but fluctuate between those and present day values. In the Labrador Sea, SSTs were also higher than today, but Sarnthein et al. (2009) identified a freshening and cooling of the East Greenland Current in the Late Pliocene. The emerging high-resolution datasets reveal that the Pliocene climate was dynamical and variable, especially in the Nordic Seas (Bachem et al., 2016; Herbert et al., 2016; Risebrobakken et al., 2016), and not a perfect analogue for a future globally warm climate. Nevertheless, the Late Pliocene remains a key interval to understand the processes and mechanisms contributing to a future globally warmer climate with most likely reduced Arctic sea ice (e.g. Dowsett et al., 2010).

Currently, there is only one study based on direct proxy evidence suggesting that sea ice on the Yermak Plateau developed between 4.00 and 2.50 Ma (Fig. 1; Knies et al., 2014). Other studies reconstructing Pliocene sea ice conditions in the Arctic Ocean (e.g. Darby, 2008) and in the Nordic Seas (e.g. Schreck et al., 2013; Stein and Stax, 1996) are based on indirect evidence such as ice-rafted debris (IRD), faunal assemblages, terrigenous coarse fractions in marine sediments and/or decrease in surface-water productivity. A compilation of the

available indirect evidence by the Pliocene Research, Interpretation and Synoptic Mapping (PRISM) Project has resulted in using seasonally sea ice-free Northern Hemisphere summers and setting winter sea ice equivalent to modern summer cover as the most plausible sea ice extent (e.g. Dowsett, 2007 and refs therein). These indirect reconstructions bear, however, large uncertainties, when identifying the optimal model and forcing combination for the mid-Pliocene sea ice cover (Howell et al., 2016), which is one of the greatest limitations and weaknesses in these model studies. Thus, not only higher temporal resolution and spatial distribution of different proxy records for surface water parameters (such as temperature or salinity) are needed to improve data-model comparisons (Howell et al., 2016; Matthiessen et al., 2009), but also reliable estimates of past sea ice extent.

Given the importance of the Nordic Seas and sea ice within the global climate system, we aim to provide a better understanding about the Late Pliocene sea-surface conditions in the Iceland Sea, by (1) reconstructing the sea ice cover, (2) documenting the paleoproductivity and (3) determining the paleo sea surface temperature. To address these goals, we here present a new, relatively high-resolution (~7–8 ka) time series of biomarkers (IP_{25}, sterols, alkenones) and a lower resolution marine palynomorph record from ODP Site 907 in the Iceland Sea between 3.50 and 2.40 Ma. The time interval we investigate includes (1) the mid-Pliocene (3.26–3.03 Ma), target interval of the PRISM project (Dowsett et al., 2010) and an often used analogue for the projected future climate; and (2) the intensification of the Northern Hemisphere glaciation (here 2.90–2.40 Ma), which marks a transitional period from the relative warm Pliocene climate towards the intense glacial/interglacial cycles of the Quaternary.

2. Oceanography

The Nordic Seas (Iceland Sea, Greenland Sea, Norwegian Sea) is the main link between the Arctic Ocean and the North Atlantic (Fig. 1; Blindheim and Østerhus, 2005). Today, the relatively warm (~10 ºC) and saline (~35 psu) North Atlantic Drift (NAD) enters the Nordic Seas over the Greenland-Scotland Ridge (GSR; Blindheim and Østerhus, 2005) through the Faeroe-Shetland Channel. In the eastern Nordic Seas, the NAD continuous northward along the Norwegian margin in the Norwegian Atlantic Current (NwAC). In the north, the NwAC divides into two branches: a considerable part flows eastwards into the Barents Sea (~1.5 Sv; Ingvaldsen et al., 2004), but the main portion (2.7 Sv; Orvik and Skagseth, 2001) forms the West Spitsbergen Current (WSC), which submerges and flows subsurface into the Arctic Ocean via the eastern Fram Strait (Blindheim and Østerhus, 2005). The WSC is deflected southwestward as the Return Atlantic Current (RAC) where it mixes in the western Fram Strait with cold waters exiting the Arctic Ocean as the intermediate water layer below the

East Greenland Current (EGC; Blindheim and Østerhus, 2005; Rudels et al., 2002). The EGC itself is the dominant surface current in the western Nordic Seas and exports sea ice, cold (<0 ºC), low salinity (30 psu) and nutrient-depleted polar surface waters. Together with arctic Atlantic water as well as deeper water masses, it flows over the Denmark Strait (e.g. Aagaard and Coachman, 1968) back into the North Atlantic (Rudels et al., 2012). A small part of the EGC bifurcates north of Iceland to form the East Icelandic Current (EIC), a water mass restricted to a depth of 0–50 m (Rudels et al., 2002). West of Iceland, warm Atlantic water enters the Nordic Seas as the Irminger Current (IC). Today, saline and warm waters of Atlantic origin (IC, a branch of the NwAC; Fronval and Jansen, 1996) and low salinity, cold polar waters (EGC, EIC) are mixing in the convective gyres of the Greenland and Iceland Sea (Jansen et al., 1996). Where water masses from the Atlantic and polar regime are mixing, they form Arctic waters. The front between the Atlantic and Arctic regime is called Arctic Front (AF). The Polar Front (PF) defines the boundary of polar, less saline and ice-covered waters of the EGC and thus the limit of sea ice extent (Fig. 1; Shipboard Scientific Party, 1996; Swift and Aagaard, 1981).

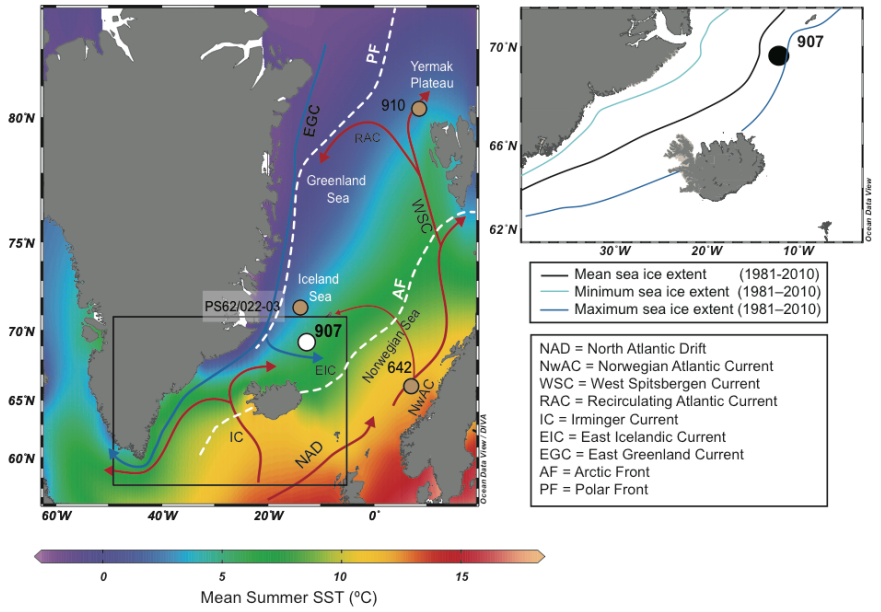

Fig. 1: *Map of the Nordic Seas, with location of ODP Site 907. Other core locations discussed in the text (PS62/022-03, ODP 642, ODP 910) are also indicated. Left map shows modern averaged July-August-September SSTs from 1955–2012 from the World Ocean Atlas 2013 (Locarnini et al., 2013). Major warm (red arrows) and cool (blue arrows) surface currents in the Nordic Sea are shown. Right map shows a close-up of the study area with minimum, mean and maximum sea ice extent between 1981 and 2010 (http://nsidc.org). Maps were generated with Ocean Data View (http://odv.awi.de/).*

The modern ocean surface circulation in the Nordic Seas likely found its origin in the Early Pliocene, when a modern-like zonal gradient developed in the Nordic Seas (Bachem et al., 2017; De Schepper et al., 2015). This occurred even though there were significant differences in the paleogeography of the region: the Barents Sea was sub-aerially exposed (until ~1.5–1 Ma; Butt et al., 2002; Zieba et al., 2017) essentially directing all warm Atlantic water via the Fram Strait into the Arctic Ocean (Hill, 2015 and refs therein). Also, the Canadian Arctic Archipelago (CAA) region was closed (Matthiessen et al., 2009), potentially leading to increased outflow of the Arctic Ocean via the EGC and an increase sea ice formation and sea surface cooling in the Iceland Sea (Otto-Bliesner et al., 2017).

3. Material and methods

3.1. Material

ODP Hole 907A (69°14.989'N, 12°41.894'W, 1800.8 m water depth; Fig. 1) was recovered from the Iceland Plateau with *Joides Resolution* in 1993 during Leg 151. In 1995, the site was revisited and two additional holes were drilled during Leg 162: Hole 907B (69°14.989'N, 12°41.898'W; 1812.8 m water depth) and Hole 907C (69°14.998'N, 12°41.900'W; 1812.4 m water depth) to complete the record.

In total, we analyzed 155 samples between 50.83 and 72.86 mcd from Hole 907A (between core sections 5H7, 8 cm to 8H1, 82 cm), Hole 907B (core sections 8H2, 33 cm to 8H2, 138 cm) and 907C (6H4, 86 cm to 7H5, 33 cm). We followed the splice of Channell et al. (1999) who revised the original spliced record from the Shipboard Scientific Party (1996) to eliminate mismatches in the position of polarity chron boundaries. Meter composite depth (mcd) of our samples was calculated by converting meter below sea floor (mbsf) into mcd separately for each hole and core-section following Channell et al. (1999). Relevant tie points are provided in Table 1.

3.2. Lithology

The investigated interval contains two lithological units (Fig. 2; Shipboard Scientific Party, 1995, 1996). Lithologic Unit II consists of clayey silts and silty clays, and dropstones (Shipboard Scientific Party, 1995). Small dropstones (<1.0 cm) are also found, whereas large dropstones are rare. The terrigenous components are constant throughout Unit II, while biogenic components are absent or rare. Unit IIIA also comprises clayey silts and silty clays with diatoms and has interbedded nannofossil ooze and nannofossil silty clay. A drop in biogenic content and an onset of dropstones can be seen from Unit IIIA to II (Shipboard Scientific Party, 1996).

Table 1: *Relevant tie points of ODP Hole 907A, Hole 907B and Hole 907C for the splice from Channell et al. (1999; Appendix A).*

907A	mbsf	mcd	907B	mbsf	mcd	907C	mbsf	mcd
5H-6, 150	43.3	49.25						
5H-7, 85	44.8	50.75						
6H-1, 150	45.3	51.09						
6H-2, 150	46.8	52.59						
6H-3, 150	48.3	54.09						
6H-4, 150	49.8	55.59				6H-4, 150	48.6	50.21
6H-5, 150	51.3	57.09				6H-5, 150	50.1	51.71
6H-6, 150	52.8	58.59						
6H- 7, 71	54.3	60.09						
7H-1, 150	54.8	61.53						
7H-2, 150	56.3	63.03						
7H-3, 150	57.8	64.53						
7H-4, 150	59.3	66.03				7H-4, 150	58.1	60.15
7H-5, 150	60.8	67.53				7H-5, 150	59.6	61.65
7H-6, 150	62.3	69.03						
7H-7, 64	63.8	70.53						
8H-1, 150	64.3	72.04						
8H-2, 150	65.8	73.54	8H-2, 150	61.2	69.93			
8H-3, 150	67.3	75.04	8H-3, 150	62.7	71.43			

3.3. Chronology

In this study, we use the age model of Jansen et al. (2000). The detailed paleomagnetic record by Channell et al. (1999) provides the elementary age constraints for Site 907 (Fig. 2). Jansen et al. (2000) detected a distinct 41-kyr component in the untuned IRD record, which led them to further improve the age model from Channell et al. (1999) by tuning the IRD record for the period from 3.50 to 1.00 Ma to obliquity. Due to the absence of calcareous microfossils in most of the Pliocene of Site 907, a direct tuning to the LR04 benthic isotope stack (Lisiecki and Raymo, 2005) is not achievable. The Jansen et al. (2000) age model aligns the IRD maxima with the glacial marine isotope stages (MIS) in LR04 (Fig. 3; see also Kleiven et al., 2002), allowing to make tentative links between our data and the marine isotope stratigraphy. We recognize that our time series cannot be related precisely to LR04, but are accurate within a marine isotope stage.

We refrain from using the age model of Lacasse and Bogaard (2002), which used five $^{40}Ar/^{39}Ar$ ages of K-feldspar and biotite phenocrysts of tephra layers. This is mainly because of the incompatibility of the $^{40}Ar/^{39}Ar$ age at 61.0 mbsf (3.01 ± 0.05 Ma), which shows a large age difference with the paleomagnetic reversals at 57.0 mbsf (3.04 Ma), 59.3 mbsf (3.11 Ma) and 61.2 mbsf (3.22 Ma; Fig. 2).

Our study interval (73.11–50.83 mcd) covers the time interval from 3.50 to 2.41 Ma with a sampling resolution across this interval being on average ~7 ka for the Late Pliocene (3.50–2.58 Ma) and ~8 ka for the Early Pleistocene (2.58–2.41 Ma).

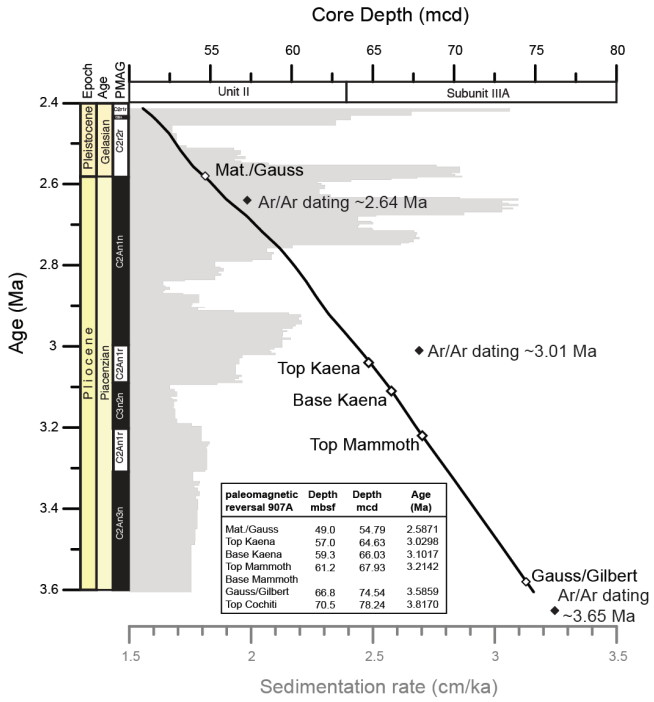

Fig. 2: *Age model for ODP Site 907 of Jansen et al. (2000), where the IRD record was tuned to obliquity using the paleomagnetic reversals (Channell et al., 1999) as tiepoints (empty diamonds; inset table). Lithology units are as identified by the Shipboard Scientific Party (1995, 1996). Grey shaded curve shows the sedimentation rate (cm/ka). The Ar/Ar-dating points from Lacasse and Bogaard (2002) are also indicated (filled diamonds), but not included in the age model.*

3.4. Approach

3.4.1. Biomarkers as proxies for reconstructing environmental conditions

The biogeochemical proxy IP_{25} (Belt et al., 2007) has been applied to reconstruct past spring sea ice cover in the Arctic and subarctic Oceans during the late Quaternary (e.g. Belt et al., 2015; Cabedo-Sanz et al., 2013; Hörner et al., 2016; Müller et al., 2009), the early Quaternary to Pliocene (Knies et al., 2014) and even the Late Miocene (Stein et al., 2016). This indicates a good stability of the biomarker over longer geological times. IP_{25} is a highly branched isoprenoid (HBI) monoene, synthesized by specific diatoms living in the sea ice (Brown et al., 2014). A weakness of IP_{25} is that it is not possible to distinguish between a fully sea ice cover and ice-free conditions because in both of those scenarios IP_{25} is absent (Belt et al., 2007; Müller et al., 2009). Therefore, Müller et al. (2011) compared IP_{25} with marine phytoplankton biomarkers (e.g. brassicasterol and dinosterol). Both IP_{25} and phytoplankton markers absence represent a permanent sea ice cover, whereas IP_{25} absence and phytoplankton marker presence indicates open-ocean conditions. Sterols are valuable

biomarkers to assign the source of organic matter in seawater and sediments (Rontani et al., 2014). Hence, brassicasterol and dinosterol are often used as indicators for marine phytoplankton production (for a critical review see Belt et al., 2013; 2015; Fahl and Stein, 1999; Xiao et al., 2013). On the other hand, β-sitosterol and campesterol are produced by vascular land plants (e.g. Volkman, 1986) and have been successfully applied for terrigenous input in the Arctic Ocean (e.g. Fahl and Stein, 1999; Xiao et al., 2013).

Our reconstruction of sea surface temperatures (SSTs) is based on long-chain C_{37} alkenones synthesized by haptophyte algae (coccolithophores) living in 0–10 m water depths (mixed layer; e.g. Brassell et al., 1986; Prahl and Wakeham, 1987). The ratio of these C_{37} alkenones, characterized by different numbers of double bonds, correlates with SST. Here, we used the simplified $U_{37}^{K\prime}$ approach (Prahl and Wakeham, 1987):

$$U_{37}^{K\prime} = C_{37:2}/(C_{37:2} + C_{37:3}) \quad (1).$$

We are using this calibration, which only includes the $C_{37:2}$ and $C_{37:3}$ alkenones since we did not detect any $C_{37:4}$ alkenones in our samples (Supplementary Fig. S1a). According to Prahl and Wakeham (1987), the error for $U_{37}^{K\prime}$ calculation is ± 0.05 $U_{37}^{K\prime}$ units for a temperature range of 0–27 °C. $U_{37}^{K\prime}$ was converted to SST according to the World Ocean surface sediment vs. measured mean annual temperature calibration (Müller et al., 1998):

$$U_{37}^{K\prime} = 0.033T + 0.044 \quad (2).$$

The error for the calculated SST values is ± 1.0 °C for the entire temperature range (Müller et al., 1998). This calibration was developed from sediment surface samples between 60 °N and 60 °S and SSTs between 0–27 °C. Therefore, the $U_{37}^{K\prime}$ is more scattered in the lower temperature range (<10 °C) than for the mean, i.e. the error might be higher. Müller et al. (1998) consider their calibration as an annual mean SST, although the correlation to spring/summer SSTs is equally significant (Filippova et al., 2016). Further, alkenone production in high-latitudes is limited to the summer months due to low solar insolation in winter (e.g. Andruleit, 1997). Hence, our SST reconstructions rather suggest summer SSTs, which has also been shown in previous studies (e.g. Bachem et al., 2016; Conte et al., 2006). Although the absolute amount of the single alkenones may decrease with increasing core depth due to degradation processes, the $U_{37}^{K\prime}$ index remains relatively constant during diagenesis (Lawrence et al., 2007 and refs therein), making the $U_{37}^{K\prime}$ index a good tool to reconstruct paleo SSTs. The combination of SST proxies and IP_{25} sea ice data helps to

interpret the proxy records more precisely in terms of sea ice variability (e.g. Stein et al., 2016; this study, see below).

3.4.2. Geochemical analyses

Subsamples (100 μg) of freeze-dried and homogenized sediment were used to measure the total organic carbon (TOC) using an ELTRA CS2000 Carbon Sulfur Detector. 4–7 g sediment was extracted using an Accelerated Solvent Extractor (DIONEX ASE 200; 100 ºC, 5 min, 1000 psi) with dichloromethane:methanol (2:1 v/v) as solvent. Prior to the extraction, the internal standards 7-hexylnonadecane, (7-HND; 0.076 μl/sample), cholesterol-d_6 (10.5 μl/sample), 19:0 (FAME; 51 μl/sample), and squalane (2.4 μl/sample) were added to the sample for quantification. Hydrocarbons, alkenones, and sterols were separated using open-column chromatography (5 ml *n*-hexane, 7 ml *n*-hexane:dichloromethane (1:1 v/v), 6 ml *n*-hexane:ethylacetate (4:1 v/v), respectively with silica gel (SiO_2) as stationary phase. Sterols were silylated with 200 μl BSTFA (bis-trimethylsilyl-trifluoroacet-amide; at 60 °C for 2 hours).

Compound analysis was performed by gas chromatography–mass-spectrometry (GC-MS). IP_{25} was analyzed using an Agilent 7890B GC coupled to an Agilent 5977A MSD using following heating program: 60 ºC (3 min), 150 ºC (rate: 15 ºC/min), 320 ºC (rate: 10 ºC/min), 320 ºC (15 min isothermal). Sterols (brassicasterol, 24-methylcholesta-5,22E-dien-3β-ol; campesterol, 24-methylcholest-5-en-3β-ol; β-sitosterol, 24-ethylcholest-5-en-3β-ol; dinosterol, 4α,23,24-trimethyl-5α-cholest-22E-en-3β-ol) were analyzed using an Agilent 6850 GC (30 m HP-5MS column, 0.25 mm inner diameter, 0.25 μm film thickness) coupled to an Agilent 5975C MSD (with 70 eV constant ionization potential, ion source temperature 230 ºC). The GC oven was heated as following: 60 ºC (2 min), 150 ºC (rate: 15 ºC/min), 320 ºC (rate: 3 ºC/min), 320 ºC (20 min isothermal). For both analyses, helium was used as carrier gas (1 ml/min constant gas flow). The injection volume was 1 μl (splitless). The identification and quantification of the IP_{25} monoene and sterols were performed as described in Fahl and Stein (2012; see also Fig. S1b). All biomarker concentrations were corrected to the amount of extracted sediment and normalized to the TOC contents of the samples.

For the alkenone analysis, the previous extracted and column chromatographed hexane:dicloromethane fraction was used. Alkenones were analyzed using an Agilent 7890A GC (column 60 m x 0.32 mm; film thickness 0.25 mm) and the following temperature program: 60 °C (3 min), 150°C (rate: 20°C/min), 320°C (rate: 6°C/min) and 320°C (40 min isothermal). For splitless injection, a cold injection system was used (60 °C (6 s), 340 °C (rate: 12 °C/s), 340 °C (1 min isothermal)). Helium was used as carrier gas (1.2 ml/min). The

individual alkenones ($C_{37:3}$ and $C_{37:2}$) were identified by their retention time and the comparison to an external standard. Instrument stability was continuously controlled by reruns of the external alkenone standard during the analytical sequences. The range of the total analytical error calculated by replicate analyses was less than 0.4 ºC based on SST.
All biomarkers were measured and analyzed at the Alfred-Wegener-Institute in Bremerhaven, Germany.

3.4.3. Palynology

Samples (10 cc) were dried and prepared using a standard palynological maceration procedure (De Schepper et al., 2017), which included adding one *Lycopodium clavatum* tablet (batch #124961), digestion cycles in cold HF and HCl, no oxidation, and sieving at 10 μm before mounting the residue on microscope slides using a 34x22 cover slips. Slides were scanned using a light microscope at x400 magnification along non-overlapping traverses. Counting was stopped when less than 25 *in situ* specimens were recorded within 10 traverses. If more specimens were recorded, the entire slide was counted or until > 300 specimens were counted.

3.5. Data storage

All raw data is available at doi.pangaea.de/10.1594/PANGAEA.877309.

4. Results

IP_{25} (Fig. 3c) was detected more frequently between 3.50 and 3.00 Ma than between 3.00 and 2.40 Ma. The highest concentration (3.72 μg/gTOC) of the entire record occurs at 3.20 Ma. After ~3.00 Ma, IP_{25} is mostly absent or below the detection limit with small peaks occurring around 2.90, 2.85–2.74 and around 2.40 Ma.
Brassicasterol (Fig. 3d) has its highest concentrations (117.59 μg/gTOC) around 3.1 Ma and is absent in a few samples. From 2.80 Ma, concentrations are decreasing. Dinosterol (Fig. 3e) is absent or below the detection level between 3.50 and 3.00 Ma except for small peaks around ~3.30 Ma (0.41 μg/gTOC), ~3.20 Ma (0.78 μg/gTOC) and ~3.00 Ma (0.91 μg/gTOC). From around 2.90 Ma, dinosterol concentrations are increasing with an average concentration of 1.21 μg/gTOC, and a maximum value of 5.49 μg/gTOC at ~2.81 Ma.
Since both, β-sitosterol and campesterol, are of terrigenous origin and do not differ much in our record, they are presented here together (terrigenous sterols; Fig. 3b). These terrestrial biomarkers show strong fluctuations with three major peaks at ~3.00 Ma (101.41 μg/gTOC), ~2.90 Ma (189.02 μg/gTOC) and ~2.80 Ma (108.09 μg/gTOC). Between 3.50 and 3.00 Ma the average concentration is 5.14 μg/gTOC. Maximum concentration does not exceed

14.73 μg/gTOC, whereas the sterols are absent or below the detection level in a few samples. Between 3.00 and 2.40 Ma, the average concentration of the terrestrial marker decreases to 13.1 μg/gTOC, while maximum values go up to 189.02 μg/gTOC.

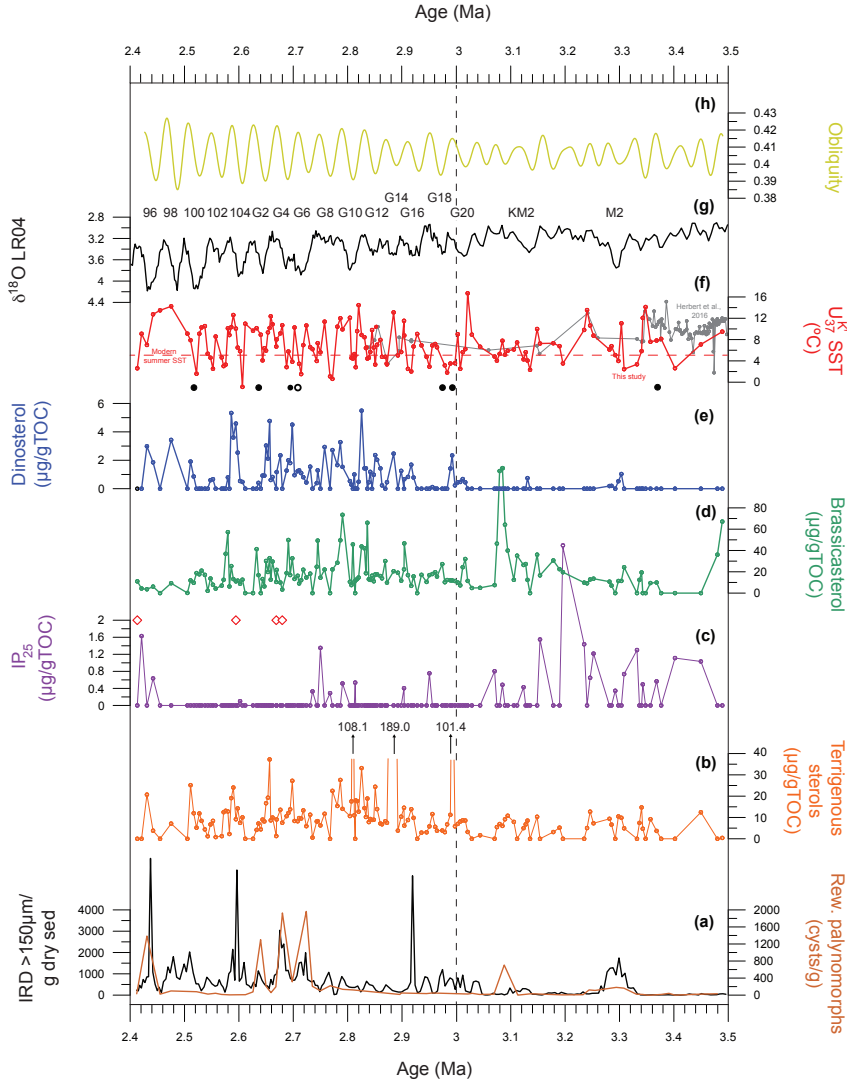

Fig. 3: *Proxy records from ODP Site 907 between 3.50 to 2.40 Ma (a–f). (a) IRD counts (Jansen et al., 2000) and reworked palynomorph concentrations (brown line, this study). Biomarker concentrations in (µg/gTOC) for (b) terrigenous sterols (campesterol and β-sitosterol), (c) IP_{25}, (d) brassicasterol, (e) dinosterol (this study). Red diamonds in panel (c) show the presence of the sea ice associated dinoflagellate species Islandinium. (f) Alkenone SSTs ($U^{K'}_{37}$) in ºC (red line, this study; gray line, Herbert et al. (2016)). Open circle in panel (f) indicates not detectable $C_{37:2}$ and $C_{37:3}$ alkenones; filled circles indicate not detectable $C_{37:2}$ alkenones in the samples. Red dashed line is the modern summer SST of ~6 ºC (from World Ocean Atlas). (g) LR04 benthic foraminifer isotope stack and glacial marine isotope stages (Lisiecki and Raymo, 2005). (h) Obliquity (Laskar et al., 2004). Note that all data is plotted using the age model of Jansen et al. (2000).*

The average SST over the entire record is 6.7 ºC (Fig. 3f). Between 3.50 and 3.00 Ma, the SST varies between 16.7 and 2.3 ºC with an average of 6.9 ºC. Between 3.00 and 2.40 Ma, the average SST drops slightly to 6.6 ºC, with a maximum SST of 14.5 ºC and minimum of 0.9 ºC. At 2.71 Ma, neither $C_{37:3}$ alkenones nor $C_{37:2}$ alkenones could be detected (Fig. 3f, open circle) and at 3.33, 2.99, 2.69, 2.64 , and 2.52 Ma, no $C_{37:2}$ alkenones could be detected (Fig. 3f, filled circles). $C_{37:4}$ alkenones were not detected in the entire record.

Between 3.50 and 3.30 Ma, dinoflagellate cyst assemblages are dominated by *Spiniferites* sp. 1 with an average concentration of 5,000 cysts per gram dry sediment (Fig. 4). After 3.30 Ma, dinoflagellate cyst concentrations dropped steeply reaching on average values of 20

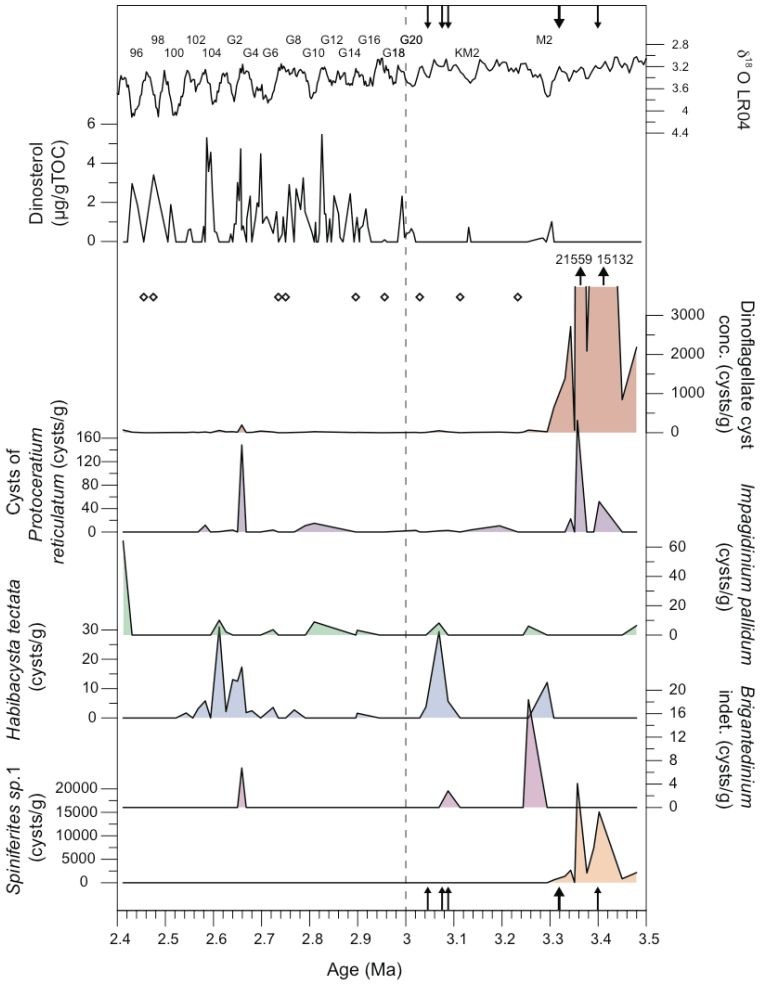

Fig. 4: *Dinoflagellate cyst concentrations (cysts per gram dry sediment) of the most abundant species and dinosterol concentration (µg/gTOC) from ODP Site 907 between 3.50 and 2.40 Ma. Black arrows indicate nannofossil layers according to the Shipboard Scientific Party (1995). Glacial MIS according to Lisiecki and Raymo (2005).*

cysts per gram dry sediment (minimum 0 and maximum of 197 cysts per gram dry sediment). Nine samples were completely barren for dinoflagellate cysts (Fig. 4, open diamonds). Four samples (3.01, 2.66, 2.61, 2.41 Ma) recorded higher concentrations (50–197 cysts per gram dry sediment) and the assemblage mainly consisted of cysts of *Protoceratium reticulatum*, *Habibacysta tectata* and *Impagidinium pallidum*. Specimens of the sea ice associated *Islandinium* were recorded at 2.68, 2.67, 2.59 and 2.41 Ma (Fig. 3c, red diamonds). The reworked palynomorphs (Fig. 3a, brown line) show two small peaks 3.30 and 3.10 Ma. Between 2.75 and 2.40 Ma four peaks with concentrations between 1302 and 1396 cysts per gram dry sediment occurred. All peaks in the reworked palynomorphs occur together with IRD peaks (Fig. 3a).

5. Discussion

Using the sea ice proxy IP_{25}, sterols for paleoproductivity, alkenone-based SSTs and palynology, we present for the first time sea ice reconstructions for the Late Pliocene to the earliest Pleistocene Iceland Sea. Our sea ice reconstruction indicates two different intervals (Fig. 3b–e): from 3.50 to 3.00 Ma, the Iceland Sea is characterized by a seasonal sea ice cover with occasionally sea ice-free intervals, whereas between 3.00 and 2.40 Ma the Iceland Sea is mainly sea ice-free with an occasional seasonal sea ice cover and ice edge conditions. The change in the biomarker record at 3.00 Ma coincides with a change in the lithology, where 3.00 Ma marks the boundary between Unit IIIA and Unit II (Shipboard Scientific Party, 1995, 1996).

5.1. Seasonal sea ice cover in the Iceland Sea between 3.5 and 3.0 Ma

Between 3.50 and 3.00 Ma, the presence of IP_{25}, absence or low concentration of marine and terrigenous biomarkers and variable SSTs between 16.7 and 2.3 ºC indicate the frequent occurrence of spring sea ice cover and ice-free summers in the Iceland Sea (Fig. 3). Higher IP_{25} values (between 1.2 and 3.2 μg/gTOC) within this interval are in the range of 1.65 μg/gTOC measured in the core top sample of a nearby sediment core (PS62/022-03: 72º29.4'N, 12º36.0'W; Müller et al., 2011). However, early diagenetic degradation of IP_{25} (Belt and Müller, 2013 and refs therein) has to be considered for our Pliocene samples, suggesting that IP_{25} concentrations were likely higher before diagenesis.

The relatively high alkenone-based SSTs throughout the entire period suggest that summers were generally ice-free and sea ice could only occur seasonally. The average paleo-SST of 7 ºC, ~2 ºC above the modern summer SST (WOA, 2013), as well as the minimum and maximum SSTs of 2 and 14 ºC (Fig. 3f), attest for generally ice-free conditions in summer. The alkenone SST record of the same site of Herbert et al. (2016) (Fig. 3f) indicates relatively

stable SSTs that are 2 ºC higher compared to our record between 3.50 and 3.30 Ma. This may be the result from different amount of extracted sediment or the researcher-specific integration of the individual $C_{37:3}$ and $C_{37:2}$ components. Between 3.30 and 3.00 Ma, the alkenone SSTs from Herbert et al. (2016) has a lower resolution and their reconstructed SSTs fall within the range of our reconstructions.

At the same time, productivity was generally very low in the Iceland Sea. The marine phytoplankton marker dinosterol, indicative of phytoplankton productivity in open waters (e.g. Belt et al., 2013; Fahl and Stein, 1999), is absent in every sample except for three minor peaks (~3.30 Ma, ~3.13 Ma, and ~3.00 Ma). Concentrations of ~1 μg/gTOC remain far below the values of 27.6 μg/gTOC measured in the core top sample (PS62/022-03; Müller et al., 2011). Comparing the dinosterol record with dinoflagellate cyst counts and concentrations in our record (Fig. 4), no correlation is apparent, an observation that has been made before in different regions (detailed review in Mouradian et al., 2007). Between 3.48 and 3.30 Ma, the only productive interval with a monospecific assemblage of the autotrophic dinoflagellate cyst *Spiniferites* sp. 1 is recorded, but this is not reflected in the dinosterol record (Fig. 4). In modern regions with seasonal sea ice cover, heterotrophic taxa are typically dominant in the sediment record (e.g. de Vernal et al., 2013b), but are also most prone to degradation due to oxidation (Zonneveld et al., 2008). The dinoflagellate cysts, including a few heterotrophs (*Brigantedinium*, round brown cysts) recorded between 3.30 and 3.00 Ma, were all in pristine condition, showing no evidence of degradation. Given the stability of the dinosterol molecule in the sediment and the low concentrations of dinoflagellate cysts concentrations, a very low biological productivity is in fact most plausible for the interval 3.30–3.00 Ma. This interpretation is in agreement with previous studies suggesting low phytoplankton productivity in this interval (Schreck et al., 2013 and refs therein). Between 3.40 and 3.00 Ma however, five layers of nannofossil ooze were recorded (Fig. 4 black arrows; Shipboard Scientific Party, 1995) indicating occasional high productivity and high carbonate preservation as a result of occasional enhanced influence of warm North Atlantic water masses (Fronval and Jansen, 1996). The increase in dinoflagellate cyst concentrations of *Spiniferites sp.* 1 and *P. reticulatum* around 3.40 Ma and *H. tectata* around 3.05 Ma (Fig. 4), could be related to an increased influence of Atlantic water masses or a shift of the Arctic Front towards the site.

Brassicasterol (Fig. 3d) also shows low concentrations between 20 and 40 μg/gTOC between 3.50 and 3.10 Ma, i.e. values far below the values of 152.6 μg/gTOC determined in nearby surface sediments (PS62/022-03; Müller et al., 2011). These low values corroborate low marine productivity in open waters, rather than indicating degradation processes (e.g. Rontani et al., 2014). However, there is an ongoing discussion about the suitability of brassicasterol as

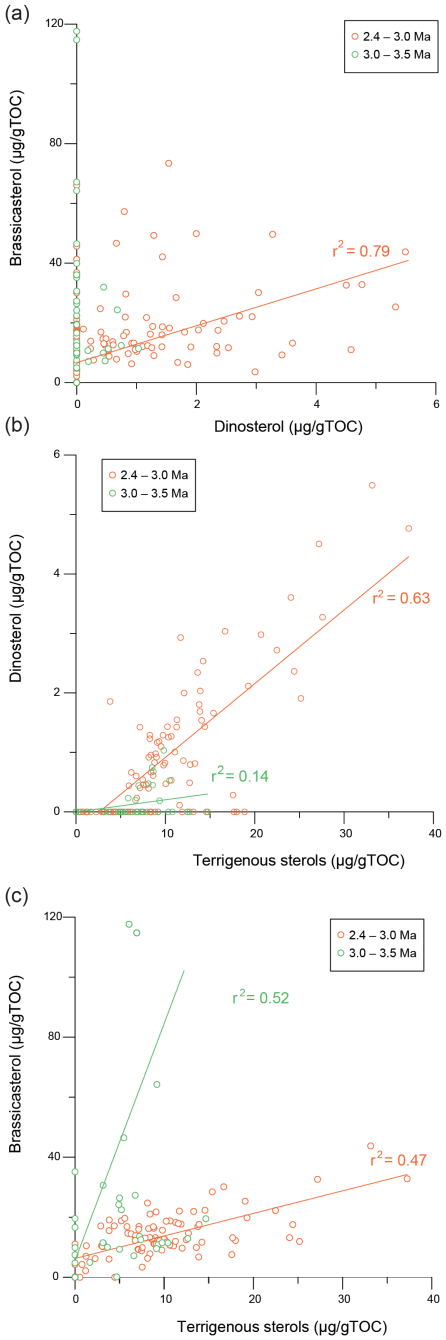

Fig. 5: *(a) Brassicasterol vs. dinosterol (marine biomarker), (b) dinosterol vs. terrigenous sterols, and (c) brassicasterol vs. terrigenous sterols from 3.50–3.00 Ma (orange dots) and 3.00–2.40 Ma (green dots) and their respective correlation coefficients. A good correlation between the compounds is interpreted as the same source of the molecules, i.e. marine or freshwater.*

a proxy for open ocean conditions especially at sea ice margins (Belt et al., 2015) due to the uncertain origin of brassicasterol (i.e. freshwater vs. marine; Belt et al., 2013; Fahl and Stein, 2012; Huang and Meinschein, 1976; Volkman, 1986) and the occasional co-occurrence of IP_{25} and brassicasterol (Belt et al., 2015; Weckström et al., 2013). Between 3.50 and 3.00 Ma, the poor correlation of dinosterol and brassicasterol (Fig. 5a) suggest that brassicasterol may had a (additional) freshwater source rather than a purely marine source. This interpretation, however, is only weakly supported by the correlation (r^2 = 0.52) of terrigenous sterols and brassicasterol (Fig. 5c). Nevertheless, it suggests that brassicasterol has a mixed marine and freshwater signal during this time. Terrigenous organic matter and freshwater-derived brassicasterol may have been derived from Greenland and/or Iceland (Xiao et al., 2017), or even from Siberia (e.g. Fahl and Stein, 1999; 2012; Xiao et al., 2013) via transport by ocean currents, drift ice and/or IRD.

At 3.10 Ma, brassicasterol increased briefly to concentrations of >80 µg/gTOC, corresponding to two nannofossil ooze layers in the sediment core (Fig. 4) and an increase in the terrigenous sterols (Fig. 3b). This peak could thus be due to increased Atlantic water influence or indicate a terrestrial origin of brassicasterol.

Generally, the presence of IP_{25}, the dominantly absence of dinosterol and low

(partly freshwater-derived) brassicasterol suggest that sea ice presence did not promote enhanced primary productivity in the Iceland Sea. The sediments of Site 907 are not rich in organic material and the accumulation rates of total organic carbon (TOC; Supplementary Fig. S2) are comparable to those observed in modern open-ocean oxic environments with low productivity (Stein and Stax, 1996 and refs therein). Incoming waters from the west (via EGC and EIC) and from the northeast (branch of the NwAC; Fig.1) form a weak cyclonic gyre in the Iceland Sea (Swift and Aagaard, 1981) and modern observations show a minimum in primary productivity in the center of the Iceland Sea close to the core location (Børsheim et al., 2014). The gyre isolates the core location from incoming nutrients, resulting in oligotrophic conditions and low primary productivity.

We cannot determine whether the sea ice was locally formed or transported to the site via the EGC. Here, additional information from mineralogical or geochemical proxies indicative for specific source areas characterized by a unique geology is needed (e.g. Andrews et al., 2016). The frequent presence of the sea ice biomarker IP_{25}, and the low dinosterol, brassicasterol and dinoflagellate cyst concentrations, however, argues for sea ice extension into the Iceland Sea, comparable to recent observations (see references in Aagaard and Carmack, 1989). This suggests that a proto-EGC, which was likely established already during the Early Pliocene (De Schepper et al., 2015; Schreck et al., 2013), might have brought cool and fresh polar water directly into the Iceland Sea (Fig. 6a). Increased fresh water can facilitate local sea ice formation in the Iceland Sea (Ólafsson, 1999). However, since seasonal sea ice was already present in the Fram Strait region since 4.00 Ma (Knies et al., 2014; Stein et al., 2014), possibly some sea ice may have been transported directly via the proto-EGC (and EIC) into the Iceland Sea. In fact, both processes are not mutually exclusive and may have operated simultaneously. Seasonal sea ice that formed locally or drifted over a short distance is most consistent with low phytoplankton productivity, high IP_{25} concentrations and highly variable SSTs between 2 and 14 ºC (Fig. 3f). Especially the highest SSTs suggest that sea ice may not have been transported over long distances.

5.2. Development of sea ice edge during the intensification of the Northern Hemisphere Glaciation

A pronounced increase in the marine productivity in the Iceland Sea from around 3.00 Ma is documented by the increase in dinosterol concentrations, although no obvious change is recorded in brassicasterol concentrations. The productivity change is accompanied by a lithology change from the presence of biogenic silica in Unit IIIA to an absence of biogenic silica and carbonate in Unit II (Shipboard Scientific Party, 1995, 1996) and increased IRD (Fig. 3a; Jansen et al., 2000), suggesting that the oceanographic conditions in the Iceland Sea

underwent changes related to the expansion of the Greenland Ice Sheet (GIS) linked to the intensification of the Northern Hemisphere Glaciation (iNHG, ~2.75 Ma).

The concentrations and accumulation of the marine phytoplankton biomarkers are substantially higher after 3.00 Ma (Fig. 3d, e; Supplementary Fig. S2), suggesting increased productivity that remains well below recent productivity rates in the Iceland Sea (Müller et al., 2011). The correlation (r^2= 0.79) of brassicasterol and dinosterol (Fig. 5a) suggest that brassicasterol is mostly of marine origin after 3.00 Ma, which is supported by a relatively weak correlation of brassicasterol and terrigenous sterols (Fig. 5c, r^2 = 0.47) after 3.00 Ma, indicating a reduced freshwater origin of brassicasterol. The increase in dinosterol might be related to increased input of terrigenous material and thus nutrients favoring phytoplankton growth as indicated from a good correlation between both sterols (Fig. 5b). Comparable to before 3.00 Ma, there is also a general mismatch between the dinoflagellate cyst concentrations and dinosterol (for discussion see chapter 5.1.): dinosterol shows a gradually increasing productivity trend from around 2.80 Ma onwards, whereas dinoflagellate cyst concentrations remain very low. The dinoflagellate cysts only show somewhat elevated numbers, and thus likely increased productivity, at 2.66 and 2.61 Ma (interglacials MIS G1 and G3; Fig. 4). On those occasions, *Habibacysta tectata* and cysts of *Protoceratium reticulatum* dominated the assemblages suggesting that Atlantic water may have reached the site, which is in agreement with IP_{25} absence and higher SSTs.

Generally, IP_{25} is absent or below the detection limit during this time interval suggesting either sea ice-free conditions or permanent sea ice cover. Given the increasing trend in sterol concentrations, a permanent sea ice cover is unlikely, i.e. dominantly ice-free conditions might have been more probable (Belt et al., 2007; Müller et al., 2011). IP_{25} occurred, however, occasionally around 2.95, 2.90, 2.81–2.74 and 2.40 Ma with maximum concentrations of 1.35 μg/gTOC at ~2.75 Ma and 1.63 μg/gTOC around 2.40 Ma. Taking degradation into account, these IP_{25} values were probably higher (Müller et al., 2011), suggesting an extended sea ice cover into the Iceland Sea during these times. Our reconstructed SST ranges between 0.9 and 14.5 ºC. Herbert et al. (2016) present only a few SST estimates after 3.00 Ma, and these are in agreement with our results (Fig. 3f). Sarnthein et al. (2003) proposed that, based on temperature estimates reconstructed by foraminiferal transfer functions, areas are covered by sea ice, when the summer SSTs is < 2.5 ºC. In our record, SST drops below 2.5 ºC in several glacials (e.g. G6–G4, 104, 100). Extremely cold surface conditions occurred during some of these glacials, where we did not record either the $C_{37:2}$ alkenone or both the $C_{37:2}$ and $C_{37:3}$ alkenones (Fig. 3f, filled and open circles, respectively). The $C_{37:2}$ alkenone cannot be synthesized when sea surface conditions are too cold. In those samples (no alkenones and < 2.5 ºC) also IP_{25} was absent. This could imply a

permanent sea ice cover, but because both dinosterol and brassicasterol were present, very cold, open-water conditions without a permanent sea ice cover were most likely.

Following the sporadic occurrences of IP_{25} at 2.95 and 2.90 Ma, a prolonged presence of IP_{25} reflects an extended time interval with seasonal sea ice in the Iceland Sea between 2.81 and 2.74 Ma. Sea ice extending into the Iceland Sea during this time might have acted as a positive feedback for the ice sheet expansion on Greenland, which became most apparent from around MIS G4–6 (ca. 2.75 Ma) when IRD peaks are recorded more frequently during consecutive glacials in the Iceland Sea (Fig. 3a; Jansen et al., 2000; Kleiven et al., 2002). The IRD also brought along a large amount of reworked terrestrial and marine palynomorphs of Mesozoic and Early Cenozoic age (Fig. 3a). Deposits of this age occur along the coast of East Greenland and were thus probably eroded during glacials MIS G6–G4, G2 and 96 (Fig. 3a) when the GIS may have expanded onto the Greenland Shelf (Vanneste et al., 1995). Such a GIS expansion would have moved the EGC and associated sea ice edge eastward and thus closer to Site 907, where it would enhance primary productivity (Fig. 3, 6b; Stein and Stax, 1996).

After 2.75 Ma, SSTs and sterols show a strong variability (less visible in brassicasterol) that may be related to a shift in seasonality, which become more extreme in glacials after MIS G3 (~2.67 Ma) onwards (Hennissen et al., 2015; Pross and Klotz, 2002). The shift towards stronger seasonality in the Pliocene is related to the large-scale expansion of the Greenland, Scandinavian and North American ice sheets (e.g. Bailey et al., 2013; Kleiven et al., 2002). Around this time (2.75–2.60 Ma), a pronounced cooling in the North Atlantic (Lawrence et al., 2009) and a southward shift of the Arctic Front (Hennissen et al., 2014) is documented. An Arctic Front located further southward would have hampered Atlantic water from entering the Iceland Sea, implying that productivity shifts are more likely linked to shifts in the sea ice edge rather than Atlantic water influence. These shifts in the sea ice edge and EGC possibly related to the waxing and waning of the GIS on glacial/interglacial timescales (Fig. 3c–e) can explain the changes in sterol concentrations after 2.75 Ma: a sea ice edge closer to Site 907 would increase productivity, whereas an edge closer to Greenland would reduce it.

It remains puzzling why IP_{25} is absent at Site 907 during the major expansions of the GIS between MIS G4–6 and 98 (Fig. 3c). Since we exclude the presence of a long-term permanent sea ice cover and propose that a stable ice edge was located between the Greenland coast and Site 907, sea ice was most likely transported southward towards the Labrador Sea. Only around 2.4 Ma (MIS 96), IP_{25} presence again supports a seasonal sea ice extent into the Iceland Sea.

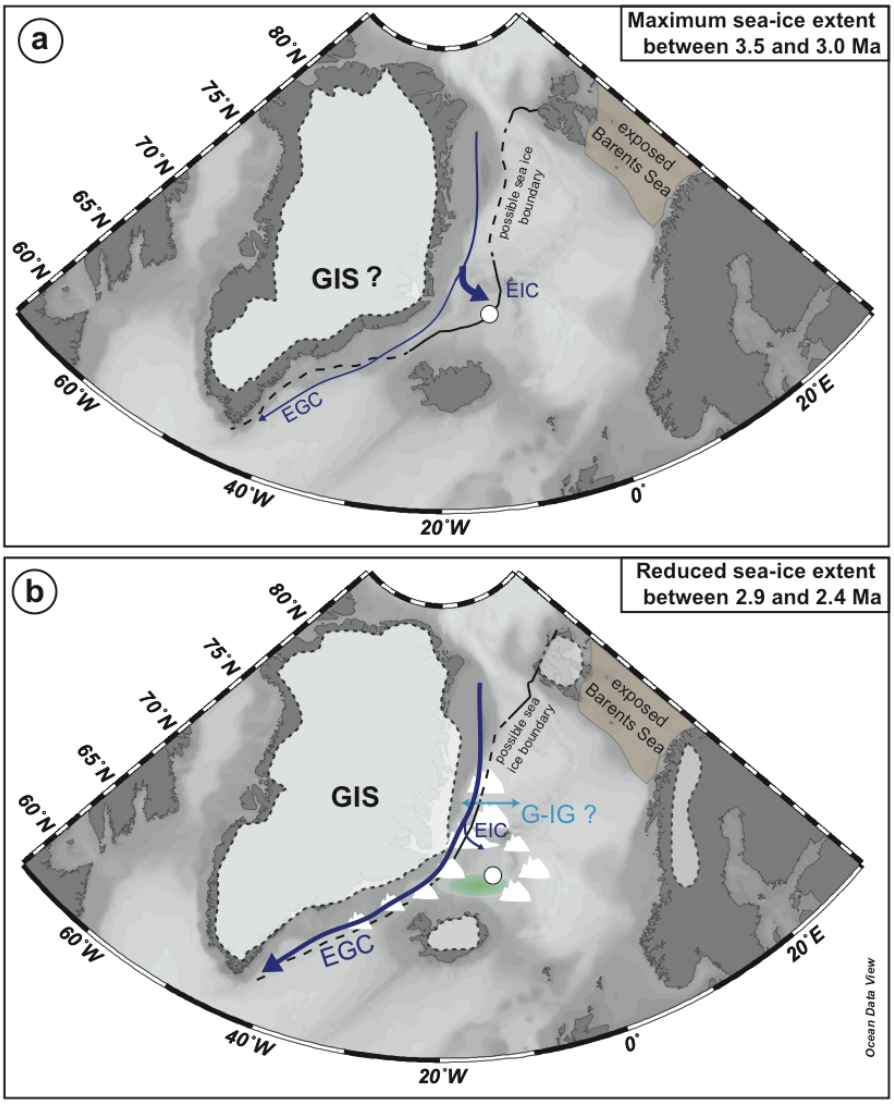

Fig. 6: *Schematic illustration of possible Late Pliocene sea ice scenarios for the Iceland Sea. (a) Seasonal sea ice cover occurs in the subarctic Ocean and the Nordic Seas from 3.50–3.00 Ma (dashed/solid black line). Dark blue line shows the East Greenland Current (EGC), which branches into an intense East Icelandic Current (EIC; thick arrow) and a possibly less intense EGC continuing southward (thin line). Greenland Ice Sheet (GIS) is after Koenig et al. (2015). (b) Sea ice extent is restricted to the East Greenland shelf and increased iceberg rafting between 2.90 and 2.40 Ma. Dark blue line shows the EGC, which branches into a weaker EIC (thin arrow) and a possibly more intense southward flowing EGC. Green area indicates enhanced phytoplankton productivity. Light blue arrow indicates a possible shift of a sea ice edge during glacial/interglacial (G-IG) times. GIS extension is shown after Vanneste et al. (1995), Iceland Ice Sheet after Geirsdóttir and Eiríksson (1994) and Scandinavian (incl. Svalbard) Ice Sheet after Knies et al. (2009).*

In summary, dominantly sea ice-free conditions occurred in the Iceland Sea between 3.00 and 2.40 Ma. Seasonal sea ice occurred for a prolonged period around 2.81–2.74 Ma in the Iceland Sea, which may have had a positive influence on the major GIS expansion around 2.75 Ma. Afterwards, a stable ice edge was present between Greenland and Site 907 and its shifts affected productivity in the Iceland Sea most likely contemporaneously with the waning and waxing of the GIS. Sea ice was absent in the Iceland Sea between 2.74 and 2.40 Ma, with sea ice most likely being transported towards the Labrador Sea.

6. Conclusion

For the first time, IP_{25} was used for reconstructing the sea ice history of the Iceland Sea during the globally warm Pliocene. Together with biomarkers for paleoproductivity, alkenone-based SSTs and palynology, we demonstrate that seasonal sea ice conditions prevailed with ice-free summers between 3.50 and 3.00 Ma, including also the mid-Piacenzian Warm Period, when global temperatures were on average 2–3 ºC higher than today. This might have been linked to an EGC (and EIC) bringing cooler and fresher waters favoring sea ice formation or in fact transporting sea ice directly into the Iceland Sea.

After 3.00 Ma, SSTs dropped more frequently below 2.5 ºC indicating cooler sea surface conditions than before 3.00 Ma. However, the Iceland Sea remained predominantly ice-free, but sea ice extended into the Iceland Sea particularly between 2.81 and 2.74 Ma, and around 2.40 Ma. Sea ice presence between 2.81 and 2.74 Ma may have acted as a positive feedback for the build-up of the GIS, which underwent a major expansion ~2.75 Ma (intensification of the Northern Hemisphere Glaciation). Thereafter, a stable ice edge developed close to Greenland possibly shifting with the expansion and retreat of the GIS affecting the productivity in the Iceland Sea. The EGC (and EIC) influence was likely reduced in the Iceland Sea resulting in more sea ice being transported southward into the Labrador Sea.

Acknowledgements

We thank Walter Luttmer for assistance in the lab, Bjørg Risebrobakken and Jens Matthiessen for discussions and comments on an earlier version of the manuscript, and Simon Belt (Biogeochemistry Research Centre, University of Plymouth/UK) for providing the 7-HND standard for IP_{25} quantification. We are grateful to Jochen Knies and a second anonymous reviewer for valuable comments, which greatly improved the manuscript. This research is supported by the Norwegian Research Council grant 229819.

References

Aagaard, K., and Carmack, E. C., 1989, The role of sea ice and other fresh water in the Arctic circulation: Journal of Geophysical Research, v. 94, no. C10, p. 14,485-414,498. doi. 10.1029/JC094iC10p14485

Aagaard, K., and Coachman, L. K., 1968, The East Greenland Current North of Denmark Strait: Part I Arctic, v. 21, no. 3, p. 181-200. doi. jstor.org/stable/40507537

Andrews, J. T., Stein, R., Moros, M., and Perner, K., 2016, Late Quaternary changes in sediment composition on the NE Greenland margin (~73° N) with a focus on the fjords and shelf: Boreas, v. 45, no. 3, p. 381-397. doi. 10.1111/bor.12169

Andruleit, H., 1997, Coccolithophore fluxes in the Norwegian-Greenland Sea: seasonality and assemblage alterations: Marine Micropaleontology, v. 31, p. 45-64. doi. 10.1016/S0377-8398(96)00055-2

Bachem, P. E., Risebrobakken, B., De Schepper, S., and McClymont, E. L., 2017, Highly variable Pliocene sea surface conditions in the Norwegian Sea: Climate of the Past, p. 1-25. doi. 10.5194/cp-2016-131

Bachem, P. E., Risebrobakken, B., and McClymont, E. L., 2016, Sea surface temperature variability in the Norwegian Sea during the late Pliocene linked to subpolar gyre strength and radiative forcing: Earth and Planetary Science Letters, v. 446, p. 113-122. doi. 10.1016/j.epsl.2016.04.024

Bailey, I., Hole, G. M., Foster, G. L., Wilson, P. A., Storey, C. D., Trueman, C. N., and Raymo, M. E., 2013, An alternative suggestion for the Pliocene onset of major northern hemisphere glaciation based on the geochemical provenance of North Atlantic Ocean ice-rafted debris: Quaternary Science Reviews, v. 75, p. 181-194. doi. 10.1016/j.quascirev.2013.06.004

Belt, S. T., Brown, T. A., Ringrose, A. E., Cabedo-Sanz, P., Mundy, C. J., Gosselin, M., and Poulin, M., 2013, Quantitative measurement of the sea ice diatom biomarker IP25 and sterols in Arctic sea ice and underlying sediments: Further considerations for palaeo sea ice reconstruction: Organic Geochemistry, v. 62, p. 33-45. doi. 10.1016/j.orggeochem.2013.07.002

Belt, S. T., Cabedo-Sanz, P., Smik, L., Navarro-Rodriguez, A., Berben, S. M. P., Knies, J., and Husum, K., 2015, Identification of paleo Arctic winter sea ice limits and the marginal ice zone: Optimised biomarker-based reconstructions of late Quaternary Arctic sea ice: Earth and Planetary Science Letters, v. 431, p. 127-139. doi. 10.1016/j.epsl.2015.09.020

Belt, S. T., Massé, G., Rowland, S. J., Poulin, M., Michel, C., and LeBlanc, B., 2007, A novel chemical fossil of palaeo sea ice: IP25: Organic Geochemistry, v. 38, no. 1, p. 16-27. doi. 10.1016/j.orggeochem.2006.09.013

Belt, S. T., and Müller, J., 2013, The Arctic sea ice biomarker IP25: a review of current understanding, recommendations for future research and applications in palaeo sea ice reconstructions: Quaternary Science Reviews, v. 79, p. 9-25. doi. 10.1016/j.quascirev.2012.12.001

Blindheim, J., and Østerhus, S., 2005, The Nordic Seas: Main Oceanographic Features, *in* Drange, H., Dokken, T., Furevik, T., Gerdes, R., and Berger, W., eds., The Nordic Seas: An Integrated Perspective, p. 11-37.

Børsheim, K. Y., Milutinović, S., and Drinkwater, K. F., 2014, TOC and satellite-sensed chlorophyll and primary production at the Arctic Front in the Nordic Seas: Journal of Marine Systems, v. 139, p. 373-382. doi. 10.1016/j.jmarsys.2014.07.012

Brassell, S. C., Eglinton, G., Marlowe, I. T., Pflaumann, U., and Sarnthein, M., 1986, Molecular stratigraphy: a new tool for climatic assessment: Nature, v. 320, p. 129-133. doi. 10.1038/320129a0

Brown, T. A., Belt, S. T., Tatarek, A., and Mundy, C. J., 2014, Source identification of the Arctic sea ice proxy IP25: Nat Commun, v. 5, p. 4197. doi. 10.1038/ncomms5197

Butt, F. A., Drange, H., Elverhøi, A., Otterå, O. H., and Solheim, A., 2002, Modelling Late Cenozoic isostatic elevation changes in the Barents Sea and their implications for oceanic and climatic regimes: preliminary results: Quaternary Science Reviews, v. 21, no. 14, p. 1643-1660. doi. 10.1016/S0277-3791(02)00018-5

Cabedo-Sanz, P., Belt, S. T., Knies, J., and Husum, K., 2013, Identification of contrasting seasonal sea ice conditions during the Younger Dryas: Quaternary Science Reviews, v. 79, p. 74-86. doi. 10.1016/j.quascirev.2012.10.028

Channell, J. E. T., Amigo, A. E., Fronval, T., Rack, F., and Lehman, B., 1999, Magnetic Stratigraphy at Sites 907 and 985 in the Norwegian-Greenland Sea and a Revision of the Site 907 Composite Section: T.D.Proceedings of the Ocean Drilling Program, Scientific Results, v. 16, p. 131-148. doi. 10.2973/odp.proc.sr.162.036.1999

Conte, M. H., Sicre, M.-A., Rühlemann, C., Weber, J. C., Schulte, S., Schulz-Bull, D., and Blanz, T., 2006, Global temperature calibration of the alkenone unsaturation index (UK'_{37}) in surface waters and comparison with surface sediments: Geochemistry, Geophysics, Geosystems, v. 7, no. 2, p. Q02005, 02001-02022. doi. 10.1029/2005gc001054

Darby, D. A., 2008, Arctic perennial ice cover over the last 14 million years: Paleoceanography, v. 23, no. 1, p. PA1S07. doi. 10.1029/2007pa001479

De Schepper, S., Beck, K. M., and Mangerud, G., 2017, Late Neogene dinoflagellate cyst and acritarch biostratigraphy for Ocean Drilling Program Hole 642B, Norwegian Sea: Review of Palaeobotany and Palynology, v. 236, p. 12-32. doi. 10.1016/j.revpalbo.2016.08.005

De Schepper, S., Schreck, M., Beck, K. M., Matthiessen, J., Fahl, K., and Mangerud, G., 2015, Early Pliocene onset of modern Nordic Seas circulation related to ocean gateway changes: Nat Commun, v. 6, p. 8659. doi. 10.1038/ncomms9659

de Vernal, A., Gersonde, R., Goosse, H., Seidenkrantz, M.-S., and Wolff, E. W., 2013a, Sea ice in the paleoclimate system: the challenge of reconstructing sea ice from proxies – an introduction: Quaternary Science Reviews, v. 79, p. 1-8. doi. 10.1016/j.quascirev.2013.08.009

de Vernal, A., Hillaire-Marcel, C., Rochon, A., Fréchette, B., Henry, M., Solignac, S., and Bonnet, S., 2013b, Dinocyst-based reconstructions of sea ice cover concentration during the Holocene in the Arctic Ocean, the northern North Atlantic Ocean and its adjacent seas,: Quaternary Science Reviews, v. 79, p. 111-121. doi. 10.1016/j.quascirev.2013.07.006

Dolan, A. M., Haywood, A. M., Hunter, S. J., Tindall, J. C., Dowsett, H. J., Hill, D. J., and Pickering, S. J., 2015, Modelling the enigmatic Late Pliocene Glacial Event — Marine Isotope Stage M2: Global and Planetary Change, v. 128, p. 47-60. doi. 10.1016/j.gloplacha.2015.02.001

Dowsett, H. J., 2007, The PRISM palaeoclimate reconstruction and Pliocene sea-surface temperature, *in* Williams, M., Haywood, A. M., Gregory, F. J., and Schmidt, D. N., eds., Deep-Time Perspectives on Climate Change, The Micropalaeontological Society Special Publications, p. 459-480.

Dowsett, H. J., Foley, K. M., Stoll, D. K., Chandler, M. A., Sohl, L. E., Bentsen, M., Otto-Bliesner, B. L., Bragg, F. J., Chan, W. L., Contoux, C., Dolan, A. M., Haywood, A. M., Jonas, J. A., Jost, A., Kamae, Y., Lohmann, G., Lunt, D. J., Nisancioglu, K. H., Abe-Ouchi, A., Ramstein, G., Riesselman, C. R., Robinson, M. M., Rosenbloom, N. A., Salzmann, U., Stepanek, C., Strother, S. L., Ueda, H., Yan, Q., and Zhang, Z., 2013, Sea surface temperature of the mid-Piacenzian ocean: a data-model comparison: Sci Rep, v. 3, p. 1-8. doi. 10.1038/srep02013

Dowsett, H. J., Robinson, M. M., Haywood, A. M., Salzmann, U., Hill, D. J., Sohl, L., Chandler, M. A., Williams, M., Foley, K., and Stoll, D., 2010, The PRISM3D paleoenvironmental reconstruction: Stratigraphy, v. 7, p. 123–139. doi. pubs.er.usgs.gov/publication/70044350

Fahl, K., and Stein, R., 1999, Biomarkers as organic-carbon-source and environmental indicators in the Late Quaternary Arctic Ocean-problems and perspectives: Marine Chemistry, v. 63, p. 293–309. doi. 10.1016/S0304-4203(98)00068-1

Fahl, K., and Stein, R., 2012, Modern seasonal variability and deglacial/Holocene change of central Arctic Ocean sea-ice cover: New insights from biomarker proxy records: Earth and Planetary Science Letters, v. 351-352, p. 123-133. doi. 10.1016/j.epsl.2012.07.009

Filippova, A., Kienast, M., Frank, M., and Schneider, R. R., 2016, Alkenone paleothermometry in the North Atlantic: A review and synthesis of surface sediment data and calibrations: Geochemistry, Geophysics, Geosystems, v. 17, no. 4, p. 1370-1382. doi. 10.1002/2015gc006106

Fronval, T., and Jansen, E., 1996, Late Neogene Paleoclimates and Paleoceanography in the Iceland-Norwegian Sea: Evidence from the Iceland and Vøring Plateaus: Proceedings of the Ocean Drilling Program, Scientific Results, v. 151, p. 455-468. doi. 10.2973/odp.proc.sr.151.134.1996

Geirsdóttir, Á., and Eiríksson, J., 1994, Growth of an Intermittent Ice Sheet in Iceland during the Late Pliocene and Early Pleistocene: Quaternary Research, v. 42, p. 115-130. doi. 10.1006/qres.1994.1061

Haywood, A. M., Dowsett, H. J., and Dolan, A. M., 2016, Integrating geological archives and climate models for the mid-Pliocene warm period: Nat Commun, v. 7, p. 10646. doi. 10.1038/ncomms10646

Hennissen, J. A., Head, M. J., De Schepper, S., and Groeneveld, J., 2014, Palynological evidence for a southward shift of the North Atlantic Current at~ 2.6 Ma during the intensification of late Cenozoic Northern Hemisphere glaciation.: Paleoceanography, v. 29, no. 6, p. 564-580. doi. 10.1002/2013PA002543

Hennissen, J. A. I., Head, M. J., De Schepper, S., and Groeneveld, J., 2015, Increased seasonality during the intensification of Northern Hemisphere glaciation at the Pliocene–Pleistocene boundary ~2.6 Ma: Quaternary Science Reviews, v. 129, p. 321-332. doi. 10.1016/j.quascirev.2015.10.010

Herbert, T. D., Lawrence, K. T., Tzanova, A., Peterson, L. C., Caballero-Gill, R., and Kelly, C. S., 2016, Late Miocene global cooling and the rise of modern ecosystems: Nature Geoscience, p. 1-5. doi. 10.1038/ngeo2813

Hill, D. J., 2015, The non-analogue nature of Pliocene temperature gradients: Earth and Planetary Science Letters, v. 425, p. 232-241. doi. 10.1016/j.epsl.2015.05.044

Hörner, T., Stein, R., Fahl, K., and Birgel, D., 2016, Post-glacial variability of sea ice cover, river run-off and biological production in the western Laptev Sea (Arctic Ocean) – A high-resolution biomarker study: Quaternary Science Reviews, v. 143, p. 133-149. doi. 10.1016/j.quascirev.2016.04.011

Howell, F. W., Haywood, A. M., Dowsett, H. J., and Pickering, S. J., 2016, Sensitivity of Pliocene Arctic climate to orbital forcing, atmospheric CO2 and sea ice albedo parameterisation: Earth and Planetary Science Letters, v. 441, p. 133-142. doi. 10.1016/j.epsl.2016.02.036

Huang, W.-Y., and Meinschein, W. G., 1976, Sterols as source indicators of organic materials in sediments: Geochimica and Cosmochimica Acta, v. 40, p. 323-330. doi. 10.1016/0016-7037(76)90210-6

Ingvaldsen, R. B., Asplin, L., and Loeng, H., 2004, Velocity field of the western entrance to the Barents Sea: Journal of Geophysical Research: Oceans, v. 109, no. C3, p. C03021. doi. 10.1029/2003JC001811

Jansen, E., Fronval, T., Rack, F., and Channell, J. E. T., 2000, Pliocene-Pleistocene ice rafting history and cyclicity in the Nordic Seas during the last 3.5 Myr: Paleoceanography, v. 15, no. 6, p. 709-721. doi. 10.1029/1999pa000435

Jansen, E., Raymo, M. E., Blum, P., and et al., 1996, New frontiers on past climate: Proceedings of the Ocean Drilling Program, Initial Reports, v. 162, p. 5-20. doi. 10.2973/odp.proc.ir.162.101.1996

Kleiven, H. F., Jansen, E., Fronval, T., and Smith, T. M., 2002, Intensification of Northern Hemisphere glaciations in the circum Atlantic region (3.5–2.4 Ma) - ice-rafted detritus evidence: Palaeogeography, Palaeoclimatology, Palaeoecology, v. 184, p. 213-223. doi. 10.1016/S0031-0182(01)00407-2

Knies, J., Cabedo-Sanz, P., Belt, S. T., Baranwal, S., Fietz, S., and Rosell-Melé, A., 2014, The emergence of modern sea ice cover in the Arctic Ocean: Nat Commun, v. 5, p. 5:5608. doi. 10.1038/ncomms6608

Knies, J., Matthiessen, J., Vogt, C., Laberg, J. S., Hjelstuene, B. O., Smelror, M., Larsen, E., Andreasen, K., Eidvin, T., and Vorren, T. O., 2009, The Plio-Pleistocene glaciation of the Barents Sea–Svalbard region: a new model based on revised chronostratigraphy: Quaternary Science Reviews v. 28, p. 812–829. doi. 10.1016/j.quascirev.20

Koenig, S. J., Dolan, A. M., de Boer, B., Stone, E. J., Hill, D. J., DeConto, R. M., Abe-Ouchi, A., Lunt, D. J., Pollard, D., Quiquet, A., Saito, F., Savage, J., and van de Wal, R., 2015, Ice sheet model dependency of the simulated Greenland Ice Sheet in the mid-Pliocene: Climate of the Past, v. 11, no. 3, p. 369-381. doi. 10.5194/cp-11-369-2015

Lacasse, C., and Bogaard, P. v. d., 2002, Enhanced airborne dispersal of silicic tephras during the onset of Northern Hemisphere glaciations, from 6 to 0 Ma records of explosive volcanism and climate change in the subpolar North Atlantic: Geology, v. 30, no. 7, p. 623-626. doi. 10.1130/0091-7613(2002)030<0623:EADOST>2.0.CO;2

Laskar, J., Robutel, P., Joutel, F., Gastineau, M., Correia, A. C. M., and Levrard, B., 2004, A long-term numerical solution for the insolation quantities of the Earth: Astronomy and Astrophysics, v. 428, no. 1, p. 261-285. doi. 10.1051/0004-6361:20041335

Lawrence, K. T., Herbert, T. D., Brown, C. M., Raymo, M. E., and Haywood, A. M., 2009, High-amplitude variations in North Atlantic sea surface temperature during the early Pliocene warm period: Paleoceanography, v. 24, no. 2, p. PA2218. doi. 10.1029/2008pa001669

Lawrence, K. T., Herbert, T. D., Dekens, P. S., and Ravelo, A. C., 2007, The application of the alkenone organic proxy to the study of Plio-Pleistocene climate, *in* Williams, M., Haywood, A. M., Gregory, F. J., and Schmidt, D. N., eds., Deep-Time Perspectives on Climate Change: Marrying the Signal from Computer Models and Biological Proxies: London, The Micropalaeontological Society, Special Publication, p. 539-562.

Lisiecki, L. E., and Raymo, M. E., 2005, A Pliocene-Pleistocene stack of 57 globally distributed benthic δ18O records: Paleoceanography, v. 20, no. 1, p. PA1003. doi. 10.1029/2004pa001071

Locarnini, R. A., Mishonov, A. V., Antonov, J. I., Boyer, T. P., Garcia, H. E., Baranova, O. K., Zweng, M. M., Paver, C. R., Reagan, J. R., Johnson, D. R., Hamilton, M., and Seidov, D., 2013, World Ocean Atlas 2013, Volume 1: Temperature, *in* Levitus, S., and Mishonov, A. V., eds., NOAA Atlas NESDIS 73, p. 40 pp.

Martínez-Botí, M. A., Foster, G. L., Chalk, T. B., Rohling, E. J., Sexton, P. F., Lunt, D. J., Pancost, R. D., Badger, M. P. S., and Schmidt, D. N., 2015, Plio-Pleistocene climate sensitivity evaluated using high-resolution CO2 records: Nature, v. 518, no. 7537, p. 49-54. doi. 10.1038/nature14145

Matthiessen, J., Knies, J., Vogt, C., and Stein, R., 2009, Pliocene palaeoceanography of the Arctic Ocean and subarctic seas: Philos Trans A Math Phys Eng Sci, v. 367, no. 1886, p. 21-48. doi. 10.1098/rsta.2008.0203

Mouradian, M., Panetta, R. J., de Vernal, A., and Gélinas, Y., 2007, Dinosterols or dinocysts to estimate dinoflagellate contributions to marine sedimentary organic matter?: Limnol. Oceanogr., v. 52, no. 6, p. 2569-2581. doi. 10.4319/lo.2007.52.6.2569

Müller, J., Massé, G., Stein, R., and Belt, S. T., 2009, Variability of sea-ice conditions in the Fram Strait over the past 30,000 years: Nature Geoscience, v. 2, no. 11, p. 772-776. doi. 10.1038/ngeo665

Müller, J., Wagner, A., Fahl, K., Stein, R., Prange, M., and Lohmann, G., 2011, Towards quantitative sea ice reconstructions in the northern North Atlantic: A combined biomarker and numerical modelling approach: Earth and Planetary Science Letters, v. 306, no. 3-4, p. 137-148. doi. 10.1016/j.epsl.2011.04.011

Müller, P. J., Kirst, G., Ruhland, G., von Storch, I., and Rosell-Melé, A., 1998, Calibration of the alkenone paleotemperature index UK'37 based on core-tops from the 37 eastern South Atlantic and the global ocean (60°N-60°S): Geochimica and Cosmochimica Acta, v. 62, no. 10, p. 1757-1772. doi. 10.1016/S0016-7037(98)00097-0

Ólafsson, J., 1999, Connections between oceanic conditions off N-Iceland, LakeMyvatn temperature, regional wind direction variability and the North Atlantic Oscillation: Rit Fiskideild, v. 16, p. 41-58. doi. n/a

Orvik, K. A., and Skagseth, M. M., 2001, Atlantic inflow to the Nordic Seas: current structure and volume fluxes from moored current meters, VM-ADCP and SeaSoar-CTD observations, 1995-1999: Deep-Sea Research I, v. 48, p. 937-957. doi. 10.1016/S0967-0637(00)00038-8

Otto-Bliesner, B. L., Jahn, A., Feng, R., Brady, E. C., Hu, A., and Löfverström, M., 2017, Amplified North Atlantic warming in the late Pliocene by changes in Arctic gateways: Geophysical Research Letters, v. 44, no. 2, p. 957-964. doi. 10.1002/2016gl071805

Prahl, F. G., and Wakeham, S. G., 1987, Calibration of unsaturationpatterns in long-chain keto compositions for palaeotemperature assesment: Nature, v. 330, p. 367-369. doi. 10.1038/330367a0

Pross, J., and Klotz, S., 2002, Palaeotemperature calculations from the Praetiglian/Tiglian (Plio–Pleistocene) pollen record of Lieth, northern Germany: implications for the climatic evolution of NW Europe.: Global and Planetary Change, v. 34, no. 3, p. 253-267. doi. 10.1016/S0921-8181(02)00119-4

Risebrobakken, B., Andersson, C., De Schepper, S., and McClymont, E. L., 2016, Low-frequency Pliocene climate variability in the eastern Nordic Seas: Palaeogeography, v. 31, p. PA002918. doi. 10.1002/ 2015PA002918.

Rontani, J.-F., Charrière, B., Sempéré, R., Doxaran, D., Vaultier, F., Vonk, J. E., and Volkman, J. K., 2014, Degradation of sterols and terrigenous organic matter in waters of the Mackenzie Shelf, Canadian Arctic: Organic Geochemistry, v. 75, p. 61-73. doi. 10.1016/j.orggeochem.2014.06.002

Rudels, B., Fahrbach, E., Meincke, J., Budéus, G., and Eriksson, P., 2002, The East Greenland Current and its contribution to the Denmark Strait overflow: ICES Journal of Marine Science, v. 59, no. 6, p. 1133-1154. doi. 10.1006/jmsc.2002.1284

Rudels, B., Korhonen, M., Budeus, G., Beszczynska-Moller, A., Schauer, U., Nummelin, A., Quadfasel, D., and Valdimarsson, H., 2012, The East Greenland Current and its impacts on the Nordic Seas: observed trends in the past decade: ICES Journal of Marine Science, v. 69, no. 5, p. 841-851. doi. 10.1093/icesjms/fss079

Sarnthein, M., Bartoli, G., Prange, M., Schmittner, A., Schneider, B., Weinelt, M., Andersen, N., and Garbe-Schönberg, D., 2009, Mid-Pliocene shifts in ocean overturning circulation and the onset of Quaternary-style climates: Climate of the Past, v. 5, p. 269-283. doi. 10.5194/cp-5-269-2009

Sarnthein, M., Pflaumann, U., and Weinelt, M., 2003, Past extent of sea ice in the northern North Atlantic inferred from foraminiferal paleotemperature estimates: Paleoceanography, v. 18, no. 2, p. PA000771. doi. 10.1029/2002pa000771

Schreck, M., Meheust, M., Stein, R., and Matthiessen, J., 2013, Response of marine palynomorphs to Neogene climate cooling in the Iceland Sea (ODP Hole 907A): Marine Micropaleontology, v. 101, p. 49-67. doi. 10.1016/j.marmicro.2013.03.003

Shipboard Scientific Party, 1995, Site 907: Proceedings of the Ocean Drilling Program, Initial Reports, v. 151, p. 57-111. doi. 10.2973/odp.proc.ir.151.105.1995

-, 1996, SITE 907 (Revisited): Proceedings of the Ocean Drilling Program, Initial Reports, v. 162, p. 223-252. doi. doi:10.2973/odp.proc.ir.162.107.1996

Stein, R., Fahl, K., and Matthiessen, J., 2014, Late Pliocene/Pleistocene changes in Arctic sea-ice cover: Biomarker and dinoflagellate records from Fram Strait/Yermak Plateau (ODP Sites 911 and 912): EGU General Assembly, v. 16, p. EGU2014-6895. doi. n/a

Stein, R., Fahl, K., Schreck, M., Knorr, G., Niessen, F., Forwick, M., Gebhardt, C., Jensen, L., Kaminski, M., Kopf, A., Matthiessen, J., Jokat, W., and Lohmann, G., 2016, Evidence for ice-free summers in the late Miocene central Arctic Ocean: Nature Communications, v. 7, p. 11148. doi. 10.1038/ncomms11148

Stein, R., and Stax, R., 1996, Organic Carbon and n-Alkane Distribution in Late Cenozoic Sediments of Arctic Gateways Sites 909 and 911 and their Paleoenvironmental Implications: Preliminary Results: Proceedings of the Ocean Drilling Program, Scientific Results, v. 151, p. 391-405. doi. 10.2973/odp.proc.sr.151.143.1996

Swift, J. H., and Aagaard, K., 1981, Seasonal transitions and water mass formation in the Iceland and Greenland seas: Deep Sea Research Part A. Oceanographic Research Papers, v. 28, no. 10, p. 1107-1129. doi. 10.1016/0198-0149(81)90050-9

Vanneste, K., Uenzelmann-Neben, G., and Miller, H., 1995, Seismic evidence for long-term history of glaciation on central East Greenland shelf south of Scoresby Sund: Geo-Marine Letters, v. 15, p. 63-70. doi. 10.1007/BF01275408

Volkman, J. K., 1986, A review of sterol markers for marine and terrigenous organic matter: Organic Geochemistry, v. 9, no. 2, p. 83-99. doi. 10.1016/0146-6380(86)90089-6

Wang, M., and Overland, J. E., 2012, A sea ice free summer Arctic within 30 years: An update from CMIP5 models: Geophysical Research Letters, v. 39, no. 18, p. L18501. doi. 10.1029/2012gl052868

Weckström, K., Massé, G., Collins, L. G., Hanhijärvi, S., Bouloubassi, I., Sicre, M.-A., Seidenkrantz, M.-S., Schmidt, S., Andersen, T. J., Andersen, M. L., Hill, B., and Kuijpers, A., 2013, Evaluation of the sea ice proxy IP25 against observational and diatom proxy data in the SW Labrador Sea: Quaternary Science Reviews, v. 79, p. 53-62. doi. 10.1016/j.quascirev.2013.02.012

Xiao, X., Fahl, K., and Stein, R., 2013, Biomarker distributions in surface sediments from the Kara and Laptev seas (Arctic Ocean): indicators for organic-carbon sources and sea-ice coverage: Quaternary Science Reviews, v. 79, p. 40-52. doi. 10.1016/j.quascirev.2012.11.028

Xiao, X., Zhao, M., Knudsen, K. L., Sha, L., Eiríksson, J., Gudmundsdóttir, E., Jiang, H., and Guo, Z., 2017, Deglacial and Holocene sea–ice variability north of Iceland and response to ocean circulation changes: Earth and Planetary Science Letters, v. 472, p. 14-24. doi. 10.1016/j.epsl.2017.05.006

Zieba, K. J., Omosanya, K. O., and Knies, J., 2017, A flexural isostasy model for the Pleistocene evolution of the Barents Sea bathymetry: Norwegian Journal of Geology, p. 1-19. doi. 10.17850/njg97-1-01

Zonneveld, K. A. F., Versteegh, G., and Kodrans-Nsiah, M., 2008, Preservation and organic chemistry of Late Cenozoic organic-walled dinoflagellate cysts: A review: Marine Micropaleontology, v. 68, no. 1-2, p. 179-197. doi. 10.1016/j.marmicro.2008.01.015

Supplementary Figures

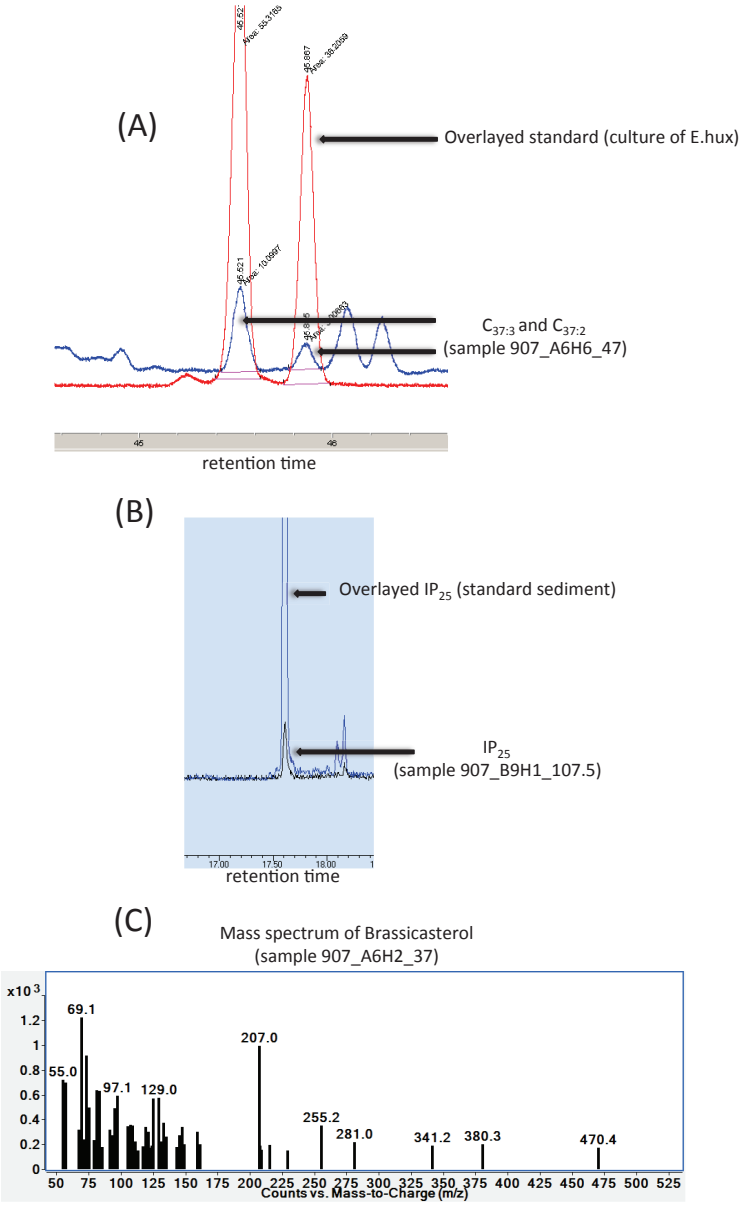

Supplementary Fig. S1: *Examples of identification of $C_{37:3}$ and $C_{37:2}$, IP_{25}, and brassicasterol. (A) GC chromatograms of alkenone standard (from culture experiments, red line) and sample 907_A6H6_47 (blue line); (B) Selected-ion monitoring chromatogram (SIM mode) of ion m/z 350 of the external IP_{25} standard (blue line) and IP_{25} (black line) analyzed from sample 907_B9H1_107.5 (overlaid chromatograms); (C) Mass spectrum of brassicasterol of sample 907_A6H2_37. The samples were selected according to low compound concentrations.*

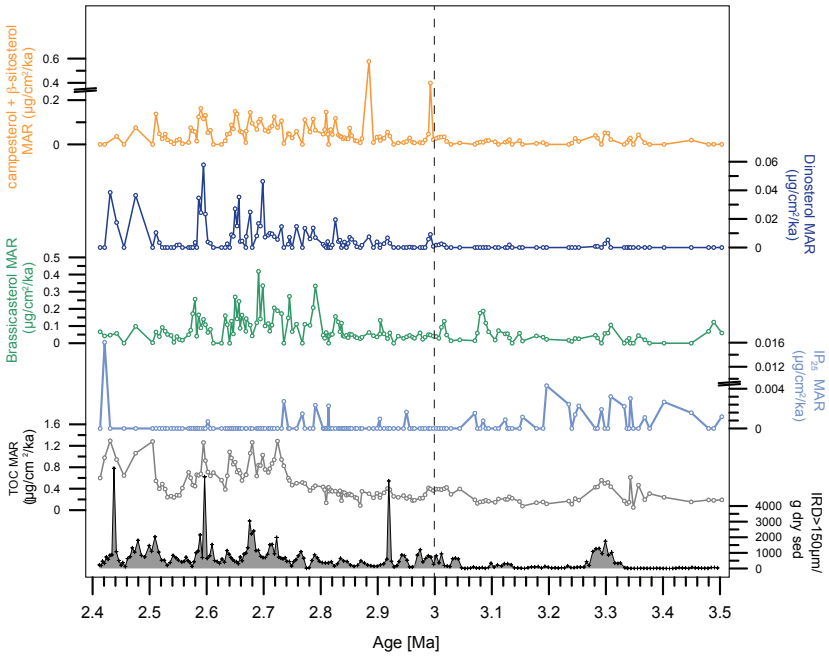

Supplementary Fig. S2: *Marine accumulation rates (MAR) of all biomarkers and total organic carbon (TOC) at ODP Site 907. IRD is shown as IRD (>150 µm) per gram dry sediment.*

7 Appendix

7.1 Paper IV

A part of my data from this thesis has also been used in another research paper. This study investigates the relationship between sea surface temperatures and species relative abundance of extinct dinoflagellate cyst and acritarch taxa from the Neogene of the Iceland Sea (ODP Site 907) by using palynological assemblages and organic geochemical (alkenone) data.
I contributed to this paper by providing alkenone data points, reading and correcting the manuscript.

Neogene Dinoflagellate Cysts and Acritarchs from the high Northern Latitudes and their Relation to Sea Surface Temperature

Schreck, M., Seung-Il, N., **Clotten, C.**, Fahl, K., De Schepper, S., Forwick, M., Matthiessen, J. (2017). Neogene Dinoflagellate Cysts and Acritarchs from the high Northern Latitudes and their Relation to Sea Surface Temperature, *Marine Micropaleontology*. doi.org/10.1016/j.marmicro.2017.09.003

NEOGENE DINOFLAGELLATE CYSTS AND ACRITARCHS FROM THE HIGH NORTHERN LATITUDES AND THEIR RELATION TO SEA SURFACE TEMPERATURE

Michael Schreck[1, 2, *], Nam Seung-Il[2], Caroline Clotten[3], Kirsten Fahl[4], Stijn De Schepper[3], Matthias Forwick[1], Jens Matthiessen[4]

[1] *Department of Geosciences, UiT The Arctic University of Norway in Tromsø, P.O. Box 6050 Langnes, 9037 Tromsø, Norway.*

[2] *Arctic Research Centre, Korea Polar Research Institute, 26 Songdomirae-ro, Yeonsu-gu, 406-840 Incheon, Korea.*

[3] *Uni Research Climate, Bjerknes Centre for Climate Research, Nygårdsgaten 112–114, 5008 Bergen, Norway.*

[4] *Alfred Wegener Institute Helmholtz Centre for Polar and Marine Research, Am Alten Hafen 26, 27568 Bremerhaven, Germany.*

[*] Corresponding author: Michael Schreck, Michael.Schreck@uit.no

Abstract

Organic-walled dinoflagellate cysts and acritarchs are a vital tool for reconstructing past environmental change, in particular in the Neogene of the high northern latitudes where marine deposits are virtually barren of traditionally used calcareous microfossils. Yet only little is known about the paleoenvironmental value of fossil assemblages that do not have modern analogues, so that reconstructions remain qualitative. Thus, extracting their paleoecological signals still poses a major challenge, in particular on pre-Quaternary timescales. Here we unravel the relationship between species relative abundance and sea surface temperature for extinct dinoflagellate cyst and acritarch taxa from the Neogene of the Iceland Sea using palynological assemblages and organic geochemical (alkenone) data generated from the same set of samples. The reconstructed temperatures for the Miocene to Pliocene sequence of Ocean Drilling Program Site 907 range from 3 to 26°C and our database consists of 68 dinoflagellate cyst and acritarch samples calibrated to alkenone data. The temperature range of five extant species co-occurring in the fossil assemblage agrees well with their present-day distribution providing confidence to inferred temperature ranges for extinct taxa. The 14 extinct dinoflagellate cyst and acritarch species clearly exhibit a temperature dependency in their

occurrence throughout the analysed section. The dinoflagellate cyst species *Batiacasphaera hirsuta, Labyrinthodinium truncatum, Cerebrocysta irregulare, Cordosphaeridium minimum, Impagidinium elongatum* and *Operculodinium centrocarpum* s.s., and the acritarch *Lavradosphaera elongatum*, which are confined to the Miocene, have highest relative abundances and restricted temperature ranges at the warm end of the reconstructed temperature spectrum. The latter five species disappear when Iceland Sea surface temperatures permanently drop below 20°C, thus indicating a distinct threshold on their occurrence. In contrast, species occurring in both the Miocene and Pliocene interval (*Batiacasphaera micropapillata, Habibacysta tectata, Reticulatosphaera actinocoronata, Cymatiosphaera*? *invaginata*) show a broader temperature range and a tolerance towards cooler conditions. *Operculodinium*? *eirikianum* may have a lower limit on its occurrence at around 10°C.

The calibration of species relative abundance versus reconstructed sea surface temperature provides a quantitative assessment of temperature ranges for extinct Miocene to Pliocene species indicating that temperature is a decisive ecological factor for regional extinctions that may explain the frequently observed asynchronous highest occurrences across different ocean basins. It demonstrates that qualitative assessments of ecological preferences solely based on (paleo) biogeographic distribution should be treated with caution. In addition to enhancing knowledge on marine palynomorph paleoecology, this study ultimately improves the application of palynomorphs for paleoenvironmental reconstructions in the Neogene of the Arctic and subarctic seas, a region essential for understanding past global climate.

Keywords

Iceland Sea | Neogene | dinoflagellate cyst | acritarch | alkenones | paleotemperatures

Introduction

Due to the nearly complete absence of biosiliceous and calcareous microfossils in Neogene deposits at high northern latitudes, organic-walled marine palynomorphs (dinoflagellate cysts and acritarchs) are important proxies for the establishment of a regional biostratigraphy and paleoenvironmental reconstructions in the Arctic and sub-arctic realm (e.g. Schreck et al., 2012, 2013; De Schepper et al., 2015, 2017). They have been proven particularly useful in upper Quaternary deposits where assemblages are comparable to modern assemblages (de Vernal et al., 2005). The distribution of modern dinoflagellate cysts (dinocysts) at high northern latitudes was first studied on locally restricted data sets, which were subsequently expanded and combined within a Northern Hemisphere reference database that currently comprises 1492 sites (Fig. 1; e.g. de Vernal et al., 2013 and references therein). The present-day n=1492 database documents the relationship between species

relative abundance and observed surface water parameters, which control assemblage composition. This extensive reference dataset has been widely used to quantitatively reconstruct sea surface temperature, salinity, productivity and sea ice cover in upper Quaternary sediments (e.g. Radi and de Vernal, 2008; de Vernal et al., 2001, 2013; Van Nieuwenhove et al., 2016) using transfer functions (e.g. Modern Analogue Technique, Guiot and de Vernal 2007).

Reconstructions of Neogene high latitude paleoceanographic and paleoclimatic variability relies heavily on marine palynomorphs, which are often the only microfossil group with a continuous record in pre-Quaternary sediments in this region. However, when going further back in the Neogene, palynomorph assemblages are increasingly dominated by extinct species of which the ecological affinities are poorly constrained. Therefore, it is of crucial importance to unravel the (paleo)ecology of these Neogene marine palynomorphs in order to improve their application for paleoceanographic studies in a region essential for understanding the Cenozoic transition from greenhouse to icehouse climates.

In the past decades, significant progress has been made in deciphering the paleoecology of extinct species using statistical analyses (e.g. Versteegh and Zonneveld, 1994), the definition of paleoenvironmental indices (Edwards et al., 1991; Versteegh, 1994), and analysis of the biogeographic distribution (Head, 1997; Masure and Vrielynck, 2009; Schreck and Matthiessen, 2013). The derived information, however, solely remains qualitative (e.g. warm/cold, oceanic/neritic). Recently, geochemical proxies for sea surface conditions have been employed to directly assess the paleoecology of extinct species (De Schepper et al., 2011; Hennissen et al., 2017). De Schepper et al. (2011) correlated the relative abundance of extant species to a sea surface temperature (SST) proxy derived from the same sample and then compared to the species' modern temperature distribution using the n=1171 dataset (the n=1492 precursor) of Radi and de Vernal (2008) and a subset thereof. The subset was restricted to 518 samples located mainly in the North Atlantic Ocean between 75°W and 15°E, and north of 25°N, with samples from the Mediterranean and northern part of Baffin Bay being omitted (De Schepper et al., 2011). Based on a dataset containing 204 samples from four drilling sites across the Plio-Pleistocene North Atlantic (Fig. 1), the authors demonstrated a strong correlation between reconstructed and present-day SST ranges of extant species. Because modern species occurring in fossil assemblages have a comparable temperature distribution as today, De Schepper et al. (2011) argued that SST ranges of extinct species could be determined with confidence. Using this approach, they documented past temperature ranges of 16 extinct dinocyst species from the Plio-Pleistocene North Atlantic in their n=204 paleo-database.

Based on this approach, we establish a quantitative relationship between high latitude marine palynomorph species and alkenone-based SST for the Miocene to Pliocene interval of Ocean Drilling Program (ODP) Hole 907A in the Iceland Sea. Both palynological assemblage and organic geochemical data are extracted from the same sample to ensure one-to-one comparability. Therefore,

this study provides independently derived temperature affinities of extinct species, and refines previous ecological interpretations that where solely based on biogeographic distribution and stratigraphic ranges. Ultimately, our study enhances the application of fossil palynomorph assemblages for paleoenvironmental reconstructions in the Neogene of the Arctic and subarctic seas, and improves our understanding of paleoceanographic implications of assemblages that do not have a modern analogue.

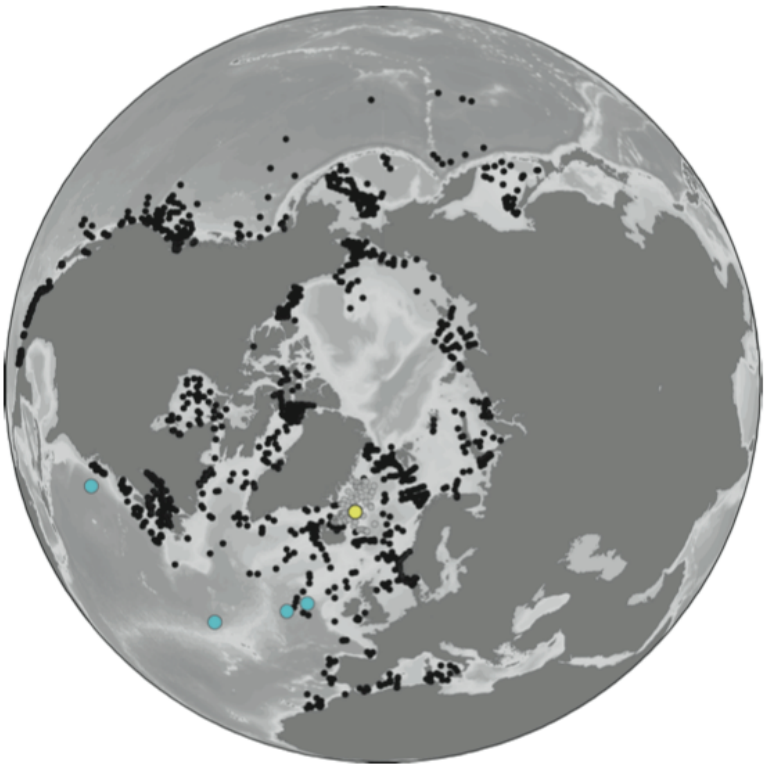

Fig. 1: Location of the study site ODP Site 907 (yellow dot) together with the n=1492 present-day Northern Hemisphere reference database of de Vernal et al., 2013 (black and grey dots) and the n=101 Nordic Seas subset (grey dots only). Blue dots represent the Pliocene to Pleistocene North Atlantic sites of the n=204 paleo-database (De Schepper et al., 2011).

Material and Methods

Material

Located on the eastern Iceland Plateau (69°14.989' N, 12°41.894' W; 2035.7 m water depth; Fig. 1), ODP Hole 907A was drilled in an undisturbed hemipelagic sequence, terminating at a total depth of 224.1 meters below sea floor (Shipboard Scientific Party, 1995). The lithology mainly consists of unlithified silty clay and clayey silt. Five lithostratigraphic units were distinguished based on their siliciclastic, biogenic calcareous, and biogenic siliceous contents (Fig. 2). Unit III is subdivided into

Subunit IIIA which is nannofossil ooze bearing, and Subunit IIIB lacking calcareous nannofossils, but having higher biogenic silica content (Shipboard Scientific Party, 1995).

Previous studies (e.g. Schreck et al., 2012, 2013) used the revised composite magnetostratigraphy of ODP Site 907 (Channell et al., 1999) adjusted to the Astronomically Tuned Neogene Time Scale 2004 (ATNTS 2004, Lourens et al., 2005). Here, we update the paleomagnetic reversals to the Geological Time Scale 2012 (Hilgen et al., 2012), which is identical to the ATNTS 2004 back to 8.3 Ma. The investigated interval spans the entire Pliocene and extends back to the early Middle Miocene. In addition to the 126 samples from Hole 907A, we included five samples from the Pliocene of Hole 907B, resulting in a total of 131 samples analysed for palynology and biomarkers.

Palynology

Subsamples (~ 15 cm^3) were processed using standard palynological techniques including acid treatment (cold HCl [10%], cold HF [38–40%]), but without oxidation or alkali treatments (see Schreck et al., 2012 for details). Two *Lycopodium clavatum* tablets were added to each sample during the HCl treatment to calculate palynomorph concentrations (Stockmarr, 1977). The residue was sieved over a 6 µm polyester mesh and mounted with glycerine jelly on microscope slides.

Six samples from Hole 907A (indicated by asterisk on Fig. 2) and the five sample from Hole 907B (not shown on Fig. 2) were processed by Palynological Laboratory Services Ltd (Holyhead, UK) using a similar processing technique, also without oxidation (details in De Schepper et al., 2017). For those samples, only one *Lycopodium clavatum* tablet was added. The residue was sieved on 10 µm and mounted with glycerine jelly on microscope slides.

Wherever possible, marine palynomorphs have been counted until a minimum of 350 dinocysts had been enumerated. All counts were conducted at 40x and 63x magnification respectively, using a Zeiss Axioplan 2 and Zeiss Axio Imager.A2 microscope. Dinocyst and acritarch nomenclature follows Williams et al. (2017), De Schepper and Head (2008a), Schreck et al. (2012), and Schreck and Matthiessen (2013, 2014). However, in contrast to De Schepper and Head (2008a), we have not distinguished *Operculodinium*? *eirikianum* on variety level. Percentage calculations for dinocysts (Figs. 3, 5–7) are based on the sum of all cysts counted to ensure comparability with previously published data. The relative abundance of acritarchs (Figs. 3 and 8) is based on the total marine palynomorph assemblage (= dinocysts + acritarchs). To evaluate the reliability of relative abundances as a function of total cyst counts and dissemination of individual species, we have calculated the simultaneous confidence intervals (95%) for each sample following Sison and Glaz (1995; Fig. 4). Except for six samples from Hole 907A (indicated with asterisk on Fig. 2) and five samples from Hole 907B (not shown on Fig. 2), all palynological data have previously been published by Schreck et al. (2012, 2013). These data can be accessed at www.pangaea.de via doi:10.1594/PANGAEA.805377 and doi:10.1594/PANGAEA.807134.

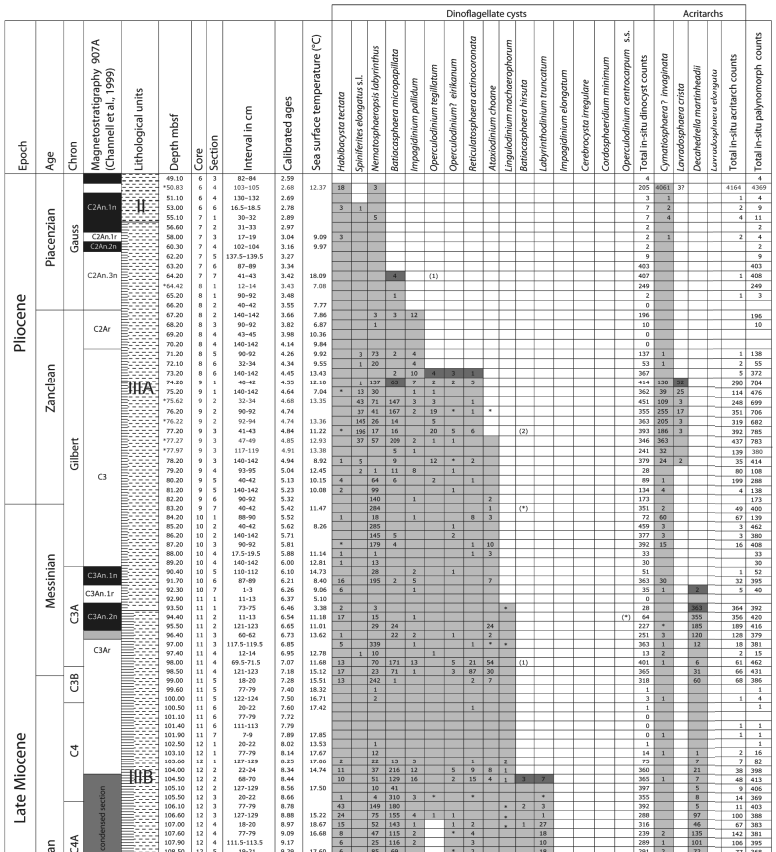

Fig. 2: Raw counts of selected dinocyst and acritarch species (data from Schreck et al., 2013) and their relation to alkenone-based sea surface temperature (data from Schreck et al., 2013; De Schepper et al., 2015; Stein et al., 2016) in ODP Hole 907A. Light shading illustrates the total stratigraphic range and dark shading the first and last occurrence respectively. * = species only encountered outside regular counts, (n) or (*) = suspected reworking. Also shown is the magnetostratigraphy (Channell et al., 1999) and the lithostratigraphic units (Shipboard Scientific Party, 1995) of ODP Hole 907A.

Alkenone paleothermometry

This study uses alkenone SST estimates previously published by Schreck et al. (2013), De Schepper at al. (2015), and Stein et al. (2016), but adds another 11 samples (see above) to the Site 907 SST record (Figs. 2 and 3). All data have been generated in the organic geochemistry laboratory of the Alfred Wegener Institute, Helmholtz Centre for Polar and Marine Research (Bremerhaven, Germany) using the following procedure: bulk sediments (2 to 7g) from the same samples as used for palynology were extracted using accelerated solvent extraction (DIONEX, ASE 200; 100°C, 1000 psi, 15min, solvent dichloromethane). Compounds have been separated by open column chromatography. The composition of alkenones was analysed with a Hewlett Packard HP 6890 gas chromatograph (n=120 samples) and an Agilent 7890A gas chromatograph (n=11 samples). Individual alkenone ($C_{37:3}$, $C_{37:2}$) identification is based on retention time and the comparison with an external standard. The instrument stability has been continuously controlled by reruns of the external alkenone standard (extracted from coccolithophore *Emiliana huxleyi* (Lohman) cultures with known growth temperature) during the analytical sequences. The range of the total analytical error calculated by replicate analyses is less than 0.4°C. The alkenone unsaturation index $U^{K'}_{37}$ and the global core top calibration (Müller et al., 1998) were used to calculate sea surface temperature (SST in °C). We used the Müller et al. (1998) calibration versus summer SSTs. $U^{K'}_{37}$ shows the best statistical relationship to mean annual SST on a global scale (Müller et al., 1998), but coccolithophore production in the modern Nordic Seas is significantly higher (factor of 10) during summer than during autumn to spring due to the availability of light for photosynthesis. This may cause a shift towards a summer bias in temperature (Schröder-Ritzrau et al., 2001; see also discussion below). The summer calibration is similar to the annual mean calibration of Müller et al. (1998) frequently used in the literature, but results in SSTs higher by a constant value of 1.2°C independent of the $U^{K'}_{37}$ value. The standard error of this calibration is reported as ± 0.055 $U^{K'}_{37}$ units or 1.7°C. Due to this uncertainty, we only present integral numbers for the alkenone SSTs. Full details of the method and the reliability of the $U^{k'}_{37}$ index in Neogene deposits of the high northern latitudes are discussed in Schreck et al. (2013) and Stein et al. (2016). The alkenone datasets can be accessed at www.pangaea.de via doi:10.1594/PANGAEA.807107, doi:10.1594/PANGAEA.848671 and, doi:10.1594/PANGAEA.855508.

Comparison database

To test whether extant taxa have a comparable SST distribution in the Neogene as in the modern ocean, we follow the approach of De Schepper et al. (2011) and first compare selected species to the Northern Hemisphere reference database n=1492 (Fig. 1). In a second step, the n=1492 database was restricted to 101 samples (n=101 database) located in the Iceland Sea and adjacent areas (between 67–78°N, and between 10°E–20°W) to provide a spatially confined representation of our study site and to

exclude sites less suitable for comparison. In both datasets species relative abundance is given as a function of summer and winter SSTs derived from the World Ocean Atlas 2001 (WOA01, Stephens et al., 2002). For the purpose of this study, we use the summer (July–September) SSTs given in the WOA01 for comparison as dinoflagellate and coccolithophore production in the Nordic Seas today is mainly restricted to the summer season (e.g. Matthiessen et al., 2005; see discussion below). We refrain from a detailed comparison with the global dataset of modern cyst distribution (Zonneveld et al., 2013), which presently consists of 2405 data points (including the Northern Hemisphere reference database), as it contains sites less suitable for meaningful comparison with our high latitude data.

In addition, the distribution of extant and extinct dinocyst species is compared to the North Atlantic paleo-database of De Schepper et al. (2011) where possible. This dataset compares Plio-Pleistocene dinocyst relative abundances with (spring–summer) SST estimates derived from the same sample by measuring Mg/Ca ratios on the planktonic foraminifera *Globogerina bulloides* (d'Orbigny). It currently comprises 204 samples (n=204 paleo-database) from four DSDP/ODP/IODP sites in the North Atlantic (Fig. 1) spanning the Late Pliocene through Early Pleistocene, and can be accessed at www.pangaea.de via doi:10.1594/PANGAEA.758713.

For most dinocyst species discussed here, however, no previous calibration of relative abundance vs. SST is available. This also applies to the acritarch taxa presented.

Comparability of proxies and general limitations of the approach

The approach used here, i.e. combining marine palynomorph assemblages with geochemical SST reconstructions, has previously been proposed by De Schepper et al. (2011). The authors show that extant species (both dominant and less abundant) occurring in fossil assemblages have a similar temperature distribution compared to today, and that these SST reconstructions can therefore be used to assess temperature ranges of extinct species. In contrast to the study of De Schepper et al. (2011), who used the Mg/Ca ratio of planktonic foraminifera *Globogerina bulloides* as a SST proxy, the virtual absence of planktonic foraminifera in the Miocene-Pliocene section of ODP Site 907 (Shipboard Scientific Party, 1995) prevents the application of the same SST proxy for calibration of species relative abundance. However, previous studies have shown that the alkenone unsaturation index $U^{K'}_{37}$ can be applied to reliably reconstruct SSTs on pre-Quaternary timescales at high northern latitudes (see discussion in Schreck et al., 2013; Stein et al., 2016; Herbert et al., 2016).

While sea surface temperature is the primary ecological factor determining the distribution of dinoflagellates (e.g. Taylor 1987), we note that the relationship between temperature and phytoplankton species abundance might be more complex. In order to compare dinoflagellate cyst abundance, alkenone-based SSTs (this study) and Mg/Ca SSTs (De Schepper et al., 2011), the producing organisms (dinoflagellates, coccolithophores, foraminifera) should have comparable habitat depth and seasonality, as these parameters determine the recorded signal.

1) Habitat depth

All dinocysts discussed here are cysts of phototrophic dinoflagellate species because of fluorescent properties of the cyst wall (cf. Brenner and Biebow, 2001). Apart from temperature, phototrophic dinoflagellates respond to light availability, and consequently they are restricted to the photic zone of the surface waters. Although capable of vertically adjusting their position in the water column, they generally inhabit a shallow and thin surface layer (e.g. Dale, 1996).

Alkenones are biosynthesized by haptophytes (e.g. coccolithophores, Herbert, 2003) and, given their phytoplanktonic source, the alkenone production must originate from the photic zone. Direct measurements of alkenones in the upper water column indicate that the zone of maximum alkenone production is in the isothermal surface mixed layer (0–20m) rather than within the deeper chlorophyll maximum layer (e.g. Rosell-Melé and McClymont, 2007, and references therein). Indeed, calibration of the $U^{K'}_{37}$ is best when using temperatures from 0–10m water depth (Müller et al., 1998), suggesting that temperatures derived from alkenone producing coccolithophores reflect surface conditions.

The planktonic foraminifera *Globogerina bulloides* generally occupies a habitat restricted to the upper 60m in the North Atlantic (Ganssen and Kroon, 2000; Chapman, 2010) and the average calcification depth lies around ± 50 m (Vázquez-Riveiros et al., 2016). Therefore, this species records slightly deeper surface water conditions compared to alkenones.

2) Seasonality of production

In the Nordic Seas, a generally restricted production period has been observed and the export of fossilizable plankton groups (including dinoflagellates, coccolithophores, foraminifera) occurs during 4–6 months of the year. Hence, the signal recorded in the sediments mainly represents the summer to autumn seasons (Schröder-Ritzrau et al., 2001, and references therein).

While studies of dinocysts in surface sediments are numerous, sediment trap studies focussing on the seasonal production of dinoflagellates and their cysts are rare. Most studies are limited to coastal marine environments, upwelling regions and very restricted marine settings such as fjords and inlets. While on global scale dinoflagellate cyst relative abundance in surface sediments shows a good correlation to summer, autumn and annual mean SSTs (Zonneveld et al., 2013), in the Arctic and Subarctic realm dinoflagellates undergo a pronounced seasonal cycle in production. They are most abundant during summer due to the prevailing light regime and nutrient availability, but never during the spring bloom (see Matthiessen et al., 2005, and references therein). Indeed, the few sediment trap studies from the high latitudes revealed a trend towards summer production of dinoflagellate cysts (e.g. Dale and Dale, 1992; Howe et al., 2010; Heikkilä et al., 2016). Therefore, we consider dinoflagellate cysts as recorders of summer surface conditions in the study area.

The same limitations as discussed for dinocysts also apply to production of coccolithophores in high latitude settings. In the modern Nordic Seas, the production of coccolithophores is significantly higher (factor of 10) during summer than in the non-production period from late autumn to early summer due to the availability of light for photosynthesis (Andruleit, 1997; Schröder-Ritzrau et al., 2001), and high cell densities are usually not observed before August (Samtleben et al., 1995). This is also documented by the vertical flux of coccolithophores recorded in sediment traps (Samtleben and Bickert, 1990). Therefore, we interpret the alkenone-derived SSTs to reflect summer SSTs in the study area.

The foraminifer *Globogerina bulloides* reflects the northward migrating North Atlantic spring bloom, February-March between 30° and 40°N, and May-June at higher latitudes (Ganssen and Kroon, 2000). In fact, recently published isotopic temperatures suggest *G. bulloides* to calcify their tests during the summer season between 40–60°N (Vázquez-Riveiros et al., 2016). In the eastern North Atlantic it reaches highest abundances in late spring and summer (Chapman, 2010). Therefore, De Schepper et al. (2011) discussed this species as a recorder of spring to summer SSTs in the North Atlantic n=204 paleo-database. The SST estimates presented by De Schepper et al. (2011) are derived using the North Atlantic calibration of Elderfield and Ganssen (2000).

3) Limitations of the approach

Despite the fact that dinoflagellate cysts and alkenone producing coccolithophores have a comparable habitat and seasonality in the study area, certain limitations apply to this approach. In particular, dispersal with ocean currents has to be considered when comparing fossil and modern species distribution (Dale and Dale, 1992), but also alkenone distribution (e.g. Mollenhauer et al., 2005) The East Greenland current flowing along the Greenland continental shelf and slope is the main oceanographic feature influencing the Iceland Sea (e.g. Blindheim and Østerhus, 2005). Its north to south configuration limits lateral transport from the Greenland fjords and shelf into the open waters of the study site. Indeed, palynological assemblages of ODP Site 907 indicate an open ocean environment throughout most of the analysed interval with only occasional input from the outer shelf (De Schepper et al., 2015). Thus, ODP Site 907 reflects local conditions with only minimal influence by oceanic transport. Another bias to the fossil assemblage may be introduced by species-selective degradation (e.g. Zonneveld et al., 2008). However, this factor does not exert a major influence on the ODP Site 907 palynomorph assemblages in the productive intervals of both the Miocene and the Pliocene (see Schreck et al., 2013 for discussion). Finally, the overall SST range reconstructed for ODP Site 907 (3–26°C) is largely comparable to that in the present-day n=1492 database (-1.8–30.5°C, de Vernal et al., 2013) and the Plio-Pleistocene North Atlantic paleo-dataset (7.7–25.2°C, De Schepper et al., 2011). However, our dataset contains more samples from the presumably warmer Middle to Late Miocene than from the cooler Pliocene, thus partially introducing an offset towards

higher SSTs when compared to the modern n=1492 and n=101 reference datasets (de Vernal et al., 2013). Therefore, we may record the warm end of species distribution rather than its minimum SST requirements. Due to these limitations, we refrain from defining exact upper and lower temperature limits for the occurrence of extinct species, but rather provide temperature ranges in which extinct species occurred based on independently derived SST estimates. We note that additional data from different sites needs to be incorporated into the developing paleo-database to allow for more precise assessment of species temperature affinities.

Results and Discussion

Alkenone sea surface temperatures

The alkenone SST data used here represent a stack record of data previously published by Schreck et al. (2013), De Schepper at al. (2015) and Stein et al. (2016). They are discussed in detail in the respective publications. In addition, this study adds 11 samples with alkenone-based SST estimates to the ODP Site 907 record. In summary, 86 of the 131 analysed samples yielded sufficient alkenones to allow the application of the $U^{k'}_{37}$ index to calculate summer SST. The $U^{k'}_{37}$ index varies from 0.116 to 0.863, which translates into SSTs ranging from 3 to 26°C (Figs. 2–3). Modern mean annual SSTs are 2°C at the study site while summer SSTs are 5°C (Fig. 3). Thus, the ODP Site 907 record suggests warmer than present-day conditions throughout most of the analysed interval. Highest temperatures are observed in the Middle Miocene. SSTs subsequently decrease towards the end of the latest Pliocene (Figs. 2–3), where SSTs close to modern values have been recorded. The long-term temperature evolution in the Iceland Sea therefore follows the general global Neogene cooling trend (Zachos et al., 2008). However, samples with low amounts of alkenones preventing a reliable calculation of the $U^{k'}_{37}$ index cluster in the early Middle Miocene (Langhian stage) and latest Pliocene. The Late Pliocene interval coincides with samples almost barren of palynomorphs (Figs. 2–3; Schreck et al., 2013) and diatoms (Stabell and Koç, 1996), which has been assigned to a combination of factors such as sea ice cover, nutrient availability, bottom water ventilation and selective degradation in relation to waxing and waning of the Greenland Ice Sheet. That may also account for the low amounts of alkenones. In contrast, the Langhian (Middle Miocene) samples are characterized by high palynomorph and diatom abundance and diversity, so that the controlling factors for the low alkenone abundance remains speculative.

Dinoflagellate cysts and acritarchs

The details and raw data of the palynological investigation are presented in Schreck et al. (2013) and summarized together with our new data in Figs. 2–3. Several species exhibit restricted stratigraphic ranges with well-defined range tops. This is exemplified in clusters of highest occurrences (HO) in the early Late Miocene and Early Pliocene (Fig. 3). From the 86 samples with SST estimates (see above)

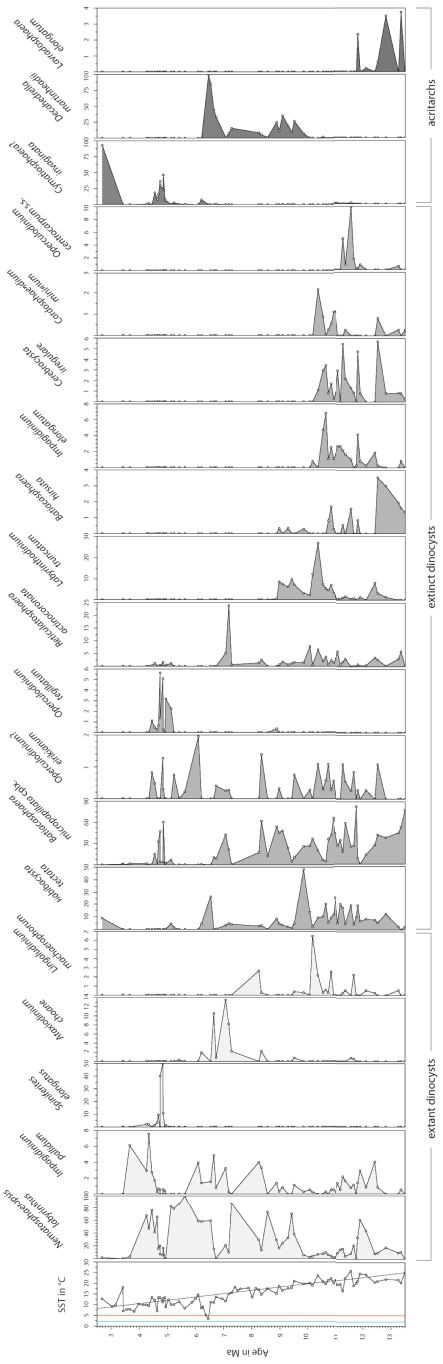

Fig. 3: Relative abundance of extant and extinct dinoflagellate cysts and acritarchs in ODP Site 907. Also shown is the reconstructed alkenone sea surface temperature (SST in °C). Black line depicts the gradual cooling trend observed in ODP Site 907. Red line presents the present-day sea surface temperature in the sudy area, while the blue line presents the present-day annual mean sea surface temperature.

18 were virtually barren (< 50 palynomorphs counted, Fig. 2). These 18 samples have been removed from the dataset due to the large statistical uncertainty introduced by the low number of counts. Of the remaining 68 samples, 48 samples yielded more than 350 cysts while 7 samples contained less than 150 cysts (Figs. 2 and 4). In order to account for the variability in the number of counts per sample and to evaluate the statistical error it introduces, we have calculated the simultaneous confidence interval (95%) for each sample using the method of Sison and Glaz (1995), which takes the total number of counts per sample into account, but also the distribution of counts for each individual species. This corresponds to confidence intervals on the relative abundance of ± 0.6 to ± 12.9% in any given sample, and an average of 5.3% on the entire dataset (Fig. 4). In general, higher count numbers result in smaller confidence intervals (represented by larger dots in Figs. 5–8) and are thus more reliable. This allows to objectively assess the reliability of the relative abundance and avoid over-interpretation.

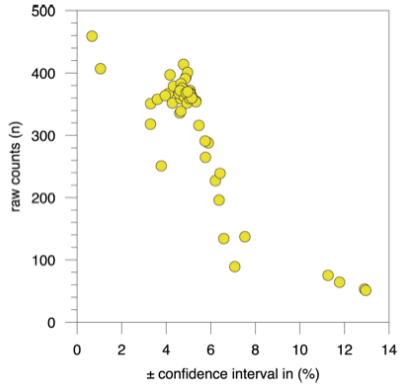

Fig. 4: The calculated simultaneous confidence interval (95%) using the method of Sison and Glaz (1995) for all samples in our Miocene-Pliocene database (n=68). Samples with less than 50 palynomorph counts have been omitted from that figure. Larger confidence intervals (i.e. less reliable samples) are represented by smaller dots in Figs. 4–7.

In summary, this study provides 68 samples with marine palynomorph relative abundance calibrated to SST estimates from the Miocene through Pliocene. The temperature affinities of extinct species discussed in the text are summarized in Fig. 9.

Extant dinoflagellate cysts

Even though extant species are recorded almost continuously in the Middle Miocene to Late Pliocene of ODP Site 907, their relative abundances are usually low (< 1%) thus rendering conclusions on their paleoecology difficult. Extant species recorded include *Bitectatodinium tepikiense, Impagidinium aculeatum, Impagidinium patulum, Impagidinium strialatum, Operculodinium israelianum, Selenopemphix nephroides, Tectatodinium pellitum* and several *Brigantedinium* species. Only *Nematosphaeropsis labyrinthus*, *Impagidinium pallidum, Ataxiodinium choane, Spiniferites elongatus* s.l. and *Lingulodinium machaerophorum* occur continuously and in higher relative abundances (up to ~ 80%) in parts of the analysed interval, and are hence discussed here (Fig. 5). Species abundance is plotted against alkenone-based SSTs (yellow dots) and compared with their modern distribution in the Northern Hemisphere reference dataset (black and grey dots) and the n=101 subset (grey dots only). The present-day data are plotted as a function of summer SST derived from the WOA01 (Stephens et al., 2001) because they provide the best comparison with our alkenone-based SSTs, which reflect

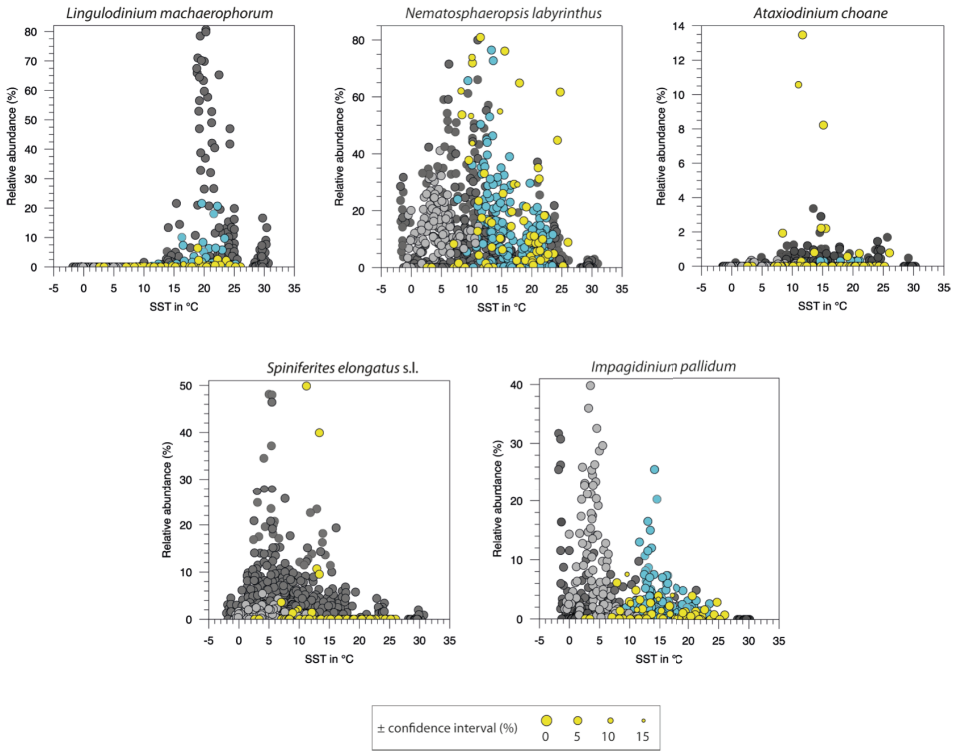

Fig. 5: Relative abundance (in %) of extant dinoflagellate cysts in relation to sea surface temperatures (SST in °C). Species relative abundance (yellow dots) is plotted against alkenone-based SST. Species relative abundance in the modern ocean (n=1492 = black and grey dots, n=101 = grey dots only) is plotted against present-day summer SST derived from the World Ocean Atlas 2001 (Stephens et al., 2002). For the Pliocene-Pleistocene n=204 paleo-database (blue dots) species relative abundances is plotted vs. foraminiferal Mg/Ca-derived (spring-summer) SST (De Schepper et al., 2011).

summer temperatures at the study site (see discussion above). In addition, we compare their Miocene-Pliocene distribution with that observed in the n=204 paleo-dataset from the Plio-Pleistocene North Atlantic (blue dots), where species relative abundance is plotted against Mg/Ca spring-summer SST (De Schepper et al., 2011).

At ODP Site 907, *Lingulodinium machaerophorum* is restricted to the comparatively warm Miocene, where it occurs at SSTs ranging from 15 to 24°C (Fig. 5). This compares favourably with its distribution in the present-day n=1492 database where it is restricted to SSTs between 14 to 30°C (de Vernal et al., 2013), and also with its distribution in the Plio-Pleistocene North Atlantic where it mainly occurs between 16 to 24°C (De Schepper et al., 2011). *Lingulodinium machaerophorum* is a temperate to tropical species today (Zonneveld et al., 2013) and accordingly has not been observed in the n=101 subset from the Nordic Seas, where present-day summer SSTs are around 5°C. It is only a minor component of the ODP Site 907 dinocyst record and thus the data has to be treated with caution due to the uncertainties related to the low numbers of counts. However, our paleo-dataset suggests a

preference for warm waters during the Neogene in accordance with its present-day and its Plio-Pleistocene distribution, indicating a similar lower limit on its occurrence as observed today (> 15°C).

Nematosphaeropsis labyrinthus exhibits a broad temperature range in both the Mio-Pliocene Iceland Sea (Fig. 5, 7–26°C) and the modern ocean (-1.8–30°C). Its Neogene distribution compares particularly well at the warm end of its temperature distribution with both present-day datasets (n=1492 and n=101), but clearly misses elevated relative abundances below 5°C. A similar distribution is observed in the n=204 paleo-database (De Schepper et al., 2011), which compares favourably with our data. However, both paleo-datasets (n=204 and this study), do not facilitate comparison at the lowermost end of this species present day SST range as they only contain two samples with temperatures < 5°C compared to the strong representation of this temperature interval in the modern dataset. Nonetheless, it is interesting to note that *N. labyrinthus* becomes successively more abundant over the course of the gradual Neogene cooling observed in ODP Hole 907A (Fig. 3). Besides few exceptions, however, relative abundances > 40% are confined to the interval from 8 to 15°C in both paleo-datasets, while such relative abundances are observed between 7–12°C in the present-day distribution of this cosmopolitan species.

Ataxiodinium choane occurs in subpolar to temperate regions of the Northern Hemisphere today and has been rarely observed in the Southern Hemisphere (Zonneveld et al, 2013). In the Mio-Pliocene of the Iceland Sea, it occurs at temperatures ranging from 8 to 21°C, exceptionally as high as 26°C, which is similar to its present-day distribution in the n=1492 database (0–25°C, Fig. 5, de Vernal et al, 2013), in particular at the warm end of its temperature distribution. It can apparently occur at lower temperatures today (< 5°C) but then it is only rare (< 1%). *Ataxiodinium choane* accounts for up to 3% of the modern dinocyst assemblage but constitutes as much as 8–14% of the dinocyst assemblage in the Neogene of the Iceland Sea. It is important to note that its maximum relative abundance at the study site is related to similar SSTs (10–15°C) as its maximum abundance in the modern ocean, thus lending confidence to our reconstruction. In the Plio-Pleistocene North Atlantic this species is only a rare component of the dinocyst assemblage (< 0.5%, data supplement in De Schepper et al., 2011), but it occurs at temperatures ranging from 11 to 21°C in the n=204 paleo-database, thereby more or less supporting our Mio-Pliocene temperature assessment.

In the modern ocean, *Spiniferites elongatus* s.l. is a polar to subtropical species restricted to the Northern Hemisphere (Zonneveld et al., 2013). It occurs at SSTs ranging from -1.8 to 25°C (Fig. 5), occasionally as high as 30°C, but has highest relative abundances (> 10%) between 2 and 15°C (de Vernal et al., 2013). At ODP Site 907, *S. elongatus* s.l. is mainly confined to the cooler Pliocene interval and is present in only two samples from the Miocene. It occurs at restricted SSTs between 7 to 13°C, and is particularly abundant between 5–4 Ma when ODP Site 907 received increased IRD input (Fronval and Jansen, 1996), which may suggest a tolerance for colder surface waters similar to its present-day distribution.

In contrast, the Middle Miocene to Pliocene record of *Impagidinium pallidum* suggests a preference for warmer conditions than its distribution in the modern ocean. Today this species occurs at SSTs ranging from -2.1 to 25.7°C (Zonneveld et al., 2013), but is most abundant (> 10% of the assemblage) in the Northern Hemisphere at SSTs ranging between -1.8 and 6.5°C, clearly suggesting a cold-water affinity (Fig. 5, de Vernal et al., 2013). This species apparently has a similar overall SST range (7–26°C) and reaches highest relative abundance (6–8% of the assemblage) at the colder end of its temperature spectrum (7–10°C) in the Mio-Pliocene Iceland Sea, but does not exhibit increased abundances at similarly lower temperatures as observed in the present-day database. In fact, *I. pallidum* never constitutes more than 10% to the dinocyst assemblage at ODP Site 907, which is in contrast to its high relative abundance in the present-day Iceland Sea (Matthiessen, 1995; Marret et al., 2004). The overall temperature range in the Iceland Sea agrees well with the distribution observed in the Plio-Pleistocene North Atlantic and, in particular, its occurrence at temperatures exceeding 15°C supports the tolerance of *I. pallidum* for higher SSTs in the past as suggested by De Schepper et al. (2011). However, De Schepper et al. (2011) reported highest relative abundances (> 10%) of *I. pallidum* at SST values between 10–15°C only at DSDP Site 610 from the eastern North Atlantic, while in the Iceland Sea it reaches maximum relative abundance at SSTs between 7–10°C, thus being closer to present-day values. Nonetheless, the occurrence of *I. pallidum* at warmer conditions in the geological past, in particular in the eastern North Atlantic, is in clear contrast with its present-day distribution (Fig. 5), which suggests other factors, such as nutrient availability, may play a decisive role in controlling its occurrence. While its present-day distribution reflects affinities with cold and rather oligotrophic environments this might have been different in the past. However, we note that the modern database does not include warm oligotrophic sites. It is worth mentioning, that *I. pallidum* is stratigraphically long-ranging and extends back into at least the Middle Eocene (Bujak, 1984; Head and Norris, 1989). Its existence during those periods, which were much warmer than today, already suggests some tolerance for warmer conditions. Moreover, its longevity, in particular from the late Paleogene to the present-day, also suggests a potential for adaption to changing environments. However, given the fact that *I. pallidum* reaches highest relative abundances in the present-day Nordic Seas and the eastern Arctic Ocean (Matthiessen, 1995), reduced habitat competition in these hostile environments may also explain the observed differences. On the other hand, it may also reflect the existence of two cryptic species and therefore explain the observed differences in distribution. We therefore corroborate the questionable value of *I. pallidum* as a reliable cold-water indicator in older (pre-Quaternary) deposits (this study, De Schepper et al., 2011).

Extinct dinoflagellate cysts

The majority of the Miocene to Pliocene samples of ODP Site 907 is dominated by extinct species. Despite the high diversity of the palynomorph record, however, only 10 dinocyst species continuously

occur in significant numbers to reliably perform a correlation exercise. Most species are rare (< 2% of the assemblage) or occur in a few samples only (see Schreck et al., 2013 for details), thus circumventing conclusions on their ecological affinities. Therefore, only the most relevant species are shown in Figs. 6–7 and 9, and discussed here. All Miocene to Pliocene data (yellow dots) are plotted versus alkenone-derived summer SSTs. *Habibacysta tectata* and *Operculodinium*? *eirikianum* have also been recorded by De Schepper et al. (2011) from the Plio-Pleistocene North Atlantic, hence allow to compare their distribution with the n=204 paleo-database (Fig. 6).

Based on its geographical distribution in the Pliocene of the Labrador Sea, North Atlantic and North Sea basin, *Habibacysta tectata* has been considered a cool-water tolerant (Head 1994) to cold-water species (Versteegh 1994), while recent quantitative data indicate a broader temperature tolerance with a cool-water affinity (De Schepper et al., 2011; Hennissen et al., 2017). This species has also been recorded from the Middle Miocene of the Mediterranean (Jiménez-Moreno et al., 2006), and the upper Miocene of the Gulf of Mexico (as *Tectatodinium* sp. B in Wrenn and Kokinos, 1986) and the Caribbean Sea (Wrenn pers. com. in Head 1994) respectively, suggesting a much wider thermal preference. In Iceland Sea ODP Hole 907A, which covers both the Miocene and the Pliocene, *H. tectata* indeed exhibits a much broader temperature range (8–26°C, Figs. 6 and 9) than in the study of De Schepper et al. (11–17°C, 2011), suggesting that temperature may not be the only factor controlling this species distribution. Even though it can occur at temperatures below 10°C, it clearly shows a centre of distribution at temperatures > 15°C. Given its wide temperature distribution across the Middle Miocene to Pliocene in the Iceland Sea (this study), its more restricted range in the Plio-

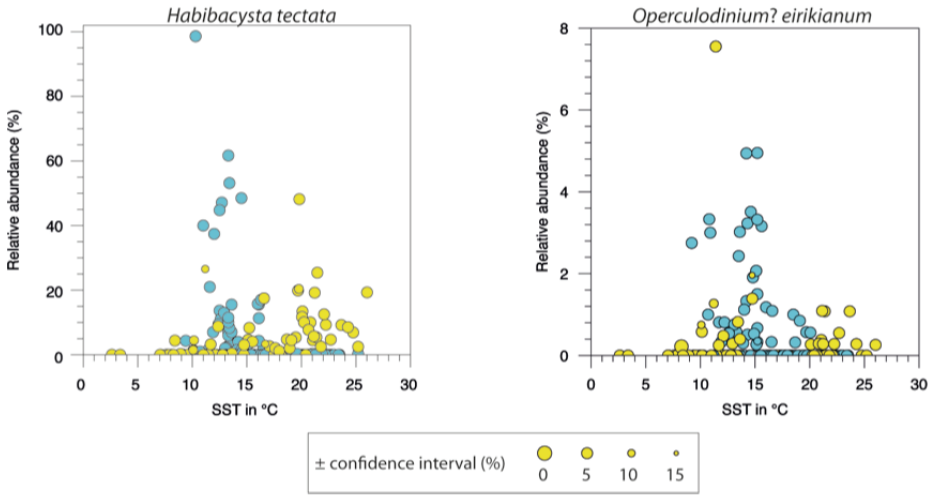

Fig. 6: Relative abundance (in %) of extinct dinoflagellate cysts in relation to sea surface temperatures (SST in °C). Species relative abundance (yellow dots) is plotted against alkenone-based SST, and for the Pliocene-Pleistocene n=204 paleo-database (light blue dots) species relative abundance is plotted vs. foraminiferal Mg/Ca-derived (spring-summer) SST (De Schepper et al., 2011).

Pleistocene North Atlantic and its overall biogeographic distribution ranging from subtropical/tropical (in the Miocene) to subpolar (in the Plio-Pleistocene), this may suggest an adaptation of this species towards cooler conditions occurring in concert with the general global cooling observed during the Neogene, with optimum temperatures > 15°C. Based on the clear decrease in relative abundance around 10°C, and comparable to the conclusion of Hennissen et al. (2017) we consider *H. tectata* as a cold-tolerant species rather than a strictly cold-water indicator.

Operculodinium? *eirikianum* is only a minor component of the Mio-Pliocene palynomorph assemblage in the Iceland Sea, and thus conclusions should be treated with caution. However, similarly low counts of *O.*? *eirikianum* have been reported from the Miocene and Pliocene of the North Atlantic and North Sea basin suggesting this species is typically a minor but consistent component of Neogene assemblages (e.g. Louwye, 2002; Louwye et al., 2007; Louwye and De Schepper et al., 2010; De Schepper et al., 2011; Quaijtaal et al., 2014). It is present from 8 to 26°C in the Mio-Pliocene of the Iceland Sea (Figs. 6 and 9), but in significant numbers (> 5%) only in one sample at 12°C, thus clearly restricting interpretations of its paleoecological preferences. Nonetheless, the lower limit of distribution compares well with the n=204 North Atlantic paleo-database where both subspecies (*O.*? *eirikianum* var. *eirikianum* and *O.*? *eirikianum* var. *crebrum*) have not been recorded at SSTs below 9°C (De Schepper et al., 2011). This may suggest a certain temperature threshold on its occurrence and supports the interpretation of this species being cold-intolerant (Head, 1997).

The species stratigraphically restricted to the Miocene (*Cerebrocysta irregulare, Cordosphaeridium minimum, Operculodinium centrocarpum* s.s., *Impagidinium elongatum, Batiacasphaera hirsuta, and Labyrinthodinium truncatum*) all show a preference towards higher temperatures (Figs. 7 and 9). *Cerebrocysta irregulare*, *Cordosphaeridium minimum, Operculodinium centrocarpum* s.s. and *Impagidinium elongatum* are all confined to the early Late Miocene and occur at SSTs between 19 and 26°C, with only one sample recorded at a lower temperature (16°C) outside this restricted SST range. All four species disappear around 10.5 Ma when temperatures permanently drop below 20°C (Figs. 2–3). In addition, siliciclastic sedimentation becomes predominant and the first drop stone is recorded at the study site (Shipboard Scientific Party, 1995). This suggests incisive environmental changes in the study area causing these species to disappear. It seems likely that a critical temperature threshold on the occurrence of these species might have been crossed, but a lower temperature limit cannot be assessed with certainty based on the limited data available. Similarly, *Batiacasphaera hirsuta* persistently occurs with relative abundances greater than 1% of the dinocyst assemblage at SSTs in excess of 20°C (Fig. 7). In contrast to *C. irregulare*, *C. minimum, O. centrocarpum* s.s., and *I. elongatum*, which all disappear around 10.5 Ma, *B. hirsuta* still occurs, although sporadically and in very low numbers only, at temperatures as low as 16°C until its highest occurrence (HO) in ODP Hole 907A at around 8.5 Ma (Figs. 2–3). *Labyrinthodinium truncatum*

clearly shows a centre of distribution at SSTs between 16 and 22°C, occasionally occurring at even higher temperatures (Figs. 7 and 9). It has a similar stratigraphic range as *B. hirsuta*, but in contrast to the latter it occurs continuously and in greater numbers until its HO around 8.5 Ma (Fig. 3). While the contemporaneous disappearance suggests a similar temperature threshold for the occurrence of both species, *L. truncatum* appears to be more tolerant towards cooler conditions than *B. hirsuta* judged by its higher relative abundances.

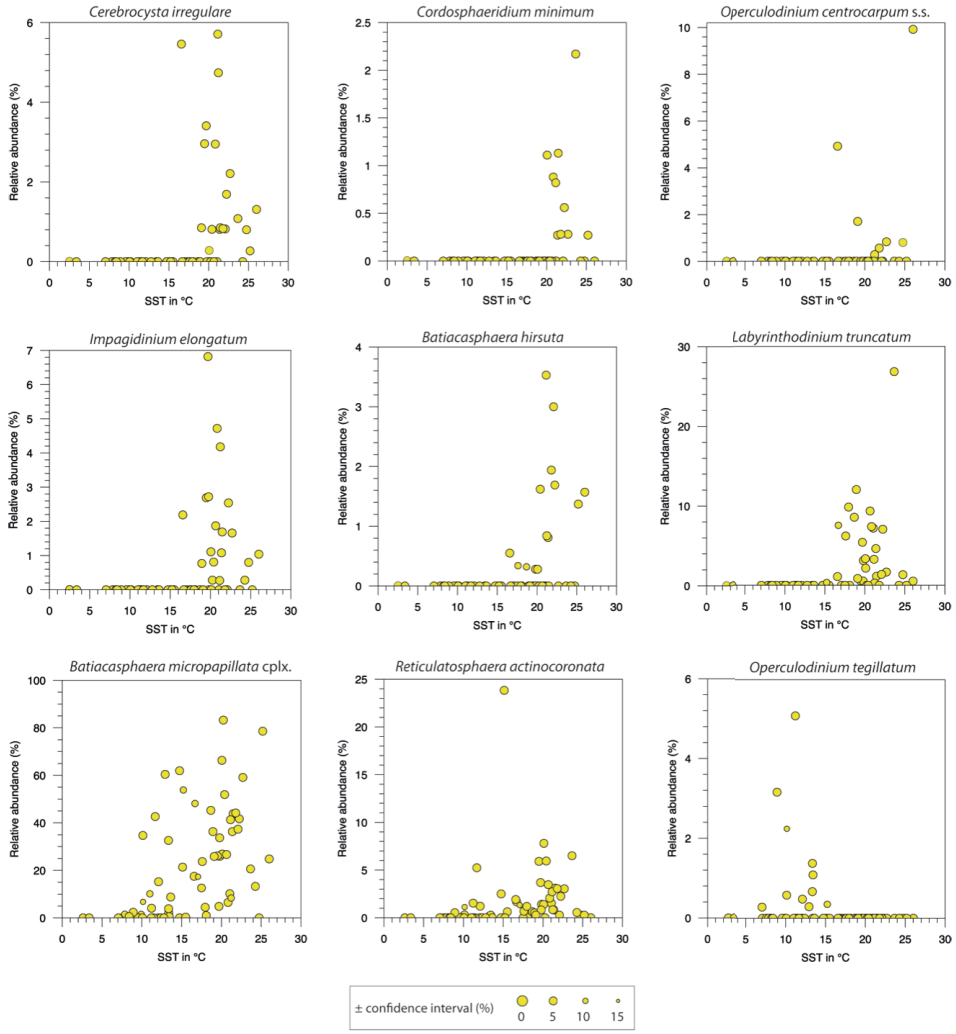

Fig. 7: Relative abundance (in %) of extinct dinoflagellate cysts in relation to sea surface temperatures (SST in °C). Species relative abundance (yellow dots) is plotted against alkenone-based SST.

All six Miocene species exhibit very restricted temperature ranges in ODP Hole 907A, but with distinctively varying thermal affinities indicating a strong individual adaptation to the warm conditions prevailing during most of the Miocene. *Cerebrocysta irregulare*, *C. minimum, O. centrocarpum* s.s. and *I. elongatum* disappear in an interval when the first drop stone is observed and temperatures constantly drop below 20°C, suggesting an intolerance towards cooler conditions. *Batiacasphaera hirsuta* and *L. truncatum* occur at SSTs as low as 16°C, the latter probably being more tolerant to these temperatures judged by its higher relative abundances. However, none of the six taxa has been recorded at temperatures lower than 15°C clearly suggesting them all to be warm-water species. They all disappear from the Nordic Seas and the North Atlantic in the early Late Miocene in concert with general Neogene climate deterioration (Figs. 2–3).

In contrast, the *Batiacasphaera micropapillata* complex and *Reticulatosphaera actinocoronata,* which both range up into the Early Pliocene across the North Atlantic, occur at a much broader temperature range (Figs. 7 and 9). The *B. micropapillata* complex ranges from 8 to 26°C, but highest relative abundances are recorded at the warm end of the SST spectrum reconstructed for Iceland Sea ODP Site 907. It contributes to the dinocyst assemblage at temperatures below 10°C, but relative abundance only starts to increase at SSTs > 10°C. Previous interpretations of this species complex as being warm- to cool-temperate based on its (paleo) biogeographic distribution (Schreck and Matthiessen, 2013) may have to be reconsidered since high relative abundances at SSTs in excess of 15°C clearly suggests a warm water affinity. *Reticulatosphaera actinocoronata* has a similar temperature range and occurs at SSTs between 9 and 25°C. Relative abundances of 2.5% and above are usually associated with SST values greater than 18°C and it only occurs sporadically at temperatures lower than 15°C. This indicates a lesser tolerance of this species versus colder waters compared to the *B. micropapillata* complex, which is still common (e.g. > 10%) at SSTs between 10 and 15°C (Fig 3). In addition, *R. actinocoronata* disappears earlier than the *B. micropapillata* complex across the North Atlantic during Pliocene cooling supporting the interpretation of *R. actinocoronata* being less tolerant towards colder conditions. However, both taxa tolerate a wide range of temperatures, thus favouring their cosmopolitan distribution in the Neogene (see Schreck et al., 2012, and references therein). Both species disappear in the Iceland Sea during the Early Pliocene in concert with a fundamental reorganisation of the Nordic Seas surface circulation (Schreck et al., 2013; De Schepper et al., 2015).

Operculodinium tegillatum is only a minor constituent of the dinocyst assemblage at ODP Site 907, and interpretations should thus be considered tentative. It is largely confined to the Early Pliocene interval and only occurs sporadically in the warmer Miocene (Figs. 2–3). It exhibits a restricted temperature range and its occurrence is related to SSTs between 7 and 15°C (Figs. 7 and 9), indicating a tolerance versus cool-temperate conditions. We note, however, that occurrences at both ends of the temperature spectrum are confined to very low relative abundances. Contemporaneously

with *B. micropapillata* and *R. actinocoronata*, this species disappears at 4.5 Ma from the record of ODP Hole 907A (Fig. 3). This disappearance event has been related to a general reorganisation of surface water circulation in the entire Nordic Seas (De Schepper et al., 2015). As these changes in oceanographic conditions certainly affected different surface water mass properties, it leaves the question whether species disappearance is exclusively a function of temperature (e.g. cooling). As all three species have slightly different thermal preferences it seems likely that other factors such as salinity and nutrient availability also played a crucial role in their coeval disappearance.

Acritarchs

Due to their small size, unknown biological affinity and challenging taxonomy, acritarchs have often received considerably less attention than dinocysts during palynological analyses, in particular during stratigraphic studies, resulting in a loss of information (De Schepper and Head, 2014). However, significant progress in their taxonomy has been made over the last two decades, and their stratigraphic and paleoenvironmental value is progressively explored. The fossil acritarch genera *Cymatiosphaera* and *Lavradosphaera* have been frequently recorded in the Neogene of the high northern latitudes and exhibit high relative abundances in certain intervals where they may even outnumber the dinocysts (de Vernal and Mudie, 1989; Piasecki, 2003; De Schepper and Head, 2014; Schreck et al., 2013). Despite providing valuable biostratigraphic marker events (Matthiessen et al., 2009; De Schepper and Head, 2014; Mattingsdal et al., 2014; Grøsfjeld et al., 2014), the application of these high abundance intervals (acmes) for paleoenvironmental reconstructions is still restricted due to limited knowledge on their paleoecological implications. At ODP Site 907, acritarchs occur throughout most of the analysed interval and contribute substantially to the palynomorph assemblage (Figs. 2–3). Unfortunately, the Middle Miocene assemblage is dominated by various spinous forms that could not be assigned to a particular genus but have only collectively been referred to as acanthomorphic acritarchs (Schreck et al., 2013), and are hence not discussed here.

Lavradosphaera elongata is restricted to the Middle Miocene in ODP Site 907 and its highest occurrence in the upper Serravallian (Figs. 2–3) has been related to the global Mi-5 cooling event leading to the interpretation of *L. elongata* being a warm-temperate species (Schreck and Matthiessen, 2014). Indeed, its occurrence is confined to SSTs higher than 20°C (Figs. 8–9) indicating a warm water preference. It exhibits a restricted temperature range between 20 and 24°C suggesting an adaptation to warmer surface waters, which likely explains its disappearance during times of high latitude cooling. However, this species has only been recorded in the Iceland Sea to date and relative abundances are usually low, thus conclusions should be regarded tentative until more data on its distribution are available to validate the temperature range given in this study.

The acritarch *Decahedrella martinheadii* is endemic to the high northern latitudes and an excellent stratigraphic marker for the Late Miocene in the Arctic and sub-arctic seas (Schreck et al.,

2012). Based on its biogeographic distribution it has been considered a cold-water species (Manum, 1997; Matthiessen et al., 2009). Indeed, its first occurrence in Iceland Sea ODP Hole 907A around 10.5 Ma is contemporaneous with the occurrence of the first drop stone, the onset of predominantly siliciclastic deposition at the site (Figs. 2–3, Shipboard Scientific Party, 1995) and a permanent drop of SSTs below 20°C. In combination with simultaneously declining dinocyst diversity and the disappearance of several dinocyst and acritarch taxa, this suggests initiation of cooler surface water conditions in the study area at that time (Schreck et al., 2013). However, alkenone data from ODP Hole 907A indicate a broad temperature tolerance for this species as it occurs at SSTs ranging from 3 to 21°C (Figs. 8–9). Although its presence in significant numbers until 21°C contrasts previous interpretations of this species being a cold-water indicator based on biogeographic distribution, highest relative abundances (> 40% of the total marine palynomorph assemblage [dinocysts and acritarchs]) are found ≤ 12°C. In the central Arctic Ocean, *D. martinheadii* continuously occurs in samples with alkenone SST estimates ranging from 4 to 6°C (Stein et al., 2016), which indicates that, even though this species can tolerate a wide range of temperatures, it is well adapted to colder conditions in the Arctic and subarctic realm.

The genus *Cymatiosphaera* has been assigned to the prasinophytes, which today forms an important element of high latitude phytoplankton communities (Tyson, 1995, and references therein). In modern and Quaternary sediments, prasinophytes (in particular *Cymatiosphaera* species) are often associated with cooler surface waters and/or less saline conditions (Wall and Dale, 1974; Tappan, 1980; Sorrel et al., 2006). In the Pliocene of Iceland Sea ODP Hole 907A, *Cymatiosphaera*? *invaginata* reaches relative abundances > 5% of the total marine palynomorph assemblage at temperatures lower than 15°C (Fig. 8), indeed indicating a cold-water tolerance of this species. The Early Pliocene interval with elevated *C.*? *invaginata* abundance is characterized by severe cooling (Figs. 2–3, De Schepper et al., 2015) and increased occurrence of ice-rafted debris (Fronval and Jansen, 1996), both supporting this interpretation. In the generally warmer Middle Miocene, however,

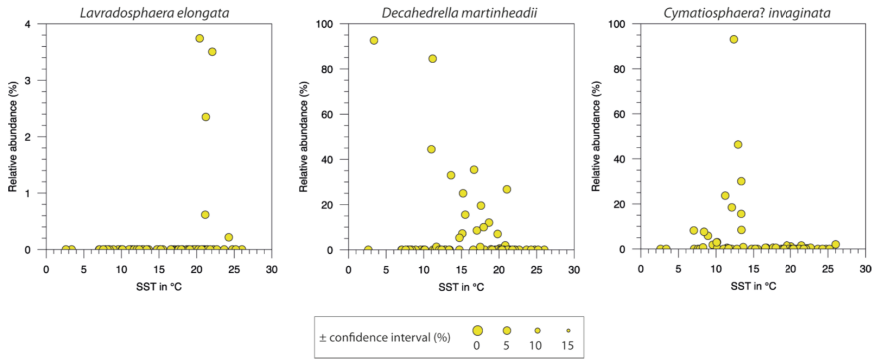

Fig. 8: Relative abundance (in %) of extinct acritarchs in relation to sea-surface temperatures (SST in °C). Species relative abundance (yellow dots) is plotted against alkenone-based SST.

it can occur at temperatures of up to 26°C, but then never exceeds more than 2% of the total marine palynomorph assemblage suggesting an occurrence close to its upper temperature limit. This species apparently tolerates a broad range of temperatures, but relative abundances in ODP Hole 907A clearly suggest an affinity for cooler surface waters.

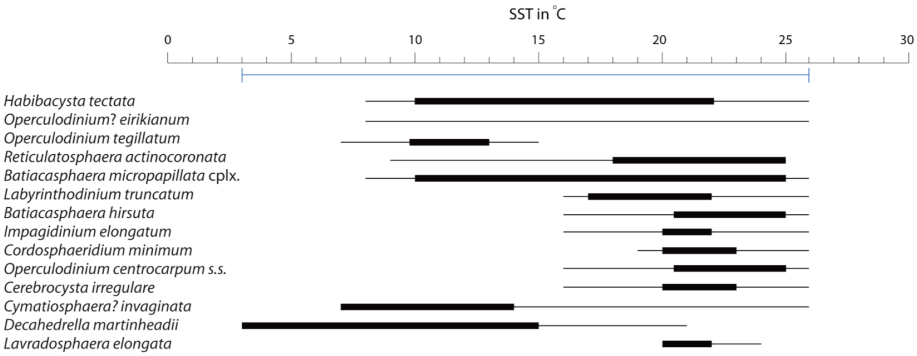

Fig. 9: Summary of the temperature ranges of the extinct dinoflagellate and acritarch species discussed in the text. Highlighted area (back) represents the centre of distribution. Blue line indicates the total reconstructed temperature range in ODP Site 907.

Conclusion

Information on the paleoecology of extinct marine palynomorphs has been mainly derived from their biogeographic distribution and thus, remained qualitative. However, the combination of dinocyst and acritarch assemblages with independently derived alkenone-based SST estimates from the same sample presented here provide an initial quantitative assessment of temperature preferences for Miocene through Pliocene species in a high latitude setting. We refrain from defining exact upper and lower temperature limits for the occurrence of extinct species, but provide temperature ranges in which extinct species may have occurred based on independently derived SST estimates, thus improving previous qualitative assignments that were solely based on biogeographic distribution. Our results indicate that:

- The Miocene dinocyst species *Cerebrocysta irregulare, Cordosphaeridium minimum, Operculodinium centrocarpum* s.s., *Impagidinium elongatum, Batiacasphaera hirsuta and Labyrinthodinium truncatum,* and the acritarch *Lavradosphaera elongata* are restricted to a narrow temperature interval and none of these are recorded at SSTs below 15°C. Therefore, these species are considered as warm-water species. Their disappearance during late Neogene cooling, indicated by a SST decrease and the first drop stone, suggests a strong adaptation to the warmer conditions prevailing during most of the Miocene.
- The stratigraphically higher ranging species *Operculodinium*? *eirikianum*, *Reticulatosphaera actinocoronata*, *Batiacasphaera micropapillata* complex and *Habibacysta tectata* tolerate a

broader temperature range. The latter two taxa still contribute to the palynomorph assemblage at temperatures below 10°C, but our data indicate that *H. tectata* is not a cold-water species as previously suggested based on (paleo)biogeographic distribution. In contrast, *B. micropapillata* complex may have a preference for warmer surface conditions than previously suggested by biogeography. *Operculodinium*? *eirikianum* is considered a cold-intolerant species that may have a lower SST limit for its occurrence at around 10°C.

- The acritarchs *D. martinheadii* and *C.*? *invaginata* have a broad temperature distribution across the Miocene to Pliocene, but high relative abundances at temperatures < 10°C in the Iceland Sea clearly suggest a preference for cooler surface water conditions. Based on our data quantitative data, however, *D. martinheadii* should not be regarded as an indicator for cold waters exclusively.
- The Miocene-Pliocene distribution of the extant *L. machaerophorum*, *N. labyrinthus, A. choane* and *S. elongatus* compares well with its occurrence in the Plio-Pleistocene North Atlantic and in the modern ocean. However, it rather corresponds to the warm end of its distribution in the modern ocean for *S. elongatus* s.l. and *N. labyrinthus*.
- Compared to present-day, the extant *I. pallidum* does not exhibit increased relative abundances at the lower end of its temperature range in both paleo-datasets, but rather show a preference for somewhat warmer waters (> 10°C) in the geological past. We thus question its use as a reliable cold-water indicator in pre-Quaternary sediments.

Although our Miocene to Pliocene record may be slightly biased towards warmer SSTs when compared to the present-day reference database, fossil and modern distribution of extant species is largely comparable. It is in good agreement with the species distribution recorded in the North Atlantic Plio-Pleistocene paleo-dataset (De Schepper et al., 2011) and therefore provides first indications on how to interpret Miocene assemblages with no modern analogue. In particular, when combining the SST range of several individual species it allows to narrow the interval of co-occurrence and thus to infer the prevailing SSTs at the study site (Fig. 9). Our new data complement the previously published paleo-dataset from the North Atlantic and expands its spatial (high northern latitudes) and temporal (into the Miocene) coverage. However, we note that our data represent an initial assignment of paleoecological affinities of extinct Mio-Pliocene species and there is a strong need to further augment data from different sites to this dataset in order to confirm the proposed relationships and to further increase the reliability of ecological assessments of extinct species.

Despite its limitations, this approach helps to decipher the paleoecology of extinct species and improves their application for paleoenvironmental reconstructions, in particular in the high northern latitudes where other microfossil groups are rare to absent. A refined understanding of temperature preferences of Neogene high latitude species and its quantitative assessment will be particularly

important to better understand paleoenvironmental changes in the Arctic Ocean and marginal seas during Earth´s transition from Greenhouse to Icehouse conditions.

Acknowledgments

This research uses samples and data provided by the Ocean Drilling Program. We gratefully thank W. Luttmer (AWI-Bremerhaven) for technical support with the alkenone analyses and M. Jones (Palynological Laboratory Services Ltd, Holyhead, UK) for palynological preparation. MS and JM acknowledge financial support from the German Research Foundation (DFG MA 3913/2), and MS is additionally thankful to the Basic Research Program (No. PE16062) of the Korea Polar Research Institute, and a National Research Foundation of Korea grant from the government of Korea (MSIP) (No. 2014R1A2A2A09049496). SDS and CC acknowledge funding from the Norwegian Research Council (project 229819).

Appendix: List of taxa discussed in the text and their full authorial citations.

Ataxiodinium choane Reid, 1974

Batiacasphaera hirsuta Stover, 1977

Batiacasphaera micropapillata Stover, 1977

Cerebrocysta irregulare Schreck et al., 2012

Cordosphaeridium minimum (Morgenroth, 1966) Benedek, 1972

Habibacysta tectata Head et al., 1989

Impagidinium elongatum Schreck et al., 2012

Impagidinium pallidum Bujak, 1984

Labyrinthodinium truncatum Piasecki, 1980

Lingulodinium machaerophorum (Deflandre and Cookson, 1955) Wall, 1967

Nematosphaeropsis labyrinthus (Ostenfeld, 1903) Reid, 1974

Operculodinium centrocarpum (Deflandre and Cookson, 1955) Wall, 1967

Operculodinium tegillatum Head, 1997

Operculodinium? *eirikianum* Head et al, 1989 emend. Head, 1997

Reticulatosphaera actinocoronata (Benedek, 1972) Bujak and Matsuoka, 1986 emend. Bujak and Matsuoka, 1986

Spiniferites elongatus Reid, 1974

Cymatiosphaera? *invaginata* Head et al., 1989

Decahedrella martinheadii Manum, 1997

Lavradosphaera elongata Schreck and Matthiessen, 2014

References

Andruleit, H., 1997. Coccolithophore fluxes in the Norwegian-Greenland Sea: seasonality and assemblage alterations. Marine Micropaleontology 31, 45–64.

Blindheim, J., Østerhus, S., 2005. The Nordic Seas, main oceanographic features. In: Drange, H., Dokken, T., Furevik, T., Gerdes, R. (Eds.), The Nordic Seas - An integrated perspective. American Geophysical Union, Washington D.C., pp. 11–38.

Brenner, W., Biebow, N., 2001. Missing autofluorescence of recent and fossil dinoflagellate cysts - an indicator of heterotrophy? Neues Jahrbuch für Geologie und Paläntologie - Abhandlungen 219, 229–240.

Bujak, J.P., 1984. Cenozoic dinoflagellate cysts and acritarchs from the Bering Sea and northern North Pacific, DSDP Leg 19. Micropaleontology 30, 180–212.

Channell, J.E.T., Amigo, A.E., Fronval, T., Rack, F., Lehman, B., 1999. Magnetic stratigraphy at Sites 907 and 985 in the Norwegian-Greenland Sea and a revision of the Site 907 composite section. In: Raymo, M.E., Jansen, E., Blum, P., Herbert, T.D. (Eds.), Proceedings of the Ocean Drilling Program, Scientific Results 162. College Station, TX, pp. 131–148.

Chapman, M., 2010. Seasonal production patterns of planktonic foraminifera in the NE Atlantic Ocean: implications for paleotemperature and hydrographic reconstructions. Paleoceanography 25, PA1101. doi:10.1029/2008PA001708.

Dale, B., 1996. Dinoflagellate Cyst Ecology: Modelling and Geological Applications. In: Jansonius, J., McGregor, D.C. (Eds.), Palynology: principles and applications, Vol. 3. AASP Foundation, Dallas, TX, pp. 1249–1275.

Dale, A.L., Dale, B., 1992. Dinoflagellate contributions to the sediment flux of the Nordic Sea. In: Honjo, S. (Eds.), Dinoflagellate contribution to the deep sea. Ocean Biocoenosis Series No. 5, Woods Hole Oceanographic Institution, Massachusetts, pp. 45–75.

Dale, B., Dale, A., 2002. Environmental applications of dinoflagellate cysts and acritarchs. In: Haslett, K. (Eds.), Quaternary environmental micropaleontology. Oxford University Press, London, pp. 207–240.

De Schepper, S., Head, M.J., 2008a. New dinoflagellate cyst and acritarch taxa from the Pliocene and Pleistocene of the eastern North Atlantic (DSDP Site 610A). Journal of Systematic Palaeontology 6, 101–107.

De Schepper, S., Head, M.J., 2008b. Age calibration of dinoflagellate cyst and acritarch events in the Pliocene-Pleistocene of the eastern North Atlantic (DSDP Hole 610A). Stratigraphy 5, 137–161.

De Schepper, S., Head, M.J., 2014. New Pliocene and Pleistocene acritarchs: correlation potential in high latitude oceans. Journal of Systematic Palaeontology 12, 493–519.

De Schepper, S., Fischer, E.I., Groeneveld, J., Head, M.J., Matthiessen, J., 2011. Deciphering the palaeoecology of Late Pliocene and Early Pleistocene dinoflagellate cysts. Palaeogeography, Palaeoclimatology, Palaeoecology 309, 17–32.

De Schepper, S., Schreck, M., Beck, K.M., Matthiessen, J., Fahl, K., Mangerud, G., 2015. Early Pliocene onset of modern Nordic Seas circulation related to ocean gateway changes. Nature Communication 6, doi:10.1038/ncomms9659.

De Schepper, S., Beck, K.M., Mangerud, G., 2017. Late Neogene dinoflagellate cyst and acritarch biostratigraphy for Ocean Drilling Program Hole 642B, Norwegian Sea. Review of Palynology and Palaeobotany 236, 12–32.

de Vernal, A., Mudie, P., 1989. Pliocene and Pleistocene palynostratigraphy at ODP Sites 646 and 647, eastern and southern Labrador Sea. In: Srivastava, S.P., Arthur, M., Clement, B. (Eds.), Proceedings of the Ocean Drilling Program, Scientific Results 105. College Station, TX, pp. 401–422.

de Vernal, A., Henry, J., Matthiessen, J., Mudie, P., Rochon, A., Boessenkool, K.P., Eynaud, F., Grosfjeld, K., Guiot, J., Hamel, D., Harland, R., Head, M.J., Kunz-Pirrung, M., Levac, E., Loucheur, V., Peyron, O., Pospelova, V., Radi, T., Turon, J.L., Voronina, E., 2001. Dinoflagellate cyst assemblages as tracers of sea-surface conditions in the northern North Atlantic, Arctic, and sub-Arctic seas: the new "n=677" data base and its application for quantitative paleoceanographic reconstruction. Journal of Quaternary Science 16, 681–698.

de Vernal, A., Eynaud, F., Henry, M., Hillaire-Marcel, C., Londeix, L., Mangin, S., Matthiessen, J., Marret, F., Radi, T., Rochon, A., Solignac, S., Turon, J.L., 2005. Reconstruction of sea-surface conditions at middle to high latitudes of the Northern Hemisphere during the Last Glacial Maximum (LGM) based on dinoflagellate cyst assemblages. Quaternary Science Reviews 24, 897–924.

de Vernal, A., Rochon, A., Fréchette, B., Henry, M., Radi, T., Solignac, S., 2013. Reconstructing past sea ice cover of the Northern Hemisphere from dinocyst assemblages: status of the approach. Quaternary Science Reviews 79, 122–134.

Edwards, L.E., Mudie, P.J., de Vernal, A., 1991. Pliocene paleoclimatic reconstruction using dinoflagellate cysts: Comparison of methods. Quaternary Science Reviews 10, 259–274.

Elderfield, H., Ganssen, G., 2000. Past temperature and $\delta^{18}O$ of surface ocean waters inferred from foraminiferal Mg/Ca ratios. Nature 405, 442–445.

Fronval, T., Jansen, E., 1996. Late Neogene paleoclimates and paleoceanography in the Iceland-Norwegian Sea: Evidence from the Iceland and Vøring Plateaus. In: Thiede, J., Myhre, A.M., Firth, J.V., Johnson, G.L., Ruddiman, W.F. (Eds.), Proceedings of the Ocean Drilling Program, Scientific Results 151. College Station, TX, pp. 455–468.

Ganssen, G.M., Kroon, D., 2000. The isotopic signature of planktonic foraminifera from NE Atlantic surface sediments: implications for the reconstruction of past oceanic conditions. Journal of the Geological Society 157, 693–699.

Grøsfjeld, K., De Schepper, S., Fabian, K., Husum, K., Baranwal, S., Andreassen, K., Knies, J., 2014. Dating and palaeoenvironmental reconstruction of the sediments around the Miocene/Pliocene boundary in Yermak Plateau ODP Hole 911A using marine palynology. Palaeogeography, Palaeoclimatology, Palaeoecology 414, 382–402.

Guiot, J., de Vernal, A., 2007. Transfer functions: methods for quantitative paleoceanography based on microfossils. In: Hillaire-Marcel, C., de Vernal, A. (Eds.), Proxies in Late Cenozoic Paleoceanography. Elsevier, Amsterdam, pp. 523–563.

Head, M.J., 1994. Morphology and paleoenvironmental significance of the Cenozoic dinoflagellate genera *Tectatodinium* and *Habibacysta*. Micropaleontology 40, 289–321.

Head, M.J., 1997. Thermophilic dinoflagellate assemblages from the mid Pliocene of eastern England. Journal of Paleontology 71, 165–193.

Head, M.J., Norris, G., 1989. Palynology and dinocyst stratigraphy of the Eocene and Oligocene in ODP Leg 105, Hole 647A, Labrador Sea. In: Srivastava, S.P., Arthur, M., Clement, B. (Eds.), Proceedings of the Ocean Drilling Program, Scientific Results 105. College Station, TX, pp. 515–550.

Heikkilä, M., Pospelova, V., Forest, A., Stern, G.A., Fortier, L., Macdonald, R.W., 2016. Dinoflagellate cyst production over an annual cycle in seasonally ice-covered Hudson Bay. Marine Micropaleontology 125, 1–24.

Hennissen, J.A., Head. M.J., De Schepper, S., Groeneveld, J., 2017. Dinoflagellate cyts paleoecology during the Pliocene-Pleistocene transition in the North Atlantic. Palaeogeography, Palaeoclimatology, Palaeoecology 470, 81–108.

Herbert, T., 2003. Alkenone Paleotemperature Determinations. In: Holland, H.D., Turekian, K.K. (Eds.), Treatise of Geochemistry - Volume 6: The Oceans and Marine Geochemistry. Elsevier, Amsterdam, pp. 391–432.

Herbert, T., Lawrence, K.T., Tzanova, A., Peterson, L.C., Caballero-Gill, R., Kelly, C.S., 2016. Late Miocene global cooling and the rise of modern ecosystems. Nature Geoscience 9, 843–847.

Hilgen, F.J., Lourens, L.J., Van Dam, J.A., 2012. The Neogene Period. In: Gradstein, F., Ogg, J., Schmitz, M., Ogg, G. (Eds.), The Geological Time Scale 2012. Elsevier, Amsterdam, pp. 923–978.

Howe, J.A., Harland, R., Cottier, F.R., Brand, T., Willis, K.J., Berge, J.R., Grøsfjeld, K., Eriksson, A., 2010. Dinoflagellate cysts as proxies for palaeoceanographic conditions in Arctic fjords, in: Howe, J.A., Austin, W.E.N., Forwick, M., Paetzel, M. (Eds.), Fjord Systems and Archives. Geological Society of London, London, pp. 61–74.

Jiménez-Moreno, G., Head, M.J., Harzhauser, M., 2006. Early and Middle Miocene dinoflagellate cyst stratigraphy of the Central Paratethys, Central Europe. Journal of Micropalaeontology 25, 113–119.

Lourens, L., Hilgen, F., Shackleton, N.J., Laskar, J., Wilson, J., 2005. The Neogene. In: Gradstein, F.M., Ogg, J.G., Smith, A.G. (Eds.), A Geological Timescale 2004 Cambridge University Press, Cambridge, U.K., 409–430. (Imprinted).

Louwye, S., 2002. Dinoflagellate cyst biostratigraphy of the Upper Miocene Deurne Sands (Diest Formation) of northern Belgium, southern North Sea Basin. Geological Journal 37, 55–67.

Louwye, S., De Schepper, S., 2010. The Miocene–Pliocene hiatus in the southern North Sea Basin (northern Belgium) revealed by dinoflagellate cysts. Geological Magazine 147, 1–17.

Louwye, S., Foubert, A., Mertens, K., Van Rooij, D., and IODP Expedition 307 Scientific Party, 2007. Integrated stratigraphy and palaeoecology of the Lower and Middle Miocene of the Porcupine Basin. Geological Magazine 145, 321–344.

Manum, S.B., 1997. *Decahedrella martinheadii* gen. et sp. nov. - a problematic palynomorph from the Northern Atlantic Miocene. Palynology 21, 67–77.

Marret, F., Eiríksson, J., Knudsen, K.L., Turon, J.-L., Scourse, J.D., 2004. Distribution of dinoflagellate cyst assemblages in surface sediments from the northern and western shelf of Iceland. Review of Palaeobotany and Palynology 128, 35–53.

Masure, E., Vrielynck, B., 2009. Late Albian dinoflagellate cyst paleobiogeography as indicator of asymmetric sea surface temperature gradient on both hemispheres with southern high latitudes warmer than northern ones. Marine Micropaleontology 70, 120–133.

Mattingsdal, R., Knies, J., Andreassen, K., Fabian, K., Husum, K., Grøsfjeld, K., De Schepper, S., 2014. A new 6 Myr stratigraphic framework for the Atlantic–Arctic Gateway. Quaternary Science Reviews 92, 170–178.

Matthiessen, J., 1995. Distribution patterns of dinoflagellate cysts and other organic-walled microfossils in recent Norwegian-Greenland Sea sediments. Marine Micropaleontology 24, 307–334.

Matthiessen, J., De Vernal, A., Head, M.J., Okolodkov, Y., Puerto, A., Zonneveld, K.A.F., Harland, R., 2005. Modern organic-walled

dinoflagellate cysts in Arctic marine environments and their (paleo-) environmental significance. Paläontologische Zeitschrift 79, 3–51.

Matthiessen, J., Brinkhuis, H., Poulsen, N.E., Smelror, M., 2009. *Decahedrella martinheadii* Manum 1997 - a stratigraphically and paleoenvironmentally useful Miocene acritarch of the northern high latitudes. Micropaleontology 55, 171–186.

Mollenhauer, G., Kienast, M., Lamy, F., Meggers, H., Schneider, R.R., Hayes, J.M., Eglinton, T.I., 2005. An evaluation of 14C age relationships between co-occurring foraminifera, alkenones, and total organic carbon in continental margin sediments. Paleoceanography 20, PA1016

Müller, P.J., Kirst, G., Ruhland, G., von Storch, I., Rosell-Melé, A., 1998. Calibration of the alkenone paleotemperature index $U^{k'}_{37}$ based on core-tops from the eastern South Atlantic and the global ocean (60°N-60°S). Geochimica et Cosmochimica Acta 62, 1757–1772.

Radi, T., de Vernal, A., 2008. Dinocysts as proxy of primary productivity in mid-high latitudes of the Northern Hemisphere. Marine Micropaleontology 68, 84–114.

Piasecki, S., 2003. Neogene dinoflagellate cysts from Davis Strait, offshore West Greenland. Marine and Petroleum Geology 20, 1075–1088.

Rosell-Melè, A., McClymont, E., 2007. Biomarkers as paleoceanographic proxies. In: Hillaire-Marcel, C., de Vernal, A. (Eds.), Proxies in Late Cenozoic Paleoceanography. Elsevier, Amsterdam, pp. 441–490.

Samtleben, C., Bickert, T., 1990. Coccoliths in sediment traps from the Norwegian Sea. Marine Micropaleontology 16, 39–64.

Samtleben, C., Schäfer, P., Andruleit, H., Baumann, A., Baumann, K.H., Kohly, A., Matthiessen, J., Schröder-Ritzrau, A., 1995. Plankton in the Norwegian-Greenland Sea: from living communities to sediment assemblages - an actualistic approach. Geologische Rundschau 84, 108–136.

Schreck, M., Matthiessen, J., Head, M.J., 2012. A magnetostratigraphic calibration of Middle Miocene through Pliocene dinoflagellate cyst and acritarch events in the Iceland Sea (Ocean Drilling Program Hole 907A). Review of Palaeobotany and Palynology 187, 66–94.

Schreck, M., Meheust, M., Stein, R., Matthiessen, J., 2013. Response of marine palynomorphs to Neogene climate cooling in the Iceland Sea (ODP Hole 907A). Marine Micropaleontology 101, 49–67.

Schreck, M., Matthiessen, J., 2013. *Batiacasphaera micropapillata*: Palaeobiogeographic distribution and palaecological implications of a critical Neogene species complex. In: Lewis, J., Marret, F., Bradley, L. (Eds.), Biological and Geological Perspectives of Dinoflagellates. The Micropalaeontological Society, Special Publications: Geological Society, London, pp. 301–314.

Schreck, M., Matthiessen, J., 2014. *Batiacasphaera bergenensis* and *Lavradosphaera elongata* - New dinoflagellate cyst and acritarch species from the Miocene of the Iceland Sea (ODP Hole 907A). Review of Palaeobotany and Palynology 211, 97–106.

Schröder-Ritzrau, A., Andruleit, H., Jensen, S., Samtleben, C., Schäfer, P., Matthiessen, J., Hass, C., Kohly, A., Thiede, J., 2001. Distribution, Export and Alteration of Fossilizable Plankton in the Nordic Seas. In: Schäfer, P., Ritzrau, W., Schlüter, M., Thiede, J. (Eds.), The Northern North Atlantic - A changing environment. Springer-Verlag, Berlin, pp. 81–104.

Shipboard Scientific Party, 1995. Site 907. In: Myhre, A.M., Thiede, J., Firth, J.V. (Eds.), Proceedings of the Ocean Drilling, Initial Reports 151. College Station, TX, pp. 57–111.

Sison, C.P., Glaz, J., 1995. Simultaneous confidence intervals and sample size determination for multinomial proportions. Journal of the American Statistical Association 90, 366–369.

Sorrel, P., Popescu, S.M., Head, M.J., Suc, J.P., Klotz, S., Oberhänsli, H., 2006. Hydrographic development of the Aral Sea during the last 2000 years based on a quantitative analysis of dinoflagellate cysts. Palaeogeography, Palaeoclimatology, Palaeoecology 234, 304–327.

Stabell, B., Koç, N., 1996. Recent to Middle Miocene diatom productivity at Site 907, Iceland Plateau. In: Thiede, J., Myhre, A.M., Firth, J.V., Johnson, G.L., Ruddiman, W.F. (Eds.), Proceedings of the Ocean Drilling Program, Scientific Results 151. College Station, TX, pp. 483–492.

Stein, R., Fahl, K., Schreck, M., Knorr, G., Niessen, F., Jensen, L., Forwick, M., Gebhardt, C., Kaminski, M., Kopf, A., Matthiessen, J., Jokat, W., Lohmann, G. (2016). Evidence for ice-free summers in the late Miocene central Arctic Ocean. Nature Communications 7, doi:10.1038/ncomms11148.

Stephens, C., Conkright, M.E., Boyer, T.P., Antonov, J.I., Baranova, O.K., Garcia, H.E., Gelfeld, R., Johnson, D., Locarnini, R.A., Murphy, P.P., O'Brien, T.D., Smolyar, I., 2002. In: Levitus, S. (Ed.), World Ocean Database 2001, Volume 3: temporal distribution of conductivity–temperature–depth (pressure) profiles. NOAA Atlas NESDIS 44. U.S. Government Printing Office, Washington, D.C., 47 p.

Stockmarr, J., 1977. Tablets with spores used in absolute pollen analysis. Pollen et Spores 13, 615–621.

Tappan, H., 1980. The paleobiology of plant protists. W.H. Freeman and Company, San Francisco, 1028 pp.

Taylor, F. J. R., 1987. The Biology of Dinoflagellates. Oxford: Blackwell Scientific Publications, 785 pp.

Tyson, R.V., 1995. Sedimentary Organic Matter - Organic Facies and Palynofacies. Chapman & Hall, London, 615 pp.

Van Nieuwenhove, N., Baumann, A., Matthiessen, J., Bonnet, S., de Vernal, A., 2016. Sea surface conditions in the southern Nordic Seas during the Holocene based on dinoflagellate cyst assemblages. The Holocene 26, 722–735.

Vázquez-Riveiros, N., Govin, A., Waelbroeck, C., Mackensen, A., Michel, E., Moreira, S., Bouinot, T., Caillon, N., Orgun, A., Brandon, M., 2016. Mg/Ca thermometry in planktic foraminifera: Improving paleotemperature estimations for *G. bulloides* and *N. pachyderma* left. Geochemistry, Geophysics, Geosystems 17, 1–16.

Versteegh, G.J.M., 1994. Recognition of cyclic and non-cyclic environmental changes in the Mediterranean Pliocene: A palynological approach. Marine Micropaleontology 23, 147–183.

Versteegh, G.J.M., Zonneveld, K.A.F., 1994. Determination of (palaeo-)ecological preferences of dinoflagellates by applying Detrended and Canonical Correspondence analysis to Late Pliocene dinoflagellate cyst assemblages of the south Italian Singa section. Review of Palaeobotany and Palynology 84, 181–199.

Wall, D., Dale, B., 1974. Dinoflagellates in the Late Quaternary deep-water sediments of the Black Sea. In: Degens, E.T., Ross, D.A. (Eds.), The Black Sea - Geology, Chemistry and Biology. American Association of Petroleum Geologists, Tulsa, TX, pp. 364–380.

Williams, G.L., Fensome, R.A., MacRae, R.A., 2017. The Lentin and Williams Index of Fossil Dinoflagellates, 2017 Edition. American Association of Stratigraphic Palynologists, Contribution Series 48, TX, 1097 pp.

Wrenn, J.H., Kokinos, J.P., 1986. Preliminary comments on Miocene through Pleistocene dinoflagellate cysts from De Soto Canyon, Gulf of Mexico. American Association of Stratigraphic Palynologists, Contributions Series 17, TX, pp. 169-225.

Zachos, J.C., Dickens, G.R., Zeebe, R.E., 2008. An early Cenozoic perspective on greenhouse warming and carbon-cycle dynamics. Nature 451, 279–283.

Zonneveld, K.A.F., Versteegh, G., Kodrans-Nsiah, M., 2008. Preservation and organic chemistry of Late Cenozoic organic-walled dinoflagellate cysts: A review. Marine Micropaleontology 68, 179–197.

Zonneveld, K.A.F., Marret, F., Versteegh, G.J.M., Bogus, K., Bonnet, S., Bouimetarhan, I., Crouch, E., de Vernal, A., Elshanawany, R., Edwards, L., Esper, O., Forke, S., Grøsfjeld, K., Henry, M., Holzwarth, U., Kielt, J.-F., Kim, S.-Y., Ladouceur, S., Ledu, D., Chen, L., Limoges, A., Londeix, L., Lu, S.H., Mahmoud, M.S., Marino, G., Matsouka, K., Matthiessen, J., Mildenhal, D.C., Mudie, P., Neil, H.L., Pospelova, V., Qi, Y., Radi, T., Richerol, T., Rochon, A., Sangiorgi, F., Solignac, S., Turon, J.-L., Verleye, T., Wang, Y., Wang, Z., Young, M., 2013. Atlas of modern dinoflagellate cyst distribution based on 2405 data points. Review of Palaeobotany and Palynology 191, 1–197.